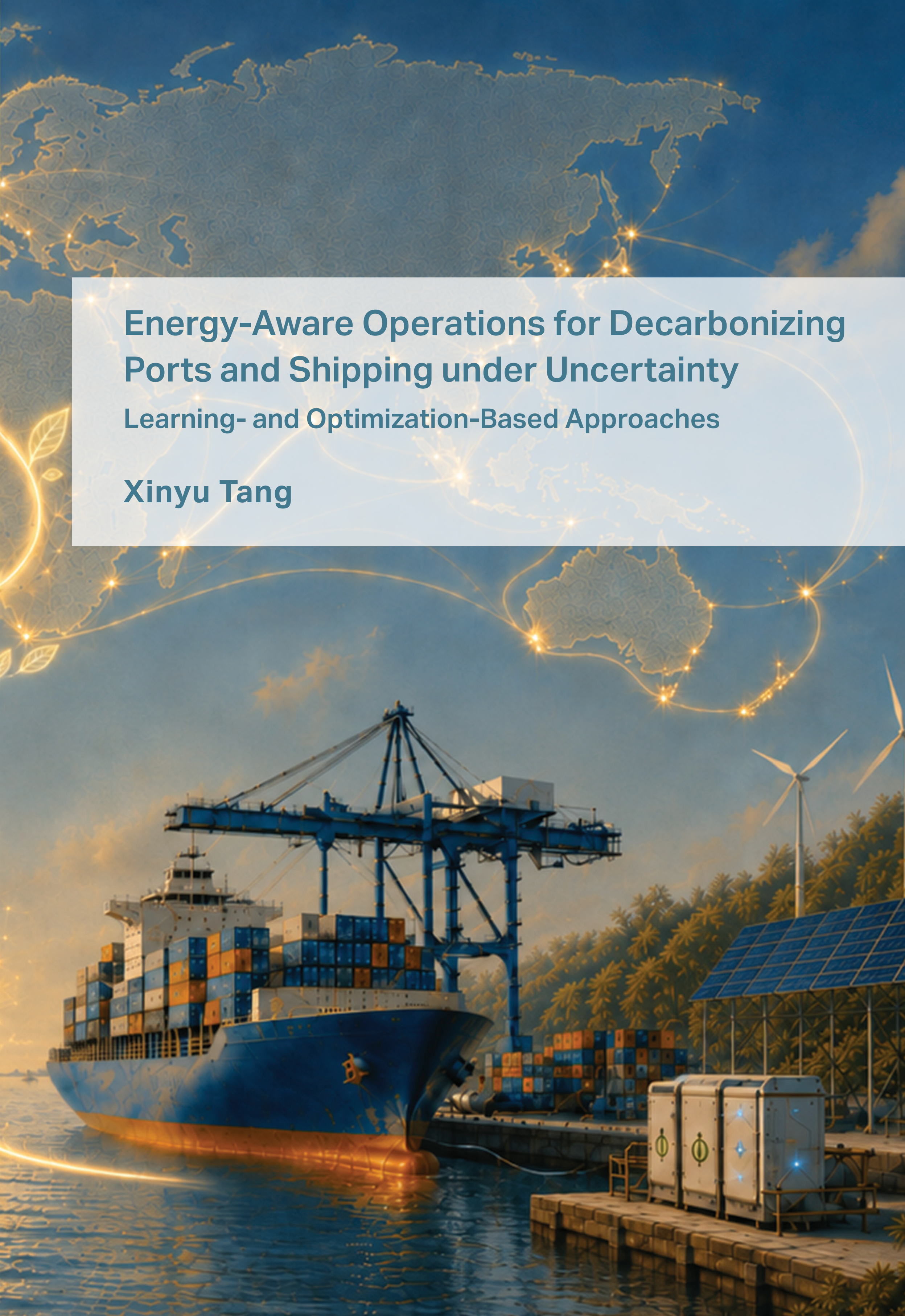

Energy-Aware Operations for Decarbonizing Ports and Shipping under Uncertainty

Learning- and Optimization-Based Approaches

Xinyu Tang

Energy-Aware Operations for Decarbonizing Ports and Shipping under Uncertainty

Learning- and Optimization-Based Approaches

Xinyu TANG

Energy-Aware Operations for Decarbonizing Ports and Shipping under Uncertainty

Learning- and Optimization-Based Approaches

Dissertation

for the purpose of obtaining the degree of doctor
at Delft University of Technology
by the authority of the Rector Magnificus, Prof. dr. ir. H. Bijl
chair of the Board for Doctorates
to be defended publicly on
Monday, 21 September 2026 at 10:00

by

Xinyu TANG

This dissertation has been approved by the promotors.

Composition of the doctoral committee:

Rector Magnificus	Chairperson
Prof. dr. R. R. Negenborn	Delft University of Technology, promotor
Dr. F. Schulte	Delft University of Technology, promotor

Independent members:

Prof. dr. ir. L. A. Tavasszy	Delft University of Technology
Prof. dr. P. Palensky	Delft University of Technology
Prof. dr. S. Yeh	Chalmers University of Technology
Dr. Ç. Iris	University of Liverpool
Dr. O. Kirichek	Delft University of Technology

The research leading to this thesis was supported by the China Scholarship Council under grant No. 202206230078.

TRAIL Thesis Series no. T2026/22, The Netherlands Research School TRAIL

TRAIL
P.O. BOX 5017
2600 GA Delft
The Netherlands
E-mail: info@rsTRAIL.nl

ISBN: 978-90-5584-397-8

Printed in the Netherlands

"Do nothing, yet leave nothing undone."

Tao Te Ching

Preface

As I write these words, my PhD journey is gradually drawing to a close. Looking back, the past four years seem both long and remarkably brief. They have been filled with curiosity, happiness and discovery, but also with uncertainty, frustration, and repeated attempts to find a way forward. There were moments when research progressed with unexpected clarity, and others when a model, a manuscript, or even a single argument had to be reconsidered many times. Yet it was through these changes of direction that I gradually learned how to approach difficult questions with greater patience and confidence. Reaching the end of this journey, I would like to express my sincere gratitude to all those who have accompanied and supported me along the way.

First, I would like to express my deepest gratitude to my promotors, Prof. Rudy R. Negenborn and Dr. Frederik Schulte. Thank you for giving me the opportunity to pursue my PhD at TU Delft and for your trust throughout these years. Your broad perspective and your ability to identify the essential question behind a complex problem have greatly influenced the way I think about research. Your guidance at important stages helped me maintain a clear direction while leaving me sufficient freedom to explore and develop my own ideas. I am especially grateful to Dr. Frederik Schulte, my daily supervisor, for accompanying me so closely throughout this journey. Our discussions were not always confined to research. These conversations made our collaboration not only intellectually rewarding but also genuinely enjoyable. You consistently encouraged me to take greater ownership of my research: to form my own judgments, make independent decisions, and pursue questions that I truly wanted to explore. Rather than simply telling me which direction to follow, you encouraged me to find and shape that direction for myself. I will always value the pleasant time we shared, as well as your patience, openness, and support during both the productive and difficult periods of my PhD. Additionally, I would like to say thank you to Prof. Jiangang Jin, my master's supervisor. Your guidance during my master's studies helped me build a solid foundation for academic research, while your encouragement gave me the confidence and motivation to pursue a PhD.

I would also like to thank my colleagues and friends at TU Delft, particularly those in the Transport Engineering and Logistics section and the Maritime and Transport Technology department. Working in such an international environment gave me the opportunity to meet people with different backgrounds, perspectives, and ways of understanding the world. My sincere thanks go to Ping He, Xiaohuan Lyu, Mingxin Li, Changyuan Chen, Qianyi Chen, Xin Xiong, Wenhua Qu, Hao Shi, Chenghua Yang, and Mingye Luan for the help encouragement, and companionship you offered in both my academic work and everyday life. I am especially grateful to my office mates, Niek Goselink, Abhishek Dhyani, and Richmond Anku, for the everyday companionship, conversations, and the quiet mutual understanding that made working days more enjoyable. I would also like to thank Keyu Chen, Yingwen Zhao, and Jiaqi Liu. The journeys and trips we shared have left me with many wonderful memories. I hope that our friendships will continue despite the different paths and distances that may lie ahead.

Beyond research, living in the Netherlands has itself been a memorable part of this journey. I will remember the sea breeze along the coast, the seemingly endless tulip fields in spring, the windmills standing among the farms and houses of the countryside, and the many remarkable museums in which history, art, and everyday life quietly meet. I will also remember cycling through changing weather, the long summer evenings, and the calm beauty of ordinary days in Delft. These scenes and experiences gave me moments of rest from research and allowed me to discover the country. Together, they form some of the most vivid and beautiful memories of my life in the Netherlands.

Above all, I would like to express my deepest gratitude to my parents. Thank you for your unconditional love, understanding, and support throughout all the years. Although we were separated by a great distance during most of my PhD, I always knew that I could rely on your encouragement and care. Your trust gave me strength during moments of doubt. Whatever I may achieve, it would not have been possible without the foundation you have given me.

Completing a PhD has been much more than an academic pursuit. It has certainly been an exploration of research questions, models, data, and methods, but it has also been an inward journey: a process of learning how to live with uncertainty, how to remain patient when progress is slow, and how to understand both my abilities and my limitations more honestly. Research taught me that meaningful results rarely emerge along a straight and predictable path. The world is vast beyond measure, while each of us occupies only a very small place within it. We may never eliminate uncertainty or fully control the direction in which life carries us. What we can do is continue to move forward with curiosity, courage, patience, and humility. Perhaps the purpose of this continuous struggle is not to arrive at complete certainty, but to gradually find a sense of fulfillment and peace within ourselves.

Xinyu Tang
Delft, August 2026

Contents

Chapter 1

Introduction

Maritime transport is a critical component of global supply chains and the world economy. The decarbonization of maritime transport and port operations has become a central objective under global climate commitments and regional policy frameworks. As ports transition toward electrified infrastructures and shipping networks adapt to carbon pricing and fuel regulations, operational planning and energy management are becoming increasingly interdependent. Decisions made at the terminal level affect electricity consumption and shore power demand, while maritime operational strategies such as sailing speed adjustment, fuel switching, and bunkering influence port energy profiles and system performance. Managing these interactions under uncertainty requires integrated modeling approaches that bridge port operations and maritime decision-making.

This thesis develops a layered and uncertainty-aware framework for energy-aware operations planning across port and maritime systems. This chapter is organized as follows. Section 1.1 presents the research background. Section 1.2 provides a literature review and highlights the research gaps. Section 1.3 presents the research motivation. Section 1.4 formulates the research questions. Section 1.5 defines the research scope and illustrates the layered structure of the thesis, followed by the main contributions in Section 1.6. Section 1.7 outlines the overall structure of the dissertation.

1.1 Background

Maritime transport is one of the pivotal pillars of global trade and supply chains, accounting for over 80% of the global trade volume (UNCTAD, 2025). Ports are therefore the essential nodes in the international logistics network. Ports emit large amounts of greenhouse gases (GHGs) from various daily operations, making ports one of the main contributors to GHG emissions in the maritime sector.

The Paris Agreement sets a long-term global climate goal to limit global warming to well below 2°C, pursuing efforts to restrict the increase to 1.5°C above pre-industrial levels (UNFCCC, 2015). This global commitment has placed increasing pressure on major emitting industries such as maritime transport. In the European Union, the European Green Deal aims to transform the EU into the world's first climate-neutral continent by 2050, making net-zero GHG emissions a legally binding objective under the European Climate Law and establishing intermediate targets such as reducing net emissions by at least 55% by 2030 compared with 1990 levels (European Commission, 2019). As part of this overarching climate strategy, the EU has introduced a suite of policy initiatives focused on the decarbonisation of the transport sector, including maritime shipping. The FuelEU Maritime Regulation sets gradual reduction targets for the greenhouse gas intensity of energy used on board ships, aiming for an overall reduction of up to 80% by 2050 compared with a 2020 baseline, and thereby promoting the uptake of low-carbon and renewable fuels in maritime transport (European Commission, 2023b). These regulations, together with supporting policies such as the Alternative Fuel Infrastructure Regulation (AFIR) and enhanced Monitoring, Reporting, and Verification (MRV) frameworks seek to accelerate the transition toward cleaner fuels, shore power use, and more energy-efficient operations.

Building upon these regulatory drivers, ports have increasingly been identified as critical actors in achieving maritime decarbonization. Port authorities and terminal operators have implemented a wide range of energy-related measures including technological upgrades, operational strategies, and energy management systems. These measures can be broadly categorized into three dimensions. First, technological interventions focus on equipment electrification and infrastructure upgrading. Ports are progressively replacing diesel-powered quay cranes, yard cranes, and terminal tractors with electric or hybrid alternatives, deploying shore power (SP) systems to eliminate auxiliary engine emissions at berth, and integrating renewable energy sources such as photovoltaic panels and wind power into terminal energy systems. Second, operational strategies aim to improve energy efficiency through optimized scheduling and coordination. Examples include energy-aware berth allocation, coordinated crane scheduling, speed optimization of yard equipment, and peak-shaving strategies to reduce electricity demand during high-price periods. Third, ports are increasingly adopting energy management systems (EMS) that enable real-time monitoring, data-driven decision-making, and demand response participation. Smart grid integration, digital platforms, and advanced metering infrastructures allow ports to dynamically adjust consumption in response to electricity prices and grid conditions.

Taken together, international climate commitments and EU regulatory frameworks are accelerating the decarbonization of the maritime and port sectors, while the existing literature highlights a wide range of technological, operational, and energy management measures adopted by ports to improve energy efficiency. However, as ports transition toward net-zero energy systems, energy consumption is no longer a purely technical issue but becomes deeply interrelated with operational planning decisions and the balance between energy demand and supply.

The current state of research reveals a space at the intersection of operations planning, energy management, and demand prediction, where uncertainty, energy demand and supply can be jointly addressed. This thesis aims to develop integrated modeling and decision-support frameworks that connect port operations and energy management under emerging regulatory constraints.

1.2 Literature review

1.2.1 Port energy and emission reduction measures

Ports are increasingly recognized as critical nodes for mitigating greenhouse gas (GHG) emissions within the maritime transport system. In response to growing environmental concerns and regulatory pressures, a wide range of measures have been proposed to improve energy efficiency and reduce emissions in port operations. Existing review studies consistently highlight that emission reduction in ports is a multi-dimensional problem requiring coordinated technological, operational, and managerial interventions (Alamoush et al., 2020; Wang et al., 2023; Iris & Lam, 2019b; Alzahrani et al., 2021).

A comprehensive categorization of port-related measures is provided in the study of Alamoush et al. (2020), where technical and operational strategies are systematically grouped into several main categories and multiple subcategories, covering both portside activities and ship-port interface operations. This classification reflects the complexity of port systems, where emissions originate from diverse sources, including cargo handling equipment, vessels at berth, and hinterland transport. Similar classifications are also discussed in sustainability-oriented studies, which group measures into technological, operational, managerial, and policy-related dimensions (Wang et al., 2023).

From a technological perspective, ports adopt various equipment and energy-related measures to reduce emissions. These include the replacement or retrofitting of cargo handling equipment with more energy-efficient technologies, electrification and hybridization of machinery, and the use of alternative fuels such as LNG, hydrogen, and biofuels (Alamoush et al., 2020; Iris & Lam, 2019b). In addition, renewable energy sources, such as solar and wind power, are increasingly integrated into port energy systems to reduce dependence on fossil fuels and enhance sustainability performance (Alamoush et al., 2020; Alzahrani et al., 2021). Among these measures, shore power (SP, which is also known as onshore power supply or cold ironing) is widely recognized as an effective solution for reducing emissions from vessels at berth by allowing ships to switch off auxiliary engines. Energy efficiency measures further focus on optimizing energy consumption through both technological solutions and management practices. These include energy-saving technologies, energy management systems, and advanced energy infrastructures such as smart grids, energy storage systems, and microgrids (Alamoush et al., 2020; Iris & Lam, 2019b). Such approaches improve the coordination between energy supply and demand, enabling more efficient and flexible energy usage within port systems.

Operational measures also play a significant role in emission reduction. These measures aim to improve the efficiency of port processes through better planning and coordination, including berth allocation, scheduling, digitalization, and automation (Alamoush et al., 2020; Wang et al., 2023). By reducing vessel waiting times, minimizing idle operations, and improving resource utilization, these strategies contribute to lower energy consumption and emissions. Furthermore, ship-port interface measures, such as just-in-time arrival, vessel speed reduction, and SP implementation, emphasize the importance of coordination between ports and shipping companies in achieving emission reduction targets.

Despite the wide range of available measures, the literature consistently emphasizes that no single strategy is sufficient to achieve substantial emission reduction. Instead, an effective decarbonization pathway requires a combination of complementary measures tailored to specific port characteristics and operational contexts. This highlights the need for integrated approaches that, for example, jointly consider operational decisions and energy management within port systems.

1.2.2 Optimization and data-driven studies for green port operations

In recent years, increasing attention has been given to the use of optimization and data-driven methods to support emission reduction and energy efficiency in port operations (Raeesi et al., 2023). Within container terminals, operational research (OR) methods have been extensively employed to improve major operational decision problems, including berth allocation, quay crane scheduling, yard management, and transport coordination. Many existing studies incorporate environmental objectives directly into optimization models, for example through minimizing energy consumption, emissions, or fuel usage during terminal operations. At the same time, the ongoing automation and electrification of container terminals (CTs) have introduced a range of new operational and planning challenges. These emerging optimization problems are often associated with energy management, equipment electrification, infrastructure sizing, and the adoption of alternative fuels and low-carbon technologies. Although such studies may not always formulate environmental performance as an explicit optimization objective, they still contribute to terminal decarbonization by improving operational efficiency and reducing unnecessary energy use indirectly (Raeesi et al., 2023). From the literature, these studies can generally be grouped into two broad streams. The first focuses on optimization for terminal energy management and infrastructure planning, while the second emphasizes operational adaptation to new technologies, clean fuels, and advanced equipment systems. More recently, an increasing number of interdisciplinary studies have attempted to bridge conventional terminal operation problems with energy-related decision-making. These "hybrid" studies integrate classical operational problems, such as berth allocation, quay crane scheduling, storage yard operations, and transport operations, with energy management considerations and low-carbon technology adoption, highlighting the growing interdependence between operational efficiency and environmental sustainability in modern container terminals (Raeesi et al., 2023).

With the increasing availability of operational and sensor data, data-driven methods have emerged as a complementary paradigm for green port research. These approaches leverage machine learning, statistical modeling, and data analytics techniques to extract patterns and predict key variables. Reliable estimation of fuel consumption, electricity demand, and emissions from major terminal resources is essential for effectively integrating environmental considerations into container terminal operations. In this context, data-driven approaches provide strong predictive capabilities for forecasting vessel and material handling equipment (MHE) energy demand, as well as the uncertain output of renewable energy sources within port microgrids Raeesi et al. (2023).

Recent studies have begun to explore the integration of optimization and data-driven methods to better support decision-making under uncertainty. In these frameworks, data-driven models are used to predict key inputs, such as energy demand or vessel arrivals, which are then incorporated into optimization models for decision-making. Existing research in this area can be mainly categorized into two approaches. The first adopts a sequential "predict-then-optimize" framework, where predictions are generated independently and used as deterministic inputs in optimization models. While straightforward to implement, this approach may lead to suboptimal decisions due to error propagation. The second approach focuses on uncertainty-aware optimization, where prediction uncertainty is explicitly incorporated into decision-making models, for example through stochastic programming or distributionally robust optimization. Although still limited in the port context, such approaches have the potential to significantly improve decision robustness.

Based on the literature, the integration between optimization models and data-driven prediction remains limited. Most existing studies treat prediction and optimization as separate tasks, and only a few works attempt to combine them into a unified framework. In addition, uncertainty is often insufficiently addressed, particularly in relation to time-varying energy demand and operational disruptions.

To address these limitations, this thesis adopts an integrated methodological framework that combines data-driven prediction and optimization. Specifically, machine learning models are used to predict time-resolved SP demand based on operational and vessel-related features, while optimization models are developed to incorporate such demand into berth allocation and scheduling decisions. Furthermore, uncertainty is explicitly considered to better capture the variability of demand and improve the robustness of energy-aware operational planning.

1.2.3 Energy-aware operations and energy management in ports

With the increasing electrification of port operations, energy consumption has gradually become an essential factor in operational decision-making. Recent studies have started to incorporate energy-related objectives into classical terminal optimization problems, aiming to balance operational efficiency and environmental performance.

At the operational level, several works integrate energy consumption into equipment scheduling problems. For instance, integrated scheduling of quay cranes, yard cranes, and internal trucks has been formulated to jointly minimize vessel delay and transportation energy consumption, revealing the inherent trade-off between efficiency and energy usage (He et al., 2015b). These studies highlight that traditional scheduling approaches focusing solely on productivity may lead to suboptimal energy outcomes. Beyond individual equipment scheduling, researchers have also explored strategies to reshape energy demand patterns. Peak shaving techniques have been proposed to reduce the maximum electricity demand of quay cranes by adjusting operational rules, demonstrating that significant reductions in peak energy costs can be achieved with only minor impacts on handling efficiency (Geerlings et al., 2018). This line of research emphasizes the importance of temporal coordination of operations to mitigate energy peaks.

At a higher system level, the concept of port microgrids and integrated energy management systems has gained increasing attention. Ports are now viewed as large-scale energy hubs where operational planning and energy management decisions are tightly coupled. Integrated models have been developed to simultaneously optimize berth allocation, equipment assignment, and energy management under smart grid environments (Iris & Lam, 2021). These approaches further incorporate renewable energy sources, energy storage systems, and demand response mechanisms, enabling ports to reduce energy costs while improving sustainability performance (Zhang et al., 2022; Mao et al., 2022).

In addition, flexible energy loads within ports, particularly reefer containers, have been identified as critical components for demand-side management. By exploiting the thermal inertia of refrigerated containers, energy consumption can be shifted across time periods to reduce peak loads and operational costs (Pei et al., 2021). Such flexibility provides new opportunities for coordinating operational decisions with energy system constraints.

Furthermore, several studies investigate the trade-off between operational efficiency and environmental objectives. For example, berth allocation and yard operations have been extended to include carbon emission considerations, demonstrating that improvements in transportation efficiency may conflict with emission reduction goals (Karakas et al., 2021). These findings underline the necessity of multi-objective optimization frameworks in port operations.

Overall, existing studies have made significant progress in integrating energy considerations into port operations at different levels, ranging from equipment scheduling to system-wide energy management. However, most of these works either focus on operational optimization with simplified energy representations or consider energy management without fully capturing the stochastic and dynamic nature of operational processes. This gap motivates the need for more integrated frameworks that explicitly account for uncertainty in both operational activities and energy demand.

1.2.4 Shore power demand estimation and operational integration

Shore power (SP, also known as onshore power supply or cold ironing) has been widely recognized as an effective measure for reducing at-berth emissions by enabling ships to switch off auxiliary engines and connect to shore-side electricity. In addition to its environmental benefits, SP has gradually become an important component of port electrification and green port development, although its wider deployment is still constrained by high infrastructure and retrofit costs, heterogeneous ship requirements, and operational complexity (Qi et al., 2020; Abu Bakar et al., 2023; Wang et al., 2024a).

From the perspective of demand estimation, existing studies have approached SP-related power demand at different levels of detail. One stream of research models shore power demand from the standpoint of infrastructure planning and deployment, focusing on the allocation of shore power capacity, berth-level adoption patterns, and the trade-off between system cost and emission reduction. In this context, SP demand is closely associated with berth configuration, installed capacity, and the operational pattern under which ships are allowed to connect to shore power (Peng et al., 2019). Related studies further show that SP utilization cannot be examined independently of berth assignment, since berth allocation decisions directly affect which ships can access electrified berths and how intensively shore power facilities are used (Peng et al., 2021).

A second stream of research addresses SP demand from a broader network or deployment perspective. In these studies, shore power demand is shaped not only by ship characteristics and berth availability, but also by the interaction between port-side and ship-side adoption decisions. This line of work highlights the dilemma in shore power development, namely that port investment depends on ship readiness while ship investment depends on infrastructure availability across the ports they visit. It also shows that actual electricity use at berth depends on mixed energy choices between shore electricity and conventional fuel, rather than being automatically realized wherever SP infrastructure exists (Sheng et al., 2025). Such findings suggest that realized SP demand may differ substantially from nominal infrastructure capacity.

Another important line of work estimates SP demand through engineering-based and simulation-driven methods. Rather than relying only on aggregate traffic counts, these approaches use real port calls, ship data, berth times, cargo-handling processes, trucks, and material handling equipment to construct detailed port energy demand models. This enables the estimation of both annual energy demand and peak power demand for SP implementation under realistic operational conditions (Uzun et al., 2024). Such studies also argue that demand estimation based solely on the number of port calls is too coarse, because port energy demand depends strongly on ship type, ship operational characteristics, and berthing conditions, making port energy demand estimation by call volume insufficient for investment planning (Uzun et al., 2024).

At the same time, review studies on cold ironing and shore power emphasize that demand estimation is influenced by multiple technical and operational factors, including auxiliary engine power, load factors, berthing duration, ship category, voltage and frequency requirements, traffic arrival patterns, and local grid characteristics (Abu Bakar et al., 2023). Existing reviews also indicate that the shore power literature has expanded rapidly but remains fragmented across several themes, such as emission inventory, practical application, deployment, and energy management, without yet converging into a unified framework for SP demand assessment Wang et al. (2024a). In parallel, management-oriented reviews stress that shore power planning is strongly shaped by the perspectives of different stakeholders, especially ports, shipowners, and governments, which further complicates how demand is represented in the literature (Qi et al., 2020).

Overall, the literature has clearly established that SP demand is not a simple electricity load, but the result of interactions among ship characteristics, berthing processes, infrastructure configuration, and operational rules. However, several limitations remain. First, many studies still estimate demand at an aggregated level, such as per vessel, per berth, or per port, without capturing sufficiently fine temporal variation during the berthing process. Second, SP demand is often embedded in deployment, allocation, or cost-benefit studies rather than being treated as a central modeling problem in its own right. Third, although operational factors are acknowledged, the explicit link between detailed port operations and time-resolved SP demand remains insufficiently developed in the existing literature. These limitations suggest the need for more operation-driven and higher-resolution approaches to SP demand estimation and modeling.

1.2.5 Uncertainty in energy-aware port planning

Uncertainty is an inherent feature of port operations and becomes even more critical when energy-related decisions are integrated into operational planning. In the literature, the uncertainties considered in energy-aware port studies can be broadly grouped into two categories: operational uncertainties, which mainly arise from vessel arrivals, handling processes, and workload fluctuations; and energy-related uncertainties, which are associated with renewable generation, electricity demand, and energy prices.

A first stream of research focuses on operational uncertainties in berth and terminal operations. Among these, vessel arrival time uncertainty is the most frequently studied source. For example, a two-stage robust programming model has been proposed for the continuous berth allocation problem under uncertain vessel arrival time, where uncertainty sets and scenarios are introduced to describe fluctuations in arrival time (Qu et al., 2023). Similarly, robust berth allocation models have been developed by considering both vessel arrival time and handling time uncertainty to improve scheduling reliability while reducing emissions (Yu et al., 2022a). In addition, stochastic programming has been applied to the deployment of electric yard cranes under uncertain workload, showing that workload variability significantly affects both operational performance and carbon efficiency (Yu et al., 2019). These studies indicate that uncertainty in port operations has been primarily characterized by arrival, handling, and workload variability, and that robust and stochastic optimization are the dominant modeling approaches in this stream. Beyond optimization-based berth planning, another group of studies addresses operational uncertainty from a data-driven perspective. Vessel arrival uncertainty has been quantitatively evaluated and predicted using machine learning methods, demonstrating that ETA inaccuracies remain a major source of disruption in port operations (Chu et al., 2023). Further studies have improved vessel arrival time prediction by integrating port call records and AIS data, and have shown that more accurate predictions can improve berth allocation decisions through predictive-operational frameworks (Chu et al., 2025, 2026). In parallel, uncertainty in the vessel service stage has also been explored, where data-driven approaches are used to predict vessel service time and capture variability in cargo handling processes (Yan et al., 2024). These studies suggest a shift from assuming uncertainty to estimating it directly from data.

A second stream of research considers *energy-related uncertainties* in electrified ports and integrated energy systems. Uncertainty in renewable energy generation is one of the most widely studied factors. For instance, integrated port operation and energy management models have been developed under smart grid environments, where renewable uncertainty is incorporated into multi-stage decision frameworks (Iris & Lam, 2021). Similarly, two-stage optimization models have been proposed to jointly schedule berth allocation and port microgrid operations while considering uncertainties in renewable generation and load demand (Zhang et al., 2022). At the integrated energy system level, photovoltaic uncertainty has been modeled using scenario generation techniques such as Latin hypercube sampling and clustering, combined with demand response mechanisms to enhance system flexibility (Zhai et al., 2020).

More recent studies extend the scope to multi-source uncertainty. For example, integrated logistics-electric frameworks have been proposed to simultaneously consider uncertainty in vessel arrivals, energy demand, and renewable generation, demonstrating that ignoring such uncertainties may lead to system infeasibility and increased emissions (Sarantakos et al., 2024). Distributionally robust optimization approaches have also been introduced in integrated seaport energy systems to address ambiguity in probability distributions, considering uncertainties in renewable output, electricity prices, and load demand (Yu et al., 2025). In addition, advanced control methods, such as reinforcement learning and model predictive control, have been explored under uncertain forecasts of demand and renewable generation (Conte et al., 2025). At a more localized level, hierarchical control strategies have been applied to reefer container parks to handle uncertainty in load demand through day-ahead and intra-day adjustments (Pei et al., 2021). These studies indicate a transition from single-source to multi-source uncertainty modeling in electrified port systems.

From a methodological perspective, the literature mainly employs several approaches to handle uncertainty. The first is stochastic programming, which models uncertainty through scenarios and is widely used in berth allocation and energy scheduling problems (Zhang et al., 2022). The second is robust optimization, which ensures solution feasibility under worst-case realizations without requiring precise probability distributions (Qu et al., 2023). Distributionally robust optimization has recently gained attention for handling ambiguity in uncertainty distributions (Yu et al., 2025). The third is data-driven prediction and control, where machine learning and forecast-based control strategies are used to reduce uncertainty impacts (Chu et al., 2025, 2026).

Despite these advances, several limitations remain. First, most studies focus on either operational uncertainty or energy-related uncertainty, while relatively few consider both in a unified framework. Second, vessel arrival time remains the dominant uncertainty studied, whereas uncertainty in service time, cargo handling processes, and SP-related demand is still insufficiently explored. Third, although data-driven approaches have improved the estimation of uncertainty, their integration into optimization-based decision-making models remains limited. These limitations highlight the need for more integrated and data-driven frameworks that can jointly capture operational and energy uncertainties in electrified port systems.

1.2.6 Research gaps

The above review highlights that, although significant progress has been made in port decarbonization, energy system integration, and uncertainty-aware optimization, several research gaps remain in the literature.

First, the integration between port operations and energy systems is still limited. While existing studies have incorporated energy consumption or emissions into operational models, they often adopt simplified or loosely coupled formulations. In particular, the interaction between operational decisions (e.g., berth allocation and scheduling) and time-varying electricity demand is not fully captured, limiting the applicability of these models in increasingly electrified port environments.

Second, SP demand modeling, prediction, and its impact on port operations remain insufficiently developed. Although various approaches have been proposed to estimate shore power demand, most studies rely on aggregated, rule-based, or case-specific methods that fail to capture fine-grained temporal dynamics and the dependence of demand on detailed port operations. Moreover, SP demand is often treated as an exogenous input, rather than being explicitly modeled as an outcome of operational processes.

Third, uncertainty in energy-aware port planning has not been fully addressed. Existing studies primarily focus on uncertainties related to vessel arrival and handling processes, while energy-related uncertainties remain underexplored. In addition, operational and energy uncertainties are often considered separately, and their joint impact on integrated port systems is rarely investigated.

Taken together, these limitations indicate a lack of unified frameworks that jointly consider (i) tight integration between operational decisions and energy systems, (ii) time-resolved SP demand modeling and prediction, and (iii) uncertainty in both operations and energy demand. Motivated by these observations, this thesis proposes a comprehensive framework that combines data-driven SP demand estimation and prediction with energy-aware berth allocation and scheduling, while explicitly accounting for uncertainty in demand and operations. The proposed approach aims to bridge the gap between SP demand modeling, operational optimization, and uncertainty management in electrified port systems.

1.3 Research motivation

The rapid electrification of port operations and increasingly stringent maritime decarbonization policies are transforming modern ports into energy-intensive and highly interconnected systems. With the large-scale deployment of shore power (SP) infrastructure and the growing adoption of low-carbon energy technologies, ports are no longer viewed solely as cargo-handling facilities, but also as critical energy hubs within maritime transportation systems. As a result, the coordination between operational decisions and energy systems has become increasingly important for supporting efficient and sustainable port operations.

In electrified ports, operational activities such as berth allocation, vessel scheduling, and cargo-handling processes directly influence the timing and magnitude of electricity demand. At the same time, energy-related constraints, including electricity capacity and fuel availability, may significantly affect operational performance and service reliability. This strong interaction creates new challenges for port planning and management, requiring more integrated approaches that jointly consider operational and energy perspectives.

The expansion of SP systems further increases the importance of accurate and time-resolved demand modeling. Compared with traditional electricity consumption, SP demand is highly dynamic and closely related to vessel operations and terminal activities. Accurate estimation and prediction of SP demand are therefore essential for infrastructure planning, energy management, and operational coordination in increasingly electrified terminals. In addition, the growing availability of operational data creates opportunities for data-driven approaches that can better support predictive and energy-aware decision-making.

Meanwhile, uncertainty has become an inherent characteristic of modern port-shipping systems. Factors such as vessel arrivals, handling operations, electricity demand, and fuel supply conditions may all vary over time and significantly affect system performance. These uncertainties often interact across different decision layers and may reduce the reliability of deterministic planning approaches. Consequently, developing uncertainty-aware frameworks has become increasingly important for improving the resilience and robustness of maritime operations.

Furthermore, port decarbonization cannot be considered independently from broader maritime transportation systems. For example, port energy demand is closely connected with vessel routing, sailing speed, and bunkering decisions, while energy and fuel availability at ports may, in turn, influence maritime operations. This interaction highlights the need for integrated approaches that support coordination between ports, shipping networks, and energy systems.

Motivated by these challenges, this thesis develops an integrated and data-driven framework for electrified port-shipping systems. The research focuses on energy-aware berth allocation and scheduling, SP demand estimation and prediction, and uncertainty-aware maritime planning involving fuel bunkering decisions. Through this layered perspective, the thesis aims to support more efficient, resilient, and sustainable maritime transportation systems.

1.4 Research questions

The main research question of this thesis is:
How can energy-aware operations planning be designed across port and maritime systems to support decarbonization objectives under uncertainty?

To answer the above question, the following sub-questions are addressed:

RQ 1: *How can terminal-level energy management and port operations be optimized under uncertain electricity prices and vessel arrival patterns?*

This question focuses on the coordination of operational scheduling and energy management within container terminals under uncertainty. Electricity price volatility and uncertain vessel arrivals introduce operational risks that affect energy costs and system efficiency. An integrated stochastic optimization framework is therefore required to jointly determine port operations and energy management. This question is investigated in Chapter 2, where a stochastic programming model is developed to optimize terminal operations and energy management under uncertainty.

RQ 2: *How to model shore power (SP) demand and predict it with raw vessel port call data?*

Accurate modeling and prediction of shore power demand are essential for energy-aware planning in electrified ports. SP demand depends on vessel characteristics, arrival and departure times, and operational patterns, making it highly dynamic and data-driven. This question explores how raw vessel port call data can be processed, modeled, and combined with machine learning techniques to construct reliable SP demand profiles. This question is addressed in Chapter 3, where data-driven methods are developed to model and predict SP demand using real port call data.

RQ 3: *How do shore power (SP) demand modeling and prediction influence berth allocation decisions and terminal shore power profiles?*

While SP demand can be predicted, it is also inherently linked to berth allocation decisions. Different berth assignments and vessel service schedules generate distinct shore power load profiles, potentially leading to capacity violations or inefficient energy use. This question examines the interaction between predicted SP demand and berth allocation. This question is also investigated in Chapter 3, where a predict-then-optimize framework is developed to analyze the impact of SP demand on berth allocation decisions.

RQ 4: *How to optimize sailing speed, fuel choice, and bunkering decisions for dual-fuel vessels considering fuel supply uncertainty from ports?*

Maritime operational decisions such as sailing speed adjustment, fuel switching, and bunkering strategies directly affect carbon emissions, fuel costs, and vessel arrival patterns. Under emerging carbon pricing schemes and uncertain fuel availability at ports, these decisions become highly interdependent and stochastic. This question develops an integrated optimization framework that determines speed, fuel choice, bunkering amount, and port selection while accounting for fuel supply uncertainty. This question is addressed in Chapter 4, where an optimization model is proposed to support fuel and speed decisions under supply uncertainty.

1.5 Research scope

Figure 1.1 illustrates the scope of this thesis. The research is structured in a layered manner, expanding from terminal-level energy management to multi-port shipping network optimization.

At the core of the framework lies port 1, representing a specific electrified container terminal. Within this terminal, multiple operational areas contribute to energy consumption, including:

- The berth area, where vessels connect to shore power (SP), and cargo handling and bunkering operation also take place in this area;
- The connection area, linking quay-side operations with inland logistics;
- The yard storage area, where electrified cargo handling equipment (e.g, yard cranes) operates;
- The gate processing area, facilitating truck interactions.

Electricity is obtained from the external market and distributed to various terminal energy consumers, such as electrified cargo handling equipment and automated guided vehicle (AGV) charging systems. Chapter 2 focuses on optimizing port operations and energy management within this terminal under uncertain electricity prices and vessel arrival patterns.

Building upon terminal-level energy management, the thesis further investigates shore power demand estimation, prediction, and its interaction with berth allocation decisions. As illustrated in the central part of the figure, shore power consumption at the berth area is influenced by vessel schedules. Chapter 3 develops a data-driven framework to estimate and predict SP demand and integrates these predictions into energy-aware berth allocation models.

The scope then expands beyond a single terminal to encompass a multi-port shipping network, represented by port 1, port 2, and port 3 connected by feeder vessels. At this broader level, vessels operate across ports while making decisions regarding sailing speed, fuel switching, bunkering quantities, and bunkering port selection. Fuel availability uncertainty at ports further complicates these decisions. Chapter 4 addresses this layer by developing a robust optimization framework that integrates bunkering strategies with sailing decisions under uncertain fuel supply conditions.

This layered structure enables a comprehensive investigation of energy-aware operations planning across port and maritime systems, bridging terminal operations, shore power management, and shipping network optimization under uncertainty.

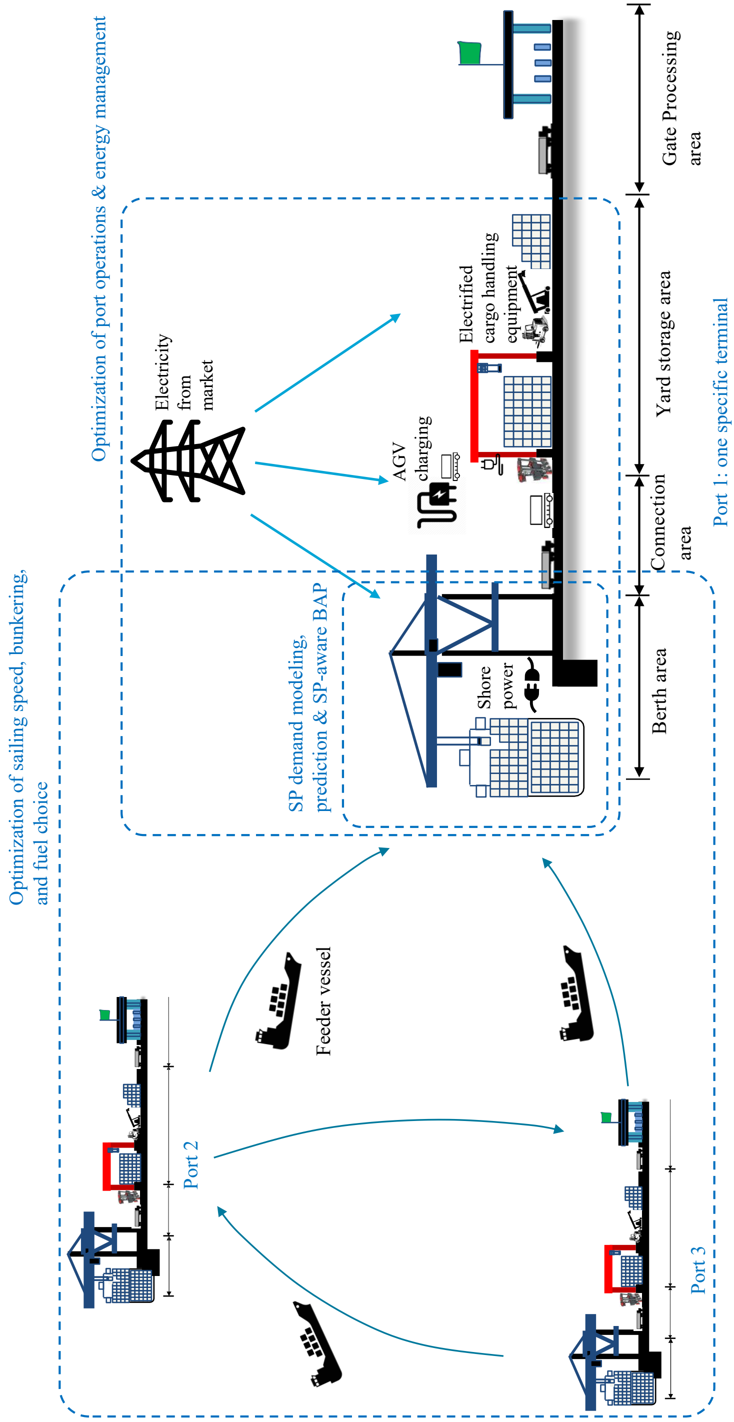

Figure 1.1: Scope of port operations, energy management and feeder vessel network framework in this thesis

1.6 Contributions

This thesis contributes to the fields of energy-aware port operations by proposing methods combining optimization and data-driven machine learning methods. The main contributions are as follows:

1. **Stochastic terminal-level energy-aware operations planning.** An integrated stochastic optimization framework is developed to coordinate terminal operations and energy management under uncertain electricity prices and vessel arrival patterns (in Chapter 2). Unlike deterministic approaches, the proposed model explicitly incorporates uncertainty and enables demand response, improving cost-efficiency and operational robustness. Part of this research has been published in Stoter et al. (2025).

2. **Data-driven modeling and prediction of shore power (SP) demand.** A data-driven predict-then-optimize framework is proposed to estimate and predict SP demand using raw vessel port call data and machine learning techniques. By transforming vessel operational data into dynamic shore power load profiles, the thesis enhances the predictive capability in energy planning for ports. Part of this research has been published in Tang et al. (2025b) and included in a manuscript submitted for publication (Tang et al., 2026b).

3. **Predictive energy-aware berth allocation under decision-dependent demand.** The thesis demonstrates how estimated and predicted SP demand influences berth allocation decisions and terminal shore power profiles. A predict-then-optimize framework is introduced to integrate SP demand forecasting into berth planning, thereby reducing capacity violations and improving energy-efficient scheduling. Part of this research has been included in a manuscript submitted for publication (Tang et al., 2026b)

4. **Integrated sailing speed, fuel bunkering, and fuel choice during sailing optimization under fuel supply uncertainty.** An integrated optimization model is developed to jointly determine sailing speeds, bunkering locations and quantities, and fuel choice during sailing under uncertain port fuel availability. The model enhances the ability to cope with uncertain port fuel availability while explicitly linking bunkering decisions with sailing operations in a unified optimization framework. Part of this research has been included in a manuscript submitted for publication (Tang et al., 2026a)

1.7 Thesis outline

Figure 1.2 illustrates the overall structure of this thesis. The dissertation is organized into five chapters, progressing from conceptual foundations to specific methodology developments and experimental studies, and finally to conclusions and future research directions.

Chapter 1 introduces the research background and motivation of the thesis. It presents the decarbonization context and outlines the research questions that guide the subsequent chapters. It also provides a literature review and highlight the research gaps that motivate the framework developed in this thesis.

Chapters 2 to 4 constitute the core methodological and research problem contributions of the thesis and are structured across different but interconnected layers of the port–maritime system.

Chapter 2 focuses on terminal-level energy management under uncertainty (**RQ 1**). It develops a stochastic operations planning framework for electrified container terminals, where multiple energy consumers—such as quay cranes, yard equipment, and other terminal facilities—are coordinated under uncertain electricity supply and demand conditions.

Chapter 3 addresses **RQ 2** and **RQ 3** by investigating terminal-level shore power (SP) consumption and its interaction with operational planning. First, a data-driven framework is proposed to learn and estimate SP demand from raw vessel port call data. Then, the predicted demand is integrated into an energy-aware berth allocation model, revealing how SP demand estimation influences berth assignment decisions and terminal shore power profiles.

Chapter 4 shifts the perspective to a more combined layer (**RQ 4**). It develops a robust optimization model for dual-fuel vessels that jointly determines sailing speed, bunkering locations and quantities, and fuel choice during sailing under fuel supply uncertainty. This chapter establishes the linkage between port-level bunkering decisions and vessel sailing optimization.

Finally, Chapter 5 concludes the thesis by summarizing the main findings, discussing managerial and policy implications, and outlining future research directions.

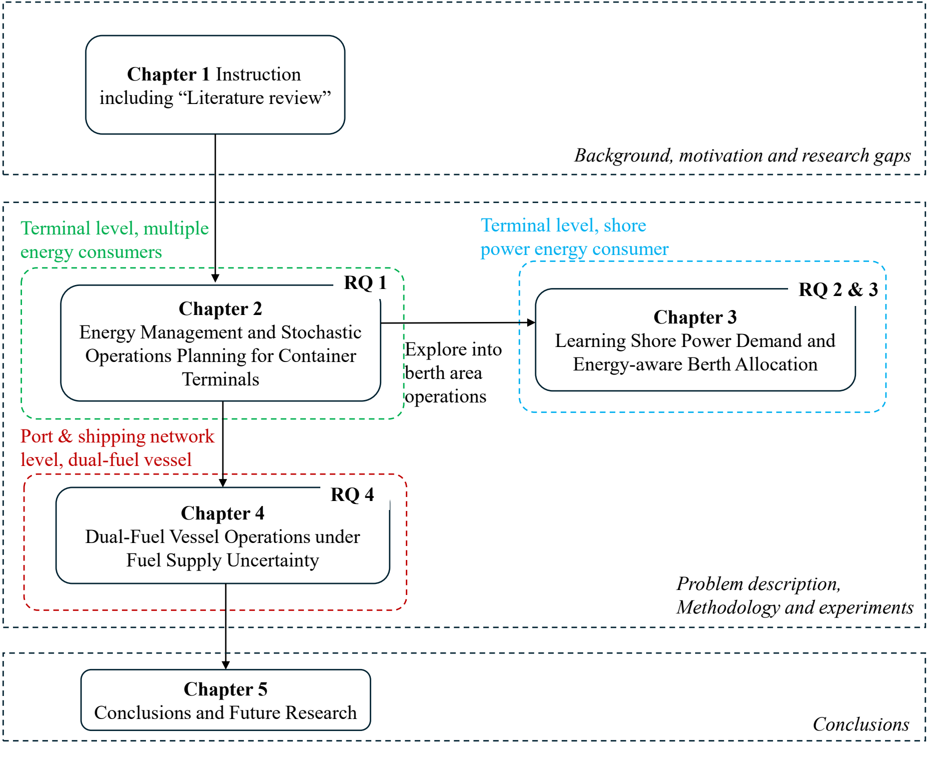

Figure 1.2: Thesis outline

Although Chapters 2 to 4 are methodologically distinct and were developed as standalone studies, they are connected by a shared vertical logic. Chapter 2 addresses the terminal as a self-contained energy system under uncertain electricity supply and vessel arrivals. Chapter 3 zooms in on the berth area within that terminal and treats shore power demand as a decision-relevant, learnable quantity that couples vessel scheduling to the terminal's electricity profile. Chapter 4 zooms out to the multi-port shipping network and treats fuel supply availability at ports as the counterpart, at the network level, of the electricity supply uncertainty modeled in Chapter 2. In this sense, the three chapters form a layered decomposition of a single integrated planning problem — terminal energy, berth-shore-power coupling, and network-level fuel supply — with uncertainty modeling as the connective tissue across layers.

Chapter 2

Energy Management and Stochastic Operations Planning for Container Terminals

---

In this chapter, we propose a two-stage stochastic programming model to optimize port operations and energy management. This chapter addresses RQ 1: How can terminal-level energy management and port operations be optimized under uncertain electricity prices and vessel arrival patterns?

The chapter is structured as follows: Section 2.1 introduces some background and briefly summarizes the research work presented in this chapter. We provide a literature review in Section 2.2 and define the problem in Section 2.3. Section 2.4 establishes the mathematical model for the problem followed by the solution procedure discussed in Section 2.5. The numerical results and their implications are presented in Section 2.6. Based on these results, managerial insights are provided in Section 2.7. Finally, Section 2.8 summarizes the conclusions and lessons learned from this chapter.

Part of this chapter is published as a journal article: Stoter, J., X. Tang, M. Cvetkovic, P. Palensky, H. Polinder, Çağatay Iris, F. Schulte (2025) Energy management and stochastic operations planning for electrified container terminals with uncertain energy supply and demand, *Journal of Cleaner Production*, 527, p. 146383.

2.1 Introduction

Electricity prices have been volatile in recent years. Between 2019 and 2022, the average electricity price in Europe increased from 38 €/MWh to 235 €/MWh, representing an increase of 518% (ENTSO-E, 2023). This price surge has resulted in higher operational costs for container terminals, particularly those with a high level of electrification, which have been significantly impacted by the rising electricity prices. Challenges related to the transition to renewable energy sources and limited grid capacity in many port regions further aggravate this situation.

Container terminal operators can reduce their energy costs (and ensure energy supply) by implementing a demand response (DR) program. DR program serves as a rationing system to change the power consumption of consumers to better match the demand for power with the supply. Rationing is usually accomplished by price incentives to shift consumption from higher-price periods to lower-price periods energy consumption is adjusted through real-time energy prices in DR system, which is more flexible than single energy prices in long-term contracts signed by container terminals to hedge against future price risks and uncertainty. By implementing demand response programs to strategically manage their energy consumption, container terminals can effectively lower energy costs.

The energy demand at a port primarily depends on logistics processes at the port system. Logistics processes within a port are uncertain, leading to complex operations planning with uncertain energy demand. Energy consumption fluctuates significantly throughout the day, depending on the scheduling (Bakar et al., 2021). Terminal operators currently possess limited knowledge about energy consumption patterns. Unlike other industries, container terminals lack continuous and recurring production cycles (Grundmeier et al., 2014). Instead, daily processes in container terminals are highly dynamic depending on the number of containers and ship arrival patterns (Grundmeier et al., 2014).

Energy management and operations planning considering uncertainty is the research issue that has a great potential for exploration. Several studies concentrate on DR with a single load, while literature focusing on energy-aware integrated planning problems involving multiple energy loads is scarce. Moreover, there is limited work considering the stochastic nature of both energy demand and supply, highlighting the research gap related to energy-aware operational problems with multiple loads considering uncertainty in both supply and demand. To the best of our knowledge, only one work (Iris & Lam, 2021) identified in the literature utilized a stochastic modeling approach that considered multiple scenarios of solar energy production to account for stochastic electricity supply. However, uncertainty in neither port operations nor energy demand has been considered. In this chapter, we consider uncertain ship arrival time (and resulting uncertainty in energy demand patterns) and uncertain energy prices in particular energy pricing schemes. Moreover, we develop a scenario decomposition algorithm to solve the model efficiently.

This chapter investigates energy management and energy-aware operations planning in container terminals, in which energy consumption is adjusted by a DR system. The goal of the chapter is to increase the efficiency of allocating energy resources and arranging operations in container terminals. The main objectives are to minimize schedule and energy-related costs, to demonstrate the impact of stochastic modeling when taking the uncertainty of energy demand

and supply and to show the impact of demand response. We optimize the operations planning problem within a container terminal, incorporating the associated energy costs into the objective function. The energy costs of the optimization process include two aspects: the cost of purchasing electricity from the wholesale market and the cost of imbalances resulting from inaccurate consumption predictions. To address the uncertainty of electricity demand and supply, we consider multiple scenarios of ship arrival times and electricity prices. We then conduct computational experiments based on the data from the HHLA Container Terminal Altenwerder (CTA) in Hamburg, Germany. We assess the impact of the uncertainty by comparing the solutions of the stochastic approach to reactive approaches. The impact of DR is presented by comparing the cost savings when applying no energy price, single energy prices and varying prices per hour.

This chapter contributes to the field in the following ways:

1. It introduces uncertainty on both energy supply and demand sides when studying operations and energy flows in container terminals. The uncertainty of energy supply and demand is represented by fluctuating energy prices and ship arrival times, respectively.
2. It considers multiple energy loads and integrates planning of Automated Guided Vehicles (AGVs), quay and yard cranes, reefer containers, and ship electricity consumption to derive total energy demand.
3. It introduces a new stochastic programming approach, using scenario decomposition with progressive hedging, and demonstrates it outperforms the reactive approaches through computational experiments based on a terminal in Port of Hamburg, Germany.
4. It quantifies the positive impact of demand response planning in real-time energy pricing schemes through the case study at the terminal in the Port of Hamburg, Germany.

2.2 Related work

Only a small number of studies have dealt with the underexplored area of energy consumption within the container terminals. In a review paper by Iris & Lam (2019b), an overview was provided on operational strategies, technologies, and energy management systems aiming to increase energy efficiency in ports. The authors emphasized the need for future research in operational strategies that incorporated energy-aware planning of operations, particularly in integrated planning problems. Additionally, the importance of an energy management system for balancing energy demand with supply was highlighted. However, this task is challenging due to the fluctuating energy supply from renewable sources, time-variant energy prices, and the difficulty in predicting energy demand resulting from the high operational complexity. Similarly, a review by Bakar et al. (2021) emphasized the growing significance of energy management in future ports. This paper conducted a review of energy-aware planning problems within container terminals. The focus of the review is the on-demand response for integrated planning problems involving multiple energy loads.

Demand response relates to shifting the energy demand to low-demand periods by solving integrated operations planning problems involving multiple energy demand generators. Several studies concentrate on demand response with a single load. In a study by van Duin et al. (2018), the demand response of reefers was considered to lower the peak load. Geerlings et al. (2018) and Kermani et al. (2018) investigated strategies to reduce the peak loads of quay cranes (QCs). These two loads account for the majority of peak demand in container terminals. Another intriguing application of demand response is the use of vehicle-to-grid (V2G) charging for automated guided vehicles (AGVs) within the terminal. Schmidt et al. (2015) explored various business cases for V2G charging with AGVs, and Harnischmacher et al. (2023) further investigated the use of AGVs for frequency containment reserves. Tang et al. (2025a) studied smart charging with demand response and energy peak shaving for reefer containers with Internet-of-Things. As the trend towards electrification continues within terminals, ships become a significant electric load through onshore power supply. Yu et al. (2022b) performed a multi-objective optimization considering energy-related costs and emissions for berth allocation and quay crane assignment (BAQAP) problems. Similarly, He (2016) quantified the impact of energy-aware planning on operational costs by comparing optimization results of an energy-saving strategy (with a constant electricity price) with a time-saving strategy (with no electricity-related cost). Additionally, the effect of energy-aware planning on yard cranes (He et al., 2015a) and automated guided vehicle (He et al., 2015b) scheduling was also investigated. Recent developments in energy system optimization and intelligent energy management, including battery thermal management systems (Oyewola et al., 2024) and real-time grid security (Xiao et al., 2024), underscore the growing importance of integrated control strategies across domains.

Literature specifically focusing on energy-aware integrated planning problems involving multiple energy loads is scarce. Table 2.1 provides an overview of the most relevant literature, categorized based on the pricing schemes considered for price-based demand response programs. Table 2.2 presents all the sources of energy demand and supply considered in these studies.

Kanellos (2017, 2019) and other scholars (Kanellos et al., 2019) conducted multiple studies on demand response in container terminals, developing a multi-agent system where different loads communicate with each other. However, these studies do not model detailed operations planning for scheduling activities at the container terminal. Mao et al. (2022) focused on loads within an integrated energy system encompassing electricity, heat, and cooling demands, employing mixed-integer programming optimization. Pu et al. (2020) also addressed an integrated energy system but estimated the total amount of fixed, reducible, and shiftable loads. In the study of Iris & Lam (2021), an integrated operations planning and energy management problem was solved using stochastic mixed-integer optimization. This chapter significantly differs from these studies as we model and obtain detailed demand response through operations planning for AGVs, QCs, YCs, reefer containers and ships with different pricing schemes and uncertainty in both energy demand and supply sides, as presented in Table 2.1 and 2.2.

When proposing energy-aware operations planning, authors often stress the importance of considering the stochastic nature of both energy demand and supply. However, only a very limited number of studies have investigated this topic, with the study of Iris & Lam (2021) as an example. It considered multiple scenarios of solar energy production to account for stochastic electricity supply, without the consideration of uncertainty in the energy demand or port operations. Sarantakos et al. (2024) presented a joint logistics-electric framework for optimal operation and power management of electrified ports, considering multiple uncertainties in the arrival time of vessels, network demand, and renewable power generation. Zhao et al. (2024) constructed a coordinative optimization problem based on the logistics-energy coupling characteristics with the aim of minimizing the port operation cost, the demand response capacity of port flexible loads and the operation constraints of an integrated energy system. Xiong et al. (2024) proposed a joint scheduling method that considers the impact of tidal patterns on the period and intensity of port operations. The method takes advantage of the strong correlations between renewable energy (solar, wind and tidal) and multi-class load to support the port microgrid operator in determining the most cost-effective scheduling of energy supply and flexible loads during port activities. The research gap lies in energy-aware operations (combined with energy management) with multiple loads considering uncertainty in both supply and demand. This chapter incorporates uncertain ship arrival times and uncertain energy prices to represent the uncertainty in the energy demand side and supply side, respectively.

2.3 Problem description

This chapter aims to assess the potential of demand response by modeling operations planning and energy flows between different components in the container terminal. Different pricing schemes, namely no pricing, single pricing, and real-time pricing, are considered to quantify the impact that demand response has on the operations in the terminal.

To model the problem, we employ a two-stage stochastic programming approach that incorporates uncertainties. Stochastic problems are those optimization problems where some of the parameters of the model are uncertain. Uncertainty can be defined by random variables in the form of probability distributions or densities. A stage of a given planning horizon is a set of consecutive time periods where the realization of one or more stochastic (i.e., uncertain) events take place. At the end of a stage, decisions are taken, considering the specific outcomes of the stochastic events of this and previous stages. In the two-stage stochastic programming, the first stage, known as the "here-and-now" decision, takes place before the values of the uncertain parameters are known.The second stage, the "wait-and-see" decision, is the response to the realization of these uncertain parameters. The formulation below gives the general mathematical formulation of a two-stage stochastic optimization with recourse:

$$
\begin{aligned}
\min_{\boldsymbol{x}} \quad & f^F(\boldsymbol{x}) + \mathbb{E}_P[f^S(\boldsymbol{x}, \boldsymbol{y}_\xi, \xi)], && (2.1a)\\
\text{s.t.} \quad & \boldsymbol{A}\boldsymbol{x} = \boldsymbol{b}, && (2.1b)\\
\text{where} \quad & f^S(\boldsymbol{x}, \boldsymbol{y}_\xi, \xi) = \min_{\boldsymbol{y}_\xi} \quad q(\boldsymbol{y}_\xi, \xi), && (2.1c)\\
\text{s.t.} \quad & \boldsymbol{T}_\xi \boldsymbol{x} + \boldsymbol{W}_\xi \boldsymbol{y}_\xi = \boldsymbol{h}_\xi. && (2.1d)
\end{aligned}
$$

In formulation (2.1), ξ is the realization of the uncertain parameters. $\mathbb{E}_P$ is the expected value of all realisations of ξ. $f\{\cdot\}$ is the objective function of first stage (F) or second stage (S). $\boldsymbol{A}, \boldsymbol{T}, \boldsymbol{W}$ are the coefficient matrices. $\boldsymbol{b}, \boldsymbol{h}_\xi$ are right-hand-side vectors. $\boldsymbol{x}$ are the first stage decision variables and $\boldsymbol{y}_\xi$ are the second stage decision variables. In linear formulation, $f^F(\boldsymbol{x})$ can be written as $\boldsymbol{c}^\top \boldsymbol{x}$, and $q(\boldsymbol{y}_\xi, \xi)$ can be written as $\sum_\xi p_\xi(\boldsymbol{q}_\xi^\top \boldsymbol{y}_\xi)$ (p_ξ is the probability for each scenario).

Table 2.1: Area of focus and pricing scheme of literature closely related to energy-aware integrated planning problems

		Uncertainty		Pricing scheme			
Reference	Focus	D	S	NP	SP	TOU	RTP
Gennitsaris & Kanellos (2019)	Demand response					√	
Iris & Lam (2021)	Port microgrid		√		√	√	√
Sarantakos et al. (2024)	Energy system	√	√				
Kanellos (2019)	Demand response					√	
Kanellos (2017)	Demand response			√			
Kanellos et al. (2019)	Demand response					√	
Mao et al. (2022)	Integrated energy system				√		√
Pu et al. (2020)	Integrated energy system			√		√	
Xiong et al. (2024)	Port microgrid					√	
Zhao et al. (2024)	Integrated energy system & Demand response	√	√			√	
This chapter	Demand response	√	√	√	√		√

Uncertainty: D (Electricity demand), S (Electricity supply)
Pricing scheme: NP (No pricing), SP (Single pricing), TOU (Time-of-use pricing), RTP (Real-time pricing)

Table 2.2: Energy demand and supply in the literature closely related to energy-aware integrated planning problems

	Demand							Supply				
Reference	SH	QC	YC	AGV	RE	ESS	Other	EG	WT	PV	ESS	Other
Gennitsaris & Kanellos (2019)	√				√			√	√			
Iris & Lam (2021)	√	√	√		√	√		√		√	√	
Sarantakos et al. (2024)	√	√	√	√	√			√	√	√	√	
Kanellos (2019)	√			√	√			√				
Kanellos (2017)				√	√			√	√			
Kanellos et al. (2019)	√			√	√			√				
Mao et al. (2022)	√				√	√	√	√	√	√	√	√
Pu et al. (2020)						√	√	√				√
Xiong et al. (2024)	√	√	√		√		√	√	√	√	√	√
Zhao et al. (2024)	√	√	√		√		√	√	√			√
This chapter	√	√	√	√	√			√				

Demand: SH (Ship), QC (Quay crane), YC (Yard crane), AGV (Automated guided vehicle), RE (Reefer), ESS (Energy storage system)
Supply: EG (Electricity grid), WT (Wind turbine), PV (Photovoltaic panel)

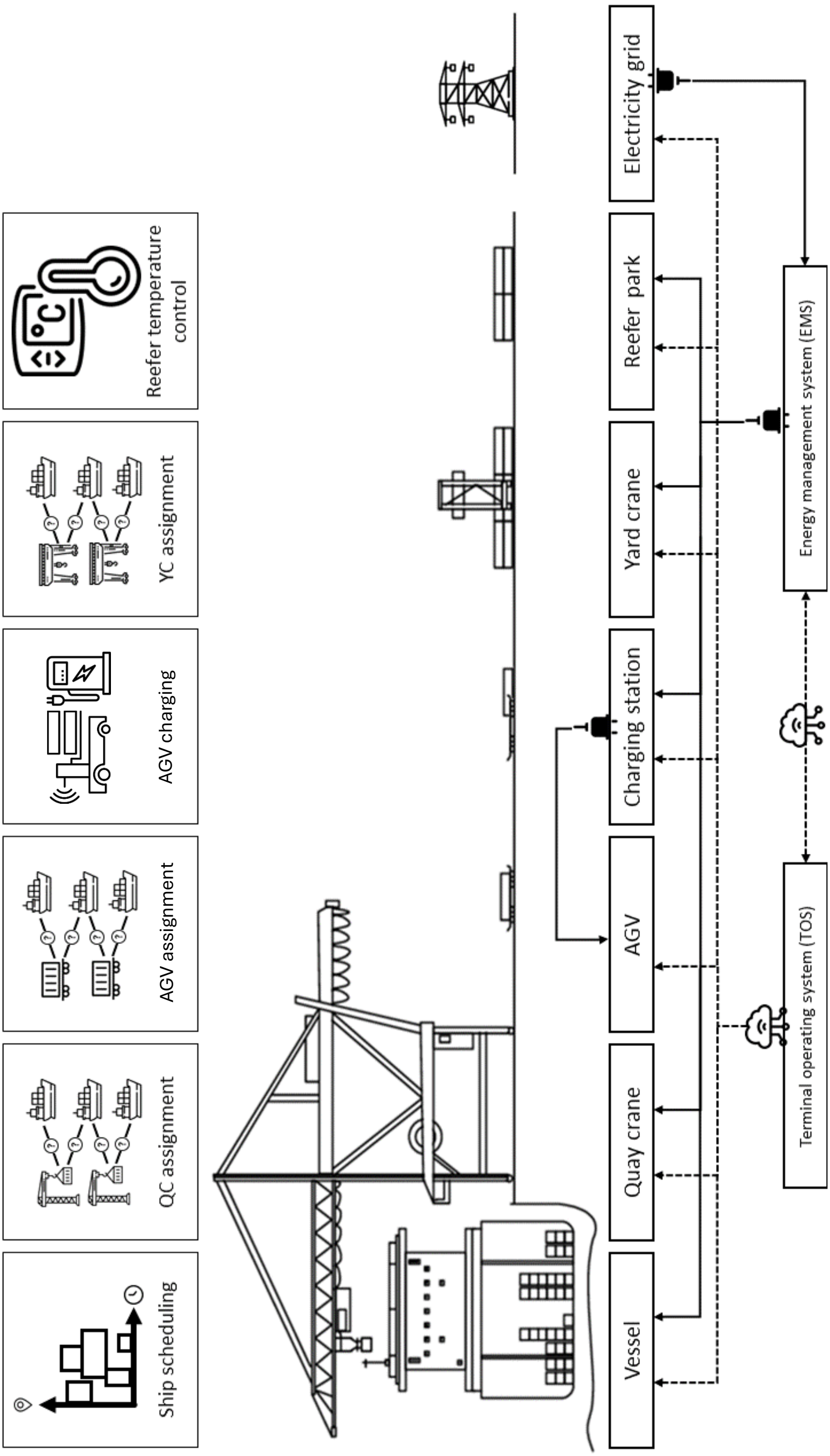

Figure 2.1: Overview of operations planning problems, energy flows and information flows in a container terminal

In the problem studied, we consider the energy consumption of vessels, quay cranes (QCs), yard cranes (YCs), reefers, and automated guided vehicles (AGVs) on the demand side. On the supply side, the energy is purchased from the electricity grid. Various operational research problems are included to accurately describe the operations within the terminal. We consider different operations including ship scheduling at berths, QC assignment, AGV assignment, YC assignment, AGV charging, and reefer temperature control. Figure 2.1 shows the energy and information flow between all the loads and the electricity grid. The information flows are controlled by the terminal operating system (TOS), while the electricity flows are coordinated by the energy management system (EMS). The terminal operating and energy management systems exchange information to match the operational and electrical requirements.

Five electric loads are considered in the problem, namely ships, QCs, YCs, AGVs and reefer containers in the yard. Ships consume energy through onshore power supply while berthed, with a constant consumption rate per hour. The energy consumption of the QCs and YCs depends on the handling rate (h_m) of each equipment m. The energy demand of AGVs materializes through the charging of the AGV batteries. All AGVs are modeled as one large battery that is depleted based on the handling rate of the AGVs.

The reefer containers consume the energy required for cooling. In the yard, all reefer containers are modeled as one large cold storage tank, with heat transfer to the ambient temperature. Container temperature is allowed to fluctuate between specific bounds. The number of reefers present in the yard is assumed to be constant.

In the model, N vessels arrive at the terminal over H hours. For every vessel, a start time S and a finish time F are decided, which results in the berthing duration. Each vessel has a specific container load of d that needs to be handled during berthing. As it is customary in berth assignment problems, a ship is allowed to berth if there is available space on the quay. Once berthed, a number of QCs, YCs and AGVs are assigned to the ship every hour to load and unload the containers. The handling rate p set is determined based on the minimum and maximum handling capacity of QCs, YCs and AGVs.

Demand response (DR) is defined as a tariff or program developed to motivate the change in energy consumption of end-users, in response to changes in the price of electricity over time, or to give incentive payments designed to induce lower electricity use at times of high market prices or when grid reliability is jeopardized (Patnam & Pindoriya, 2021). The DR considered in this chapter belongs to the category of economic-based demand response, where the system operator adopts various electricity pricing mechanisms, such as real-time pricing (RTP), critical peak pricing (CPP), and time-of-use (TOU), to influence the energy consumption behavior of different user groups, including residential, commercial, and industrial consumers. Since electricity price plays a significant role in energy usage decisions, users may adjust their consumption patterns according to the applied pricing scheme and their own operational or comfort preferences. The impact of different pricing schemes (no pricing, single pricing and real-time pricing) is investigated in some studies (Palensky & Dietrich, 2011; Patnam & Pindoriya, 2021).

The problem contains sources of uncertainty, both in the supply and demand of electricity. The uncertainty in supply is presented by electricity prices, while the uncertainty in demand is presented by ship arrival times. Notably, the prices of electricity and the arrival times of ships are the most significant uncertainties when optimizing a container terminal's operations planning. The uncertainty of the arrival times and electricity prices are considered to be independent of each other.

We formulate the problem as a two-stage optimization problem with uncertainties taken into account. The first-stage decisions are taken one day ahead of when the operations are performed. A baseline schedule is created where the expected start time S_i^{da} for every vessel and the expected energy consumption P_t^{da} for every hour are decided upon in the first stage. The decisions in the second stage are made in real time just before performing the operations. The baseline decision made in the first stage can be changed by deciding upon berthing start time in scenario w ($S_{i,w}$) and power used in scenario w ($P_{t,w}$). The second-stage objective is based on the expected value of all the different realizations. Different weights π_ξ are assigned to every realization based on the likelihood of occurrence.

A time step of one hour is considered in this model. Electricity prices from the market one day ahead of the actual operations are obtained every hour. Additionally, the energy demand of different loads is averaged over an hour assuming a constant consumption within one hour. For every hour, the amount of energy consumed is equal to the amount of energy supplied by the grid.

The real-time pricing model is present today (in e.g., Germany, or the Netherlands) under the name of dynamic pricing. If an energy customer opts for dynamic pricing (what we call real-pricing in this work) they will be exposed to the hourly wholesale market price. In this case, the customer is exposed to the fluctuations of the electricity price at the national level and will be required to remunerate their consumed energy under such fluctuating price. In contrast, what we call a single-pricing scheme is a fixed-price contract for a certain duration of time. When the customer chooses a fixed-price contract they have a guaranteed price for every unit of energy they consume.

To explore the impact of DR, we compare the ship berthing schedule, energy consumption patterns and other related variables under the real-time pricing (time-variant pricing during the planning horizon) scheme with those under no-pricing and single-pricing schemes in Section 2.6. The no-pricing scheme excludes cost-related factors when modeling, and the single-pricing scheme applies a single energy price for the entire day. The no-pricing and single-pricing schemes therefore do not include uncertain considerations. On the contrary, the real-time pricing scheme employs different energy prices for each time unit (usually hour) and considers uncertainty presented by energy prices in various scenarios.

The objective is to minimize the ship's lateness costs and energy-related costs. Deviations from the baseline schedule are minimized by considering rescheduling costs and power imbalance costs. A note on the institutional scope of the model is in order. The objective function minimizes the combined lateness, rescheduling, day-ahead energy purchase, and imbalance costs associated with terminal operations. In practice, exposure to wholesale electricity prices and imbalance settlement costs depends on the contractual arrangement between the terminal operator, the grid operator, and the balance-responsible party. In highly integrated ports, where the terminal operator directly procures electricity and bears imbalance risk, the model applies most naturally. In ports where these costs are fully passed through to shipping lines or other terminal customers, the direct financial incentive for the terminal operator to implement the proposed optimization is reduced, even though total system costs would still be lowered. The model is therefore best interpreted as identifying the total system-level savings available from energy-aware terminal planning; realizing these savings in a given port depends on the allocation of electricity and imbalance costs, on which actor controls the flexible loads, and on which actor captures the resulting savings. Chapter 5 returns to this point in the practice implications.

2.4 Mathematical model

2.4.1 Assumptions

The following assumptions are made in this problem:

1. Ships only use constant onshore power when they are berthed.
2. The berthing location of a ship does not influence energy consumption.
3. The hoisting and lowering operations of QCs consume the same amount of energy for each container, which is the same case for YCs.
4. The energy consumption of QCs, YCs and AGVs only depends on the handling rate.
5. The number of reefers in the yard is constant throughout the day.
6. The reefer cooling requirements are the same for every reefer container.
7. All the reefer containers in the storage yard can be modeled as a large reefer container.
8. The reefer energy consumption is based on the constant ambient temperature per time period.
9. The AGV fleet can be modeled with one large battery.
10. The energy consumption of the container terminal does not influence the electricity price.

2.4.2 Model formulation

In this section, a mixed-integer linear programming model is formulated for the problem described above. Table 2.3, 2.4 and 2.5 present an overview of all sets, parameters and decision variables used in the model.

Table 2.4: Parameters

Parameters	Description
k_m	The number of machinery $m \in M$ available.
h_m	Handling rate of machinery m in containers per hour.
d_i	The total demand of containers to be handled (loaded + unloaded) for ship $i \in V$.
$u_{p,m}$	The number of machinery of type m used in handling rate pattern p.
l_i^{ship}	The quay length that ship i takes up.
l^{total}	The total length of the quay.

Parameters	Description
eat_i	Expected arrival time of vessel $i \in V$.
eft_i	Expected berthing finishing time of vessel $i \in V$.
$a_{i,w}$	Actual arrival time of vessel $i \in V$ in scenario $w \in S$.
e^{ship}	Energy consumption of a ship for onshore power for one hour.
$e_m^{\text{machinery}}$	Energy consumption of machinery m for operating for one hour.
e^{charge}	Energy consumed by one charger when charging an AGV every time unit.
$e^{\text{charge,max}}$	Maximum energy consumed by all chargers when charging AGVs every time unit.
b^{min}	Minimum battery level allowed for an AGV.
b^{max}	Maximum battery level allowed for an AGV.
η^{charge}	Charging efficiency.
$e^{\text{reefer,max}}$	Maximum energy consumption of all reefer connections every time unit.
tc^{min}	Minimum temperature allowed for reefer containers.
tc^{max}	Maximum temperature allowed for reefer containers.
η^{reefer}	Cooling efficiency.
ta_t	Ambient temperature at time period t.
m	Mass of the reefer.
cp	Specific heat capacity of a reefer.
u	Heat transfer coefficient of a reefer.
a	Area of the reefer.
$c_{t,w}^{da}$	Hourly electricity price at time period t in scenario w.
c_i^{late}	Penalty cost of exceeding the expected finishing time (EFT) for vessel $i \in V$ for one hour.
c_i^{resch}	Cost of changing the initial schedule by one hour, a coefficient multiplying c_i^{late}.
c^{sur}	Cost of having a surplus of energy, a coefficient multiplying $c_{t,w}^{da}$.
c^{shor}	Cost of having a shortage of energy, a coefficient multiplying $c_{t,w}^{da}$.
M	A large positive number.
π_w	Probability of scenario w's realization.

The objective function below is designed to jointly minimize scheduling-related and energy-related costs in the terminal operations system:

$$\min \sum_{w\in S} \pi_w \Bigg(\sum_{i\in V} c_i^{late} L_{i,w} + \sum_{i\in V} c^{resch} c_i^{late} (S_{i,w}^{late} + S_{i,w}^{early}) + \sum_{t\in T} c_{t,w}^{da} P_t^{da} + \sum_{t\in T} c_{t,w}^{da} (c^{shor} P_{t,w}^{shor} - c^{sur} P_{t,w}^{sur}) \Bigg). \tag{2.2}$$

The first two components of the objective function (2.2) minimize the cost of lateness for all ships ($\sum_{i\in V} c_i^{late} L_{i,w}$) and the cost associated with deviations from the baseline schedule $\sum_{i\in V} c^{resch} c_i^{late} (S_{i,w}^{late} + S_{i,w}^{early})$. The subsequent two elements aim to minimize the cost connected to energy purchase on the day-ahead market ($\sum_{t\in T} c_{t,w}^{da} P_t^{da}$) and the cost associated with power imbalances in both shortage and surplus ($\sum_{t\in T} c_{t,w}^{da} (c^{shor} P_{t,w}^{shor} - c^{sur} P_{t,w}^{sur})$). These costs are calculated for each scenario and the weighted average of all scenarios is minimized. The model is subject to the following set of constraints.

Table 2.3: Sets

Sets	Description
V	Set of vessels to be served, $i \in 1,2,\ldots,N$, where N is the number of vessels to be served.
T	Set of time periods, $t \in 0,1,\ldots,t^{max}-1$, where t^{max} is the number of hours considered.
P_i	Set of possible handling rate pattern p that can be assigned to a ship $i \in V$.
M	Types of machinery present in the terminal, $m \in \{QC, YC, AGV\}$.
S	Set of scenarios, $w \in S$.

Table 2.5: Decision Variables

Decision variables	Description
S_i^{da}	Scheduled berthing start time of vessel $i \in V$ in the baseline plan.
$S_{i,w}$	Berthing start time of vessel $i \in V$ in scenario $w \in S$.
$S_{i,w}^{early}$	Time the vessel $i \in V$ arrives ahead of schedule in scenario $w \in S$.
$S_{i,w}^{late}$	Time the vessel $i \in V$ arrives behind schedule in scenario $w \in S$.
$F_{i,w}$	Berthing end time (time when handling ends) of vessel $i \in V$ in scenario $w \in S$.
$L_{i,w}$	Lateness of operations for ship $i \in V$ in scenario $w \in S$.
$A_{i,t,w} \in \{0,1\}$	1 if vessel $i \in V$ is assigned at to a berth in time period t in scenario $w \in S$, 0 otherwise.
$H_{i,p,t,w} \in \{0,1\}$	1 if pattern p of quay cranes, yard cranes and AGVs is assigned to serve vessel $i \in V$ at time period t in scenario $w \in S$, 0 otherwise.
$B_{t,w}$	Battery level at time period t in scenario $w \in S$.
$TC_{t,w}$	Reefer temperature at time period t in scenario $w \in S$.
$E_{t,w}^{charge}$	Energy consumed to charge AGVs at time period t in scenario $w \in S$.
$E_{t,w}^{reefer}$	Energy consumed to cool the reefers at time period t in scenario $w \in S$.
$P_{t,w}$	Power used from the utility grid at time period t in scenario $w \in S$.
P_t^{da}	Power purchased at the day-ahead market for time period t in the baseline plan.
$P_{t,w}^{sur}$	Power surplus at time period t in scenario $w \in S$.
$P_{t,w}^{shor}$	Power shortage at time period t in scenario $w \in S$.
$IM_{t,w}^{state} \in \{0,1\}$	Imbalance state, 1 if there is a surplus and 0 if there is a deficit in scenario $w \in S$

The constraint below ensures the energy consumed by the ships, quay cranes (QCs), yard cranes (YCs), automated guided vehicle (AGV) charging, and reefer cooling matches the power drawn from the grid:

$$\sum_{i \in V} e^{ship} A_{i,t,w} + \sum_{m \in M} \sum_{i \in V} \sum_{p \in P_i} u_{p,m} H_{i,p,t,w} e_m^{machinery} + E_{t,w}^{reefer} + E_{t,w}^{charge} = P_{t,w}, \quad m = \{QC, YC\} \; \forall t \in T, \forall w \in S. \tag{2.3}$$

The constraints below describe the vessel scheduling process in the terminal:

$$S_{i,w} \geq a_{i,w}, \qquad \forall i \in V, \forall w \in S, \tag{2.4}$$

$$L_{i,w} \geq F_{i,w} - eft_i, \qquad \forall i \in V, \forall w \in S, \tag{2.5}$$

$$\sum_{t \in T} A_{i,t,w} = F_{i,w} - S_{i,w}, \qquad \forall i \in V, \forall w \in S, \tag{2.6}$$

$$(t+1)A_{i,t,w} \leq F_{i,w}, \qquad \forall i \in V, \forall t \in T, \forall w \in S, \tag{2.7}$$

$$t\, A_{i,t,w} + t^{max}\, (1 - A_{i,t,w}) \geq S_{i,w}, \qquad \forall i \in V, \forall t \in T, \forall w \in S, \tag{2.8}$$

$$\sum_{i \in V} A_{i,t,w}\, l_i^{ship} \leq l^{total}, \qquad \forall t \in T, \forall w \in S. \tag{2.9}$$

Constraint (2.4) guarantees that the start time of vessel operation is either equal to or later than its expected arrival time. Constraint (2.5) defines the lateness time, which is the time a ship departs after the expected departure time. To ensure that the ships are berthed during every hour between the berthing start time and end time, constraints (2.6), (2.7) and (2.8) are introduced. Constraint (2.9) prevents overcrowding of the berth by ensuring that the total length of all berthed vessels is shorter than the quay length.

The following constraints describe the handling capacity assignment of cargo handling equipment:

$$\sum_{p \in P_i} H_{i,p,t,w} = A_{i,t,w}, \qquad \forall i \in V, \forall t \in T, \forall w \in S, \tag{2.10}$$

$$\sum_{t \in T} \sum_{p \in P_i} pH_{i,p,t,w} \geq d_i, \qquad \forall i \in V, \forall t \in T, \forall w \in S, \tag{2.11}$$

$$\sum_{i \in V} \sum_{p \in P_i} u_{p,m} H_{i,p,t,w} \leq k_m, \qquad \forall t \in T, \forall m \in M, \forall w \in S. \tag{2.12}$$

A handling rate is assigned to every ship for every hour it is berthed, which is accomplished by constraints (2.10) and (2.11). Constraint (2.12) guarantees that the machinery capacity is not exceeded for QCs, YCs, and AGVs.

The following constraints describe the deviations from the day-ahead schedule and the modeling of power imbalances under different operational scenarios:

$$S_{i,w}^{late} - S_{i,w}^{early} = S_{i,w} - S_i^{da}, \qquad \forall i \in V, \forall w \in S, \tag{2.13}$$

$$P_{t,w}^{shor} - P_{t,w}^{sur} = P_{t,w} - P_t^{da}, \qquad \forall t \in T, \forall w \in S, \tag{2.14}$$

$$P_{t,w}^{sur} \leq M \cdot IM_{t,w}^{state}, \qquad \forall t \in T, \forall w \in S, \tag{2.15}$$

$$P_{t,w}^{shor} \leq M \cdot (1 - IM_{t,w}^{state}), \qquad \forall t \in T, \forall w \in S. \tag{2.16}$$

A day-ahead schedule is formulated for both the arrivals of the ships and power consumption. Constraint (2.13) states the difference between the actual start time in each scenario and the day-ahead scheduled start time is equivalent to the deviation of the start time. Similarly, constraint (2.14) defines the energy consumption surplus and shortage. It is impossible to have a surplus and a deficit in energy consumption simultaneously. A binary variable $IM_{t,w}^{state}$ is used to keep track of whether there is a surplus or shortage, and constraints (2.15) and (2.16) model this relationship.

The model also incorporates charging and battery management constraints for AGVs, as presented by the constraints below:

$$E_{t,w}^{charge} \leq e^{charge,max}, \qquad \forall t \in T, \forall w \in S, \tag{2.17}$$

$$\begin{aligned} &E_{t,w}^{charge} \leq (k_m - \sum_{i \in V} \sum_{p \in P_i} u_{p,m} \cdot H_{i,p,t,w}) \cdot e^{charge}, \\ &m = \{AGV\}, \ \forall t \in T, \ \forall w \in S, \end{aligned} \tag{2.18}$$

$$b^{min} \leq B_{t,w} \leq b^{max}, \qquad \forall t \in T, \ \forall w \in S. \tag{2.19}$$

Constraints (2.17) – (2.19) concern the limits for energy used to charge AGVs and the AGV battery level. Constraints (2.17) and (2.18) describe that the total power used to charge the AGVs is constrained by the maximum energy limit and the number of AGVs available for charging. Constraint (2.19) ensures that the battery energy level always remains within the minimum and maximum allowed values.

Battery charging and discharging dynamics of AGVs are modeled through the constraints below:

$$\begin{aligned} &B_{t,w} = B_{t-1,w} + \eta^{charge} \cdot E_{t,w}^{charge} - \sum_{i \in V} \sum_{p \in P_i} e_m^{machinery} \cdot u_{p,m} \cdot H_{i,p,t,w}, \\ &m = \{AGV\}, \ \forall t \in T \setminus \{0\}, \ \forall w \in S, \end{aligned} \tag{2.20}$$

$$\begin{aligned} &B_{t,w} = (b^{min} + b^{max})/2 + \eta^{charge} \cdot E_{t,w}^{charge} - \sum_{i \in V} \sum_{p \in P_i} e_m^{machinery} \cdot u_{p,m} \cdot H_{i,p,t,w}, \\ &m = \{AGV\}, \ t = \{0\}, \ \forall w \in S, \end{aligned} \tag{2.21}$$

$$\begin{aligned} &\sum_{t \in T} \eta^{charge} \cdot E_{t,w}^{charge} = \sum_{t \in T} \sum_{i \in V} \sum_{p \in P_i} e_m^{machinery} \cdot u_{p,m} \cdot H_{i,p,t,w}, \\ &m = \{AGV\}, \ \forall w \in S. \end{aligned} \tag{2.22}$$

These constraints monitor the AGV battery level and guarantee the energy consumed equals the energy charged. Constraints (2.20) and (2.21) capture the principle that the state of battery charge fluctuates based on the amount of energy charged and discharged for time periods 1 to H and time period 0, respectively. We assume the initial battery level at the beginning is $(b^{min}+b^{max})/2$. Constraint (2.22) asserts that the amount of energy consumed equals the amount of energy charged.

The thermal dynamics and cooling energy consumption of reefer containers are modeled through the formulations below:

$$tc^{min} \leq TC_{t,w} \leq tc^{max}, \qquad \forall t \in T, \forall w \in S, \tag{2.23}$$

$$E_{t,w}^{reefer} \leq e^{reefer,max}, \qquad \forall t \in T, \forall w \in S, \tag{2.24}$$

$$\begin{aligned} & m \cdot cp \cdot (TC_{t,w} - TC_{t-1,w}) = u \cdot a \cdot (ta_t - (tc^{min} + tc^{max})/2) - \\ & \eta^{reefer} \cdot E_{t,w}^{reefer}, \qquad \forall t \in T \setminus \{0\}, \forall w \in S, \end{aligned} \tag{2.25}$$

$$\begin{aligned} & m \cdot cp \cdot (TC_{t,w} - (tc^{min} + tc^{max})/2) = u \cdot a \cdot (ta_t - (tc^{min} + tc^{max})/2) - \\ & \eta^{reefer} \cdot E_{t,w}^{reefer}, \qquad t = \{0\}, \forall w \in S, \end{aligned} \tag{2.26}$$

$$\sum_{t \in T} u \cdot a \cdot (ta_t - (tc^{min} + tc^{max})/2) = \sum_{t \in T} \eta^{reefer} \cdot E_{t,w}^{reefer}, \qquad \forall w \in S. \tag{2.27}$$

Constraint (2.23) indicates that the temperature of the reefers, represented by $TC_{t,w}$, should always be within the minimum and maximum temperature to ensure the good quality of the stored content. The energy consumed by the reefers at any time should not exceed the maximum rated power of all the reefer connections, as dictated by constraint (2.24). The reefers lose heat to the environment through convection. This heat loss depends on the temperature difference between the container and the environment, both of which are assumed to be constant for every hour. Constraint (2.25) is the cooling balance constraint, which stipulates that the temperature change of the reefer container depends on the heat loss and the cooling energy supplied. Constraint (2.26) requires the same cooling balance for the initial time period. Constraint (2.27) is the reefer energy constraint, which ensures that the total energy lost through heat transfer equals the total energy consumed by cooling. These constraints manage the energy consumption of ships, QCs, YCs, AGVs and reefer containers while adhering to the constraints based on the operations planning. We also add the domains of all variables in Table 2.5.

2.5 Solution procedure

This section explains the algorithmic procedure to obtain the solutions. First, the stochastic decomposition method, progressive hedging, is introduced. Then, we explain how the scenarios are obtained.

2.5.1 Stochastic decomposition with progressive hedging

Optimization problems under uncertainty are notoriously complex to solve, both in theory and practice. A practical method to tackle these problems involves the use of decomposition strategies in stochastic programming models. This process breaks down the overarching issue into manageable sub-problems, simplifying the overall optimization process and reducing computational complexity.

To handle this complexity efficiently, we implement a progressive hedging (PH) algorithm based on the original PH algorithm introduced by Rockafellar & Wets (1991). The algorithmic steps are presented in pseudo-code in Algorithm 2.1. The PH algorithm is based on the split-variable formulation of formulation (2.1), which can be compactly written as formulation (2.28):

$$
\begin{aligned}
\min \quad & f^F(\boldsymbol{x}_\xi) + \mathbb{E}_P[q(\boldsymbol{y}_\xi, \xi)], && (2.28a)\\
\text{s.t.} \quad & \boldsymbol{A}\boldsymbol{x}_\xi = \boldsymbol{b}, \quad \forall \xi \in \Xi, && (2.28b)\\
& \boldsymbol{T}_\xi \boldsymbol{x}_\xi + \boldsymbol{W}_\xi \boldsymbol{y}_\xi = \boldsymbol{h}_\xi, \quad \forall \xi \in \Xi, && (2.28c)\\
& \boldsymbol{x}_\xi - \bar{\boldsymbol{x}} = 0, \quad \forall \xi \in \Xi. && (2.28d)
\end{aligned}
$$

The PH algorithm is a practical way of splitting a large problem into smaller sub problems and solving them iteratively, thus possibly reducing the solving time considerably. The idea of the PH algorithm is to aggregate the solutions of subproblems, where artificial costs have been added. These added costs enforce that the aggregated solutions become non-anticipative and are updated in every iteration of the algorithm (Kaisermayer et al., 2021). The non-anticipativity constraint (2.28d) enforces that all decisions made in the first stage must be the same across all scenarios. The PH algorithm is based on the idea of relaxing the non-anticipativity constraint, solving all scenario subproblems separately, and then iteratively achieving consensus on the non-anticipative first-stage solution. The mathematical model presented in formulation (2.1) is decomposed into several independent optimizations for every scenario, with $\boldsymbol{x}_\xi^\nu, \boldsymbol{y}_\xi^\nu$ representing the decision variable of the first and second stages, respectively. $\boldsymbol{x}_\xi^\nu$ includes S_i^{da} and P_t^{da} in this model, and $\boldsymbol{y}_\xi^\nu$ represents all the other decision variables.

Algorithm 2.1 first sets the initial values for the iteration counter ν and the penalty parameter $\rho > 0$, and then solves the model for the first time. The initial mean value of $\boldsymbol{x}_\xi$ and the initial dual prices are calculated. In the following steps, the mathematical model of this problem is iteratively solved, with the mean value of $\boldsymbol{x}_\xi$ and dual prices λ_ξ (also called Lagrange multipliers) updated in every iteration. The model is solved in parallel for each scenario. The dual price is represented by λ_ξ^ν, and the likelihood of occurrence of each scenario is represented by π_ξ. ρ is the penalty experienced for deviations of the first-stage decision variable from the mean. The core idea of progressive hedging can be motivated by the augmented Lagrangian method, which combines classical Lagrangian methods and the penalty function. The problem is solved iteratively for ν times until sufficient convergence of $\sum_{\xi\in\Xi} \pi_\xi \|\boldsymbol{x}_\xi^{(\nu+1)} - \bar{\boldsymbol{x}}^{(\nu+1)}\|_2 < \delta_0$ is met or the maximum number of iterations is reached.

Algorithm 2.1 Progressive Hedging for a Two-Stage Stochastic Optimization

Initialization: Set iteration counter $\nu = 0$ and penalty parameter ρ;
for each $\xi \in \Xi$ **do**
Solve the scenario subproblem

$$(x_\xi^{(0)}, y_\xi^{(0)}) \in \arg \min_{x_\xi, y_\xi \in X(\xi)} f^F(x_\xi) + f^S(x_\xi, y_\xi, \xi)$$

end for
Compute the initial solution:

$$\bar{x}^{(0)} = \sum_{\xi \in \Xi} \pi_\xi x_\xi^{(0)}$$

and the initial duals:

$$\lambda_\xi^{(0)} = \rho(\boldsymbol{x}_\xi^{(0)} - \bar{\boldsymbol{x}}^{(0)}), \quad \forall \xi \in \Xi$$

while $\left(\sum_{\xi \in \Xi} \pi_\xi \| x_\xi^{(\nu+1)} - \bar{x}^{(\nu+1)} \|_2 \right) > \delta_0$ **or** $\nu \le \nu_{\max}$ **do**
for each $\xi \in \Xi$ **do**
Solve the augmented scenario subproblem

$$\boldsymbol{x}_\xi^{(\nu+1)}, \boldsymbol{y}_\xi^{(\nu+1)} = \arg\min_{\boldsymbol{x}_\xi, \boldsymbol{y}_\xi \in \boldsymbol{X}(\xi)} \quad f^F(\boldsymbol{x}_\xi) + f^S(\boldsymbol{x}_\xi, \boldsymbol{y}_\xi, \xi) + \lambda_\xi^{(\nu)} \boldsymbol{x}_\xi + \frac{\rho}{2} \| \boldsymbol{x}_\xi - \bar{\boldsymbol{x}}^{(\nu)} \|_2^2$$

end for
Update solution

$$\bar{x}^{(\nu+1)} = \sum_{\xi \in \Xi} \pi_\xi x_\xi^{(\nu+1)}$$

Update dual variables

$$\lambda_\xi^{(\nu+1)} = \lambda_\xi^{(\nu)} + \rho(x_\xi^{(\nu+1)} - \bar{x}^{(\nu+1)})$$

$\nu \leftarrow \nu + 1$
end while

2.5.2 Scenario generation

Generating and reducing scenarios accurately is crucial in stochastic programming. For efficiency and accuracy, a balance between sample size and complexity is sought, with a preference for the least number of samples (Roald et al., 2023).

For ship arrival times, we observe historical data and find that the estimated arrival time generally follows a uniform distribution. A quasi-random sampling technique, specifically Halton sampling, is utilized to obtain distinct scenarios. The arrival distribution is obtained from Kolley et al. (2023). The actual arrival time is generated by adding the uniformly distributed estimated arrival time to the deviation time obtained from quasi-random sampling that conforms to a normal distribution. This method promotes a uniform distribution and distinct scenarios, leading to more accurate optimization results. The arrival times are rounded to the nearest hour, with corresponding probabilities for each hour.

In terms of electricity price scenarios, an approach based on the clustering method in Crespo-Vazquez et al. (2018) is used. Using historical data from the German day-ahead market, a K-means clustering algorithm is implemented to group days with similar prices. We use the day with the median value in each cluster to represent each cluster, with cluster weights derived from normalizing the number of days in each cluster.

Upon obtaining the individual scenarios for both the arrival times and electricity prices, the total set of scenarios is generated using the Cartesian product of the two sets. The associated probability for each scenario is obtained as the product of the probabilities of arrival time and electricity prices. This method leads to a near-actual representation of uncertainty and less computational time for the optimization model.

We conduct computational experiments in the next section. We use the data collected from the open platform or website of HHLA Container Terminal Altenwerder (CTA) in Port of Hamburg to run various experiments and analyze the results. Details are further explained in the next section.

2.6 Computational experiments and results

This section conducts computational experiments and presents the results obtained. To find the potential for demand response, we present a case study of the HHLA Container Terminal Altenwerder (CTA) in Hamburg. Altenwerder is a state-of-the-art container terminal with a high degree of automation and has a lot of electrified equipment. Additionally, CTA has data publicly available.

The computations are all conducted using the commercial solver Gurobi v10.0.1, in combination with the Pyomo modeling language. For the stochastic decomposition, the mpi-sppy package was utilized (Knueven et al., 2020). The optimization model was run on an Intel i7-7700HQ processor with a 2.80 GHz clock speed and 8.00 GB of RAM.

All optimizations are solved using the progressive hedging (PH) algorithm. Ten iterations and a penalty parameter of 8000 are employed for each scenario's solution to converge. For all models, a mixed-integer programming optimality gap of 5% is used as a termination criterion. The solving time for each individual scenario is limited to 300 seconds. A convergence threshold of 0.01 is set. The convergence is lower than 0.01 for most of the experiments, though the threshold is not reached within 10 iterations in every experiment. The convergence metric is lower than 0.05 in all cases.

2.6.1 Model parameters

This section presents the parameters used in the mathematical model. We collect ship berthing record data from the open platform HHLA COAST. The sailing list from the CTA reveals that between April 10, 2023, and May 7, 2023, 190 ships arrived at the CTA terminal, averaging 7 ships per day (HHLA, 2025). The terminal equipment configuration data is collected on the CTA website. The terminal utilizes 14 quay cranes (QCs), 74 battery-electric automated guided vehicles (AGVs), and 52 yard cranes (YCs) for container handling (HHLA, 2023a). Containers are delivered and dispatched via ship, truck, or train. No onshore power facilities are currently applied at the CTA terminal. The length of the quay at CTA is found to be 1400 meters (HHLA, 2023a). Based on the container layout, it is estimated that the AGVs travel an average distance of 947 meters in 237 seconds to move a container (Zhang et al., 2023). Currently, there are 18 charging stations with a combined capacity of 4 MW for these AGVs (HHLA, 2023b).

The energy consumption for QCs and YCs to move one container is estimated to be 8 kWh and 2 kWh, respectively (He, 2016; He et al., 2015a; Iris & Lam, 2021). Additionally, the handling speed of both QCs and YCs is set to 30 containers per hour (He, 2016; He et al., 2015a). The average energy consumption of AGVs per meter is 0.00935 kWh (He et al., 2015b). By multiplying the energy consumption per meter by the average travel distance, the energy consumption for AGVs is estimated to be 9 kWh per container move. Furthermore, based on the travel time, the handling rate for the AGVs is calculated to be 15 containers per hour.

Three types of ships are assumed to arrive at the container terminal: feeder, short-sea, and deep-sea vessels. Following the work of Iris and Lam, it is assumed that 40% of ships are feeders, 40% are short-sea vessels, and 20% are deep-sea vessels (Iris & Lam, 2021). The ship lengths are uniformly distributed in the ranges [70, 200] for feeders, [210, 300] for short-sea vessels, and [300, 400] for deep-sea vessels (Iris & Lam, 2019a). The container demand is also assumed to be uniformly distributed in the ranges [200, 600] for feeders, [600, 1600] for short-sea vessels, and [1600, 4500] for deep-sea vessels (Iris & Lam, 2021). Based on the number of QCs, YCs, and AGVs assigned to fulfill the demand, the ship unloading rate varies. The handling rate is defined as the handling speed multiplied by the number of QCs, YCs, and AGVs assigned. For feeders, the handling rate can be one of 30, 45, 60, for short-sea vessels 60, 75, 90, 105, 120, and for deep-sea vessels 120, 135, 150, 165, 180.

The estimated time of arrival for each ship is distributed uniformly in the range [0, 24]. The actual arrival time $a_{t,w}$ is the estimated arrival time plus a deviation, which is different for every scenario. The arrival time deviations are normally distributed with a mean of 0 and a standard deviation of 3 hours, similar to the distribution in the work of Kolley et al. (2023). The estimated time of finishing is calculated by dividing the container demand by the minimum handling rate and adding the estimated time of arrival. If a ship departs later than the estimated finishing time, a penalty is applied. This penalty is obtained by converting the penalty stated by Iris & Lam (2021) to euros, assuming an exchange rate of 0.63 euro/SGD (Singapore Dollars), resulting in penalties of 630 euros, 1260 euros, and 1890 euros for feeder, short-sea, and deep-sea vessels, respectively. Additionally, a penalty of 20% of the late penalty is assumed with regards to changing the berthing schedule created on the previous day, similar to the approach used by Liu et al. (2020).

For the energy consumption of reefer containers, it is assumed that all reefers are of the same type. According to a breakdown by van Duin et al. (2018), frozen product-based reefer containers are the most common type. The temperature range allowed for frozen products like meat and fish is between -20 and -16 °C (van Duin et al., 2018). Based on the average values for a 40ft container, the mass, specific heat, heat transfer coefficient, and area of a reefer container are 24500 kg, 2.76 $\mathrm{kJ/kg \cdot K}$, 0.4 $\mathrm{W/m^2 \cdot K}$, and 135.26 $\mathrm{m^2}$, respectively (Kanellos, 2017). A cooling efficiency of 0.95 and the maximum cooling power are obtained from Kanellos (2017). At the CTA terminal, there are 2200 reefer connections, of which it is assumed that an average of 1500 are used simultaneously (HHLA, 2023a).

According to the HHLA website, it takes 1.5 hours to charge one AGV (HHLA, 2022). Based on the charging rate and the number of AGVs, it can be calculated that all AGVs together can store 24.7 MWh of electricity. A charging efficiency of 90% is assumed, similar to Kanellos (2017).

Historical electricity prices from the day-ahead market in Germany are obtained from the ENTSO-E (2023) website. A penalty of 20% of the day-ahead price is assumed for having an energy surplus or shortage, following the approach of Crespo-Vazquez et al. (2018).

While the current experiments focus on a single-terminal system, we note that the model has been successfully executed for instances involving up to 40 vessels within a 48-hour horizon, well above the typical daily number of ships for this container terminal. This suggests that the current model is, to some extent, suitable for larger terminal systems.

2.6.2 The impact of stochastic modeling

The mathematical formulation of the stochastic problem (SP) is given by formulation (2.1). We consider the uncertainty in the arrival times of ships and electricity prices. To find the impact that stochastic modeling has on the results, a comparison is made between the stochastic problem (SP) and several reactive approaches. For reactive approaches, the first-stage variables of the stochastic problem are fixed at specific values.

The following formulations give the mathematical formulation of the reactive approach and the formulation of the expected value problem:

$$\min_{\boldsymbol{x}_0, \boldsymbol{y}_\xi \in \boldsymbol{X}(\xi)} \quad f^F(\boldsymbol{x}_0) + \mathbb{E}_P[f^S(\boldsymbol{x}_0, \boldsymbol{y}_\xi, \xi)], \tag{2.29a}$$

$$\text{where} \quad \boldsymbol{x}_0 : \text{fixed.} \tag{2.29b}$$

$$\min_{\boldsymbol{x}, \boldsymbol{y}_{\bar{\xi}} \in \boldsymbol{X}(\bar{\xi})} \quad f^F(\boldsymbol{x}) + f^S(\boldsymbol{x}, \boldsymbol{y}_{\bar{\xi}}, \bar{\xi}), \tag{2.30a}$$

$$\text{where} \quad \bar{\xi} = \mathbb{E}_P[\xi]. \tag{2.30b}$$

The mathematical formulation of the reactive approach is given in formulation (2.29). In the problem described in Section 2.3, the first-stage variables are the start time of operations, S_i^{da}, and the energy purchased on the day-ahead market, P_t^{da}. Three reactive approaches are formulated: RE(reactive problem), RE+ and EEV(expectation of the expected value problem). For the RE and RE+ approaches, S_i^{da} is set to the estimated arrival time eat_i. P_t^{da} is set to 0 and the average daily consumption $\bar{P}^{da}$ for the RE and RE+ approach respectively. For the EEV, S_i^{da} and P_t^{da} are set to the solutions that can be obtained by solving the expected value problem. The mathematical formulation of the expected value problem is given by formulation (2.30). The x obtained from this problem is then used as x_0 in formulation (2.29).

For comparison, the results of the stochastic model can also be compared with the wait-and-see solution (WS). This solution gives a lower bound to the problem in case a perfect forecast of the first-stage decision variables is known. The wait-and-see solution is however not achievable in practice, since no perfect forecast exists. The mathematical formulation of WS is given as follows:

$$\min_{\boldsymbol{x}_\xi, \boldsymbol{y}_\xi \in \boldsymbol{X}(\xi)} \quad \mathbb{E}_P[f^F(\boldsymbol{x}_\xi) + f^S(\boldsymbol{x}_\xi, \boldsymbol{y}_\xi, \xi)]. \tag{2.31}$$

Table 2.6 gives the results of total costs for the RE, RE+, EEV and SP approaches. The optimization was done ten times for each approach, using different random seeds. For every approach, the cost reduction compared to the RE approach is calculated. The difference between the results from the RE approach and results from other approaches (RE+, EEV, SP) is divided by the results from RE results to get the cost saving percentage. By employing the EEV strategy, a cost reduction of 16.6% can be achieved. The stochastic problem presented in this chapter further increases the cost reduction to 20.6%. As for the wait-and-see (WS) solution, the average cost for ten iterations is 44096.5€. The hypothetical maximum reduction achievable through WS solution is 32.4%.

Based on the differences between the EEV and SP solutions, the following equations calculate the value of the stochastic solution (VSS) and the expected value of perfect information (EVPI, which represents the difference between the SP and WS solutions):

$$VSS = EEV - SP = 54411.5 - 51815.9 = 2595.6 \text{ EUR} \tag{2.32}$$

$$EVPI = SP - WS = 51815.9 - 44096.5 = 7719.4 \text{ EUR} \tag{2.33}$$

As the equations above show, the stochastic approach we use is superior to the EEV, and there is also space for improving forecasting accuracy.

2.6.3 The positive impact of demand response

To assess the impact of demand response on the solution, we consider different electricity pricing schemes: no pricing (NP), single pricing (SP), and real-time pricing (RTP) cases.

In the NP case, all energy-related costs in the objective function are disregarded. The objective function is simplified by removing the energy cost terms, resulting in formulation 2.34:

Table 2.6: Result comparison among reactive approaches and stochastic problem

	RE	RE+	EEV	SP
No.	Total cost [€]	Total cost [€]	Total cost [€]	Total cost [€]
1	62863.8	58775.9	53217.3	50138.7
2	62074.0	57967.5	53056.8	47049.1
3	69925.5	63784.6	59770.4	57459.1
4	53117.1	51103.7	40004.2	39828.8
5	81891.7	74881.7	67645.8	62538.3
6	67430.5	61454.6	53747.0	52804.4
7	75826.3	69324.2	62984.9	61154.2
8	48113.5	45913.3	41666.9	39914.3
9	71876.7	65269.8	56203.4	54556.0
10	59377.4	55685.1	55818.4	52716.3
Avg	**65249.7**	**60416.1**	**54411.5**	**51815.9**
Cost savings (%)	**0.0**	**7.4**	**16.6**	**20.6**

Note: RE (Reactive problem), EEV (Expectation of the expected value problem), SP (Stochastic problem), Cost savings (%) = $(Avg_{RE} - x) * 100/Avg_{RE}$

$$\min_{\mathbf{V},\mathbf{T}} \sum_{w \in \mathbf{S}} \pi_w \left(\sum_{i \in \mathbf{V}} c_i^{late} L_{i,w} + \sum_{i \in \mathbf{V}} c^{resch} c_i^{late} (S_{i,w}^{late} + S_{i,w}^{early}) \right). \tag{2.34}$$

In the SP case, the electricity price $c_{t,w}^{da}$ in the objective function is replaced with a single price $\bar{c}_w^{da}$ for each hour. The objective function is modified accordingly, resulting in formulation (2.35):

$$\begin{aligned} \min_{\mathbf{V},\mathbf{T}} \sum_{w \in \mathbf{S}} \pi_w \Bigg(& \sum_{i \in \mathbf{V}} c_i^{late} L_{i,w} + \sum_{i \in \mathbf{V}} c^{resch} c_i^{late} (S_{i,w}^{late} + S_{i,w}^{early}) + \\ & \sum_{t \in \mathbf{T}} \bar{c}_w^{da} P_t^{da} + \sum_{t \in \mathbf{T}} \bar{c}_w^{da} (c^{shor} P_{t,w}^{shor} - c^{sur} P_{t,w}^{sur}) \Bigg). \end{aligned} \tag{2.35}$$

Therefore, there is no uncertainty in energy prices in this case. The mathematical formulation presented in Section 2.4 remains the same for the RTP case. However, for the SP and NP cases, minor adjustments are needed. Specifically, constraint (2.22) and constraint (2.27) are replaced with constraint (2.36) and constraint (2.37) below, respectively. These changes ensure that the energy consumed by operations, such as charging and cooling, matches the energy demand for each time period without considering different prices. Constraint (2.36) and (2.37) prevent unnecessary rescheduling of charging and cooling times that would occur under the assumption of the single or no pricing scheme, as the timing of consumption becomes irrelevant in the SP and NP cases:

$$\eta^{charge} \cdot E_{t,w}^{charge} = \sum_{i \in V} \sum_{p \in P_i} e_m^{machinery} \cdot u_{p,m} \cdot H_{i,p,t,w}$$
$$m = AGV, \ \forall t \in T, \ \forall w \in S, \tag{2.36}$$

$$u \cdot a \cdot (ta_t - (tc^{min} + tc^{max})/2) = \eta^{reefer} \cdot E_{t,w}^{reefer}, \qquad \forall t \in T, \ \forall w \in S. \tag{2.37}$$

Ten optimization experiments are performed for all three pricing schemes. Electricity prices in Germany in 2022 were used for the optimization.

Figure 2.2 illustrates the planned and actual ship schedule and energy purchase and consumption for the second instance in the fourth scenario. By plotting the ship schedule and energy purchase and consumption, a visual comparison can be made between the different pricing strategies, including the decisions made in the first stage and how they changed in the second stage. In the subfigures for energy purchase and consumption, the grey bars represent the energy purchased one day ahead of the actual operations in the energy consumption shortage case (day-ahead energy purchase$<$energy consumption) or equal-use case (day-ahead energy purchase = energy consumption), while the stacked grey and blue bars represent day-ahead energy purchased in the energy consumption surplus case (day-ahead energy purchase$>$energy consumption).

For the NP alternative, power imbalances can be observed for most hours, resulting in higher energy costs. When the cost of electricity is taken into account in the SP alternative, these imbalances are significantly reduced, leading to lower energy costs. When the real-time pricing scheme (RTP scheme is implemented, imbalances occur much less frequently. Once real-time prices are considered in the optimization (RTP scenario), the energy consumption pattern also changes with the fluctuating prices. The energy consumption reduces during times of high prices, and the energy consumption increases during times of low prices. We can find visible energy consumption peaks and troughs during planning horizon when applying real-time pricing scheme. Some differences in the berthing schedule can be observed between the different alternatives, although they are minor. Most of the differences are noticeable between the RTP scenario and the other two scenarios.

Table 2.7 presents the results of different pricing strategies, including NP, SP, and RTP. The costs are divided into energy-related costs and schedule-related costs. We assume that the percentage cost savings for different costs can be calculated directly using the costs obtained under different pricing methods. For example, the cost savings of energy-related costs can be directly calculated using the energy-related costs under different pricing schemes. The cost reduction compared to the results under no-pricing scheme is calculated. The difference between the results under the no-pricing scheme and results under other pricing schemes (single-pricing and real-time pricing) is divided by the results from no-pricing scheme to get the cost saving percentage. As the table shows, the real-time pricing strategy has a noticeable decrease in energy-related costs. By considering a single price or a real-time price of electricity, the energy-related costs decrease by 6.4% and 14.4%, respectively. It appears that scheduling costs also slightly decrease. However, the average absolute difference in scheduling costs between the no pricing and real-time pricing is small, at around 400 euros. It can be concluded that the real-time pricing scheme will have a relatively less significant impact on scheduling costs than it will have on energy-related costs, though no definitive conclusions can be drawn regarding the

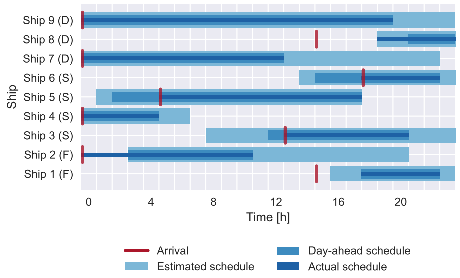

(a) Planned and actual ship schedule – No pricing

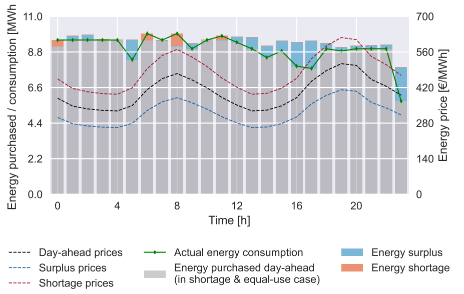

(b) Energy purchase and consumption – No pricing

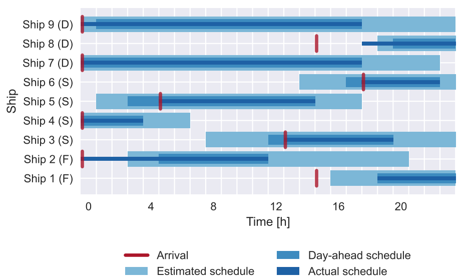

(c) Planned and actual ship schedule – Single pricing

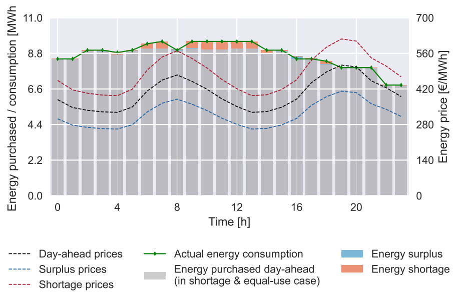

(d) Energy purchase and consumption – Single pricing

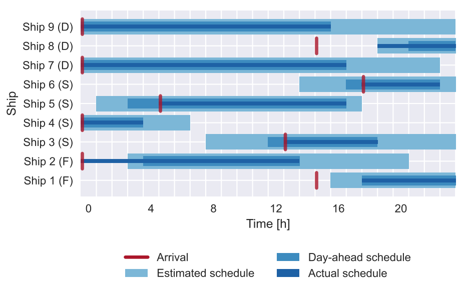

(e) Planned and actual ship schedule – Real-time pricing

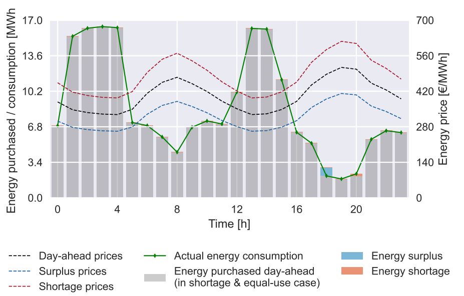

(f) Energy purchase and consumption – Real-time pricing

Figure 2.2: Ship schedule and hourly energy consumption of the second instance for different pricing strategies in the fourth scenario

impact of energy-aware optimization on scheduling costs. By considering energy prices, the total operational cost of the terminal is reduced by 5.9% and 13.2% for the single and real-time pricing schemes, respectively, with energy-related costs accounting for the majority of the reduction. It shows that the real-time pricing scheme in a demand response mechanism performs well in the energy management system. This demonstrates that incorporating real-time pricing into terminal operations can yield substantial financial benefits. Moreover, the results highlight the importance of time-sensitive electricity pricing in improving cost-saving performance within demand response frameworks.

Figure 2.3 displays the average energy consumption across all instances for the NP and RTP schemes. A negative correlation between energy consumption and electricity price is observed in the real-time pricing case. Compared to the steady consumption pattern during the planning horizon with the NP strategy, the average consumption increases at night and in the early afternoon when prices are lowest with the RTP scheme. This clear load-shifting behavior reflects how the model adapts energy usage in response to price signals, concentrating consumption in off-peak periods to reduce operational costs. The visual contrast between the two schemes illustrates the potential of real-time pricing scheme to reshape the temporal distribution of energy demand. To quantify this correlation, the Pearson correlation coefficient is calculated between energy consumption and electricity price. For the NP and SP schemes, correlation coefficients of 0.09 and 0.03 are found, indicating that almost no correlation exists between price and consumption. However, when RTP scheme is considered, the Pearson correlation coefficient becomes -0.85, indicating a strong negative correlation.

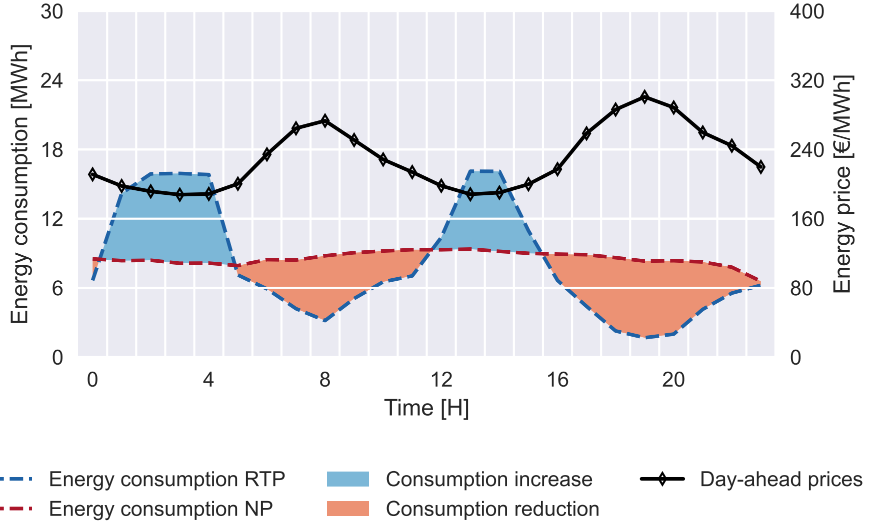

Figure 2.3: Average energy consumption for No pricing and Real-time pricing schemes

Table 2.7: Result comparison of different pricing strategies

	No pricing			Single pricing			Real-time pricing		
No.	EC [€]	SC [€]	TC [€]	EC [€]	SC [€]	TC [€]	EC [€]	SC [€]	TC [€]
1	44628.1	13482.0	58110.1	43325.8	13692.0	57017.8	38798.7	11340.0	50138.7
2	49746.6	6804.0	56550.6	47013.8	6602.4	53616.2	42317.8	4731.2	47049.1
3	53979.6	11390.4	65370.0	50921.5	10735.2	61656.7	47429.5	10029.6	57459.1
4	45266.7	3931.2	49197.9	39856.1	4989.6	44845.7	35544.8	4284.0	39828.8
5	57095.3	11793.6	68888.9	55677.2	11844.0	67521.2	52357.5	10180.8	62538.3
6	55265.5	3376.8	58642.3	52559.4	4737.6	57297.0	48559.9	4244.5	52804.4
7	55561.2	10533.6	66094.8	52899.1	9626.4	62525.5	48999.4	12154.8	61154.2
8	46231.0	4284.0	50515.0	40303.2	3780.0	44083.2	35991.5	3922.8	39914.3
9	54584.0	8618.4	63202.4	51742.4	6442.8	58185.2	47626.0	6930.0	54556.0
10	50439.0	9651.6	60090.6	45624.5	8794.8	54419.3	41401.5	11314.8	52716.3
Avg	**51279.7**	**8386.6**	**59666.3**	**47992.3**	**8124.5**	**56116.8**	**43902.6**	**7913.3**	**51815.9**
Cost savings (%)	**0.0**	**0.0**	**0.0**	**6.4**	**3.1**	**5.9**	**14.4**	**5.6**	**13.2**

Note: EC (Energy-related cost), SC (Schedule-related cost), TC (Total cost), Cost savings (%) = $(Avg_{NP} - x) * 100/Avg_{NP}$

Furthermore, increased volatility in electricity consumption for RTP can be observed in Figure 2.3. The peak-to-average ratio (PAR) is calculated for all different pricing schemes. The NP and SP schemes have PAR values of 1.17 and 1.19, respectively. In contrast, the RTP scheme exhibits a significantly higher PAR of 2.05. This means that the RTP strategy creates more volatile consumption with higher peaks. It is generally not desired since it causes more strain on the electricity grid.

Similarly to the energy demand, other decision variables can also be compared under different pricing schemes. Figure 2.4 illustrates variations in the number of berthed ships, the handling rate of cargo handling equipment combination (QCs, YCs and AGVs), the power of AGV charging, and the power of reefer cooling. Each of these variables responds to price changes. A larger difference between NP and RTP indicates greater responsiveness of the variable to price changes. From Figure 2.4, it can be visually observed that different variables change to a great extent when comparing the RTP and NP schemes. A metric called the flexibility coefficient (FC) is calculated to compare the sensitivity of each variable to price changes. The FC is defined as the standard deviation of the difference of variables between the NP and RTP schemes divided by the mean value of the variable under the NP scheme. The FC for each variable (X) can be calculated using the equation below:

$$\mathrm{FC} = \frac{\sigma(X_{NP} - X_{RTP})}{\bar{X}_{NP}} \tag{2.38}$$

When comparing the FC for the variables above, we can discover that the cooling power is the most flexible, with a normalized standard deviation of 1.48. It implies that the rate at which reefers are cooled can be adjusted more readily in response to price changes. Following this, the AGV charging power also demonstrates notable flexibility. The handling rate and the number of ships berthed exhibit relatively lower levels of flexibility compared to other variables. These results suggest that energy-intensive and temporally shiftable components are more responsive to price signals. Understanding such flexibility can help operators identify the most effective levers for cost optimization under dynamic pricing schemes.

2.7 Managerial insights

The experimental results lead to several valuable managerial insights for the operations and management of container terminals. Focusing on the implications of energy-aware optimization on the operations, the following key insights emerge:

- The growing impact of uncertainty: Properly accounting for uncertainty in the demand and supply of energy is crucial when optimizing energy consumption and operations planning in container terminals. Failing to consider this uncertainty can result in up to 20% higher costs, on average, due to the need for subsequent operational plan changes.
- The economic opportunity of energy-aware planning: Implementing an energy-aware optimization approach based on hourly varying electricity prices can lead to significant cost reductions in container terminals, with potential savings of up to 13.2% of the operational costs. These cost savings can be achieved without requiring substantial investments in, for instance, energy storage or renewable energy infrastructure.

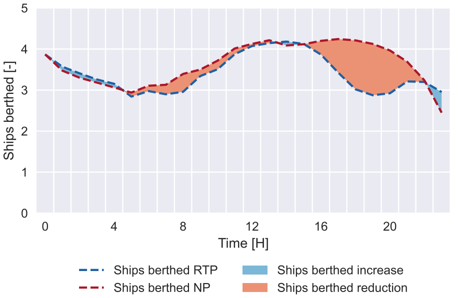

(a) Average number of ships berthed for NP and RTP schemes

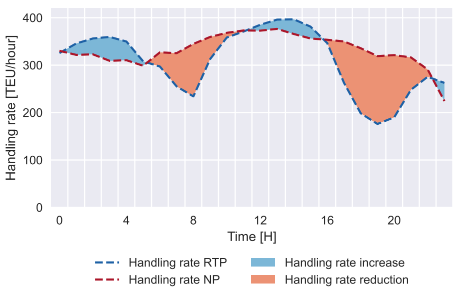

(b) Average handling rate of equipment combination for NP and RTP schemes

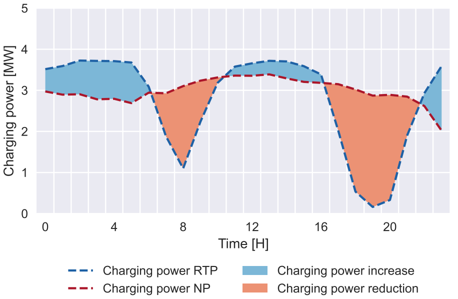

(c) Average AGV charging power for NP and RTP schemes

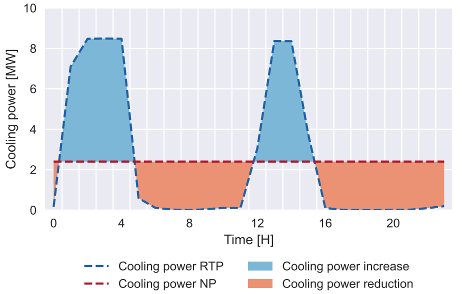

(d) Average cooling power for NP and RTP schemes

Figure 2.4: Pattern comparison for different variables between No pricing and Real-time pricing schemes

- The importance of real-time pricing: The real-time pricing scheme has a relatively more significant impact on energy-related costs than on scheduling costs. The inclusion of energy-related costs has a small impact on the scheduling costs. The decrease in energy-related costs accounts for the majority of the reduction in total costs.
- Container terminal (in this case, Alterwerder terminal) operators need to have more connection with grid operator/ electricity power supplier to take care of the fluctuation of energy consumption, especially when consumption peaks and troughs happen.
- The role of peaks: The energy consumption peak period shifts with the implementation of the real-time pricing scheme. Energy consumption during peak periods is higher with real-time pricing than with the other pricing schemes. There is still space to explore the effect of real-time pricing on peak time-related electricity costs.
- The model has the possibility to be extended to study the integration of renewable energy sources. The generation of renewable energy has a high degree of uncertainty, which can represent the uncertainty on the energy supply side. Different energy generation scenarios can be generated to be integrated into the stochastic programming model.

These insights highlight the potential for cost savings and operational improvements by considering electricity demand and implementing efficient control measures. By adopting these insights, container terminals can optimize their operations, reduce energy-related expenses, and get ready for the challenges of the transition to renewable energy sources.

2.8 Conclusions

Demand response (DR) is an effective measure to manage energy consumption and reduce energy-related costs in container terminals. It helps to adapt the power consumption of consumers in ports to better match the demand for power with the supply. Nonetheless, in academic literature, energy consumption management in ports has received limited attention, especially in the aspect of the uncertainty in energy demand and supply.

This chapter addresses RQ 1. We present an integrated energy-aware optimization approach for the operations of a container terminal in this chapter and build a stochastic programming model to formulate the operation and energy flow in container ports. The model considers vessels, quay cranes (QCs), yard cranes (YCs), reefers, and automated guided vehicles (AGVs) as multiple loads in the energy system. The uncertainty in demand is reflected in ship arrival times, and the uncertainty in supply is represented by electricity prices. We further develop a progressive hedging algorithm to efficiently solve the problem, and conduct computational experiments, based on data from Container Terminal Altenwerder (CTA) in the Port of Hamburg, to test the proposed model and explore its practical implications. The stochastic programming method consistently outperform reactive approaches. We analyze different pricing strategies to assess the potential benefits of demand-responsive planning. Results suggest the cost saving increases to 13.2% on average when applying real-time electricity prices, which is more than the cost saving achieved by the single pricing scheme. As for implications, results show that considering uncertainty in the demand and supply of energy is crucial when optimizing energy consumption and operations planning in container terminals in an integrated way. Furthermore, we observe that implementing an energy-aware optimization approach based on hourly varying electricity prices can lead to significant cost reductions in container terminals, and including energy-related costs has minimal impact on the scheduling costs. Finally, the control of reefer energy consumption and adjusting the charging times of AGVs have the most potential to alter the overall energy consumption pattern. In the next chapter, the research further extends into the berth area and investigates the modeling, prediction of shore power (SP) demand and its integration into port operations, with particular emphasis on the interaction between berth allocation decisions.

Chapter 3

Learning Shore Power Demand and Energy-aware Berth Allocation

In Chapter 2, we propose a two-stage stochastic programming model to optimize port operations and energy management. This chapter explores the energy dimension of port operations, with a particular emphasis on shore power (SP). A fine-grained temporal prediction of shore power demand is developed and subsequently integrated into the berth allocation problem. This chapter addresses RQ 2: How to model SP demand and predict it with raw vessel port call data, and RQ 3: How does SP demand modeling and prediction influence berth allocation decisions and terminal shore power profiles?

This chapter is structured as follows: Section 3.1 explains the necessity of shore power demand prediction and summarizes the research work presented in this chapter. Section 3.2 reviews related work on shore power demand estimation, prediction and integration into port operations optimization. Section 3.3 explains the problem we study and presents the mathematical formulation. Section 3.4 introduces the predict-then-optimize pipeline, which includes SP modeling method, ML method and SP-aware berth allocation problem (BAP) formulation. Section 3.5 explains the experiment process, presents and analyzes the ML performance and BAP experiments, followed by the managerial insights presented in Section 3.6. Finally, Section 3.7 concludes the chapter.

Part of this chapter is submitted as a journal paper: Tang, X., Ç. Iris, R. R. Negenborn, P. He, F. Schulte (2026b) Learning shore power demand and energy-aware berth allocation, and is published in a conference article: Tang, X., Ç. Iris, F. Schulte (2025b) Fine-grained estimation of onshore power demand via operational phase segmentation of port call data, in: *Proceedings of the 16th International Conference on Computational Logistics*, Delft, The Netherlands.

3.1 Introduction

Decarbonizing maritime transport has emerged as a key pillar in global efforts to achieve climate neutrality and sustainable development. The European Union (EU) has positioned maritime decarbonization as a central objective in its broader climate strategy, particularly under the "Fit for 55" package aimed at reducing greenhouse gas (GHG) emissions by at least 55% by 2030. In line with this goal, the EU has introduced the FuelEU Maritime Regulation European Commission (2023b) and the Alternative Fuels Infrastructure Regulation (AFIR) European Commission (2023a), which mandate that from January 2030, all passenger ships and container vessels over 5000 GT must use shore power (SP) while berthed at core Trans-European Transport Network (TEN-T) ports.

Shore power (SP) refers to supplying docked vessels with electricity from the shore grid, allowing vessels to shut down auxiliary engines and thereby reduce emissions. These regulatory requirements are expected to significantly mitigate local air pollution and GHG emissions at ports, where auxiliary engines have traditionally operated during berthing periods.

Since SP is being introduced to more and more terminals, terminal operators need to take it into account when making decisions for port operations. SP usage is intrinsically linked to operations in the berth area, such as berth allocation and quay crane assignment. As a result, the temporal distribution of SP demand directly affects the feasibility and efficiency of terminal operations, particularly under increasingly constrained port electricity infrastructure. This regulatory push substantially increases the need for accurate SP demand prediction at fine temporal granularity. For terminal operators, it is no longer sufficient to estimate aggregate energy consumption; instead, reliable hourly SP demand profiles are required to support infrastructure sizing, grid coordination, and operational planning. However, predicting SP demand at such granularity is inherently challenging. SP demand depends not only on vessel type and installed auxiliary power, but also on operational factors such as handling schedules.

Existing approaches largely rely on static, type-based power assumptions or aggregated daily estimates, which fail to capture variability and operational interactions. Moreover, studies that explicitly integrate SP into port operation optimization problems often treat SP demand as a given, exogenously specified input. In several cases, SP load profiles are assumed to be fixed or even constant over time, independent of vessel operations. Such assumptions may lead to berth allocation plans that are infeasible from an energy perspective, as the aggregated SP demand during certain time periods may exceed the available shore power capacity. This limits the ability of optimization models to account for demand variability and reduces the applicability of existing approaches for real-time energy management and operational decision support. Consequently, the interaction between SP demand prediction and port operations, such as berth allocation and vessel scheduling, remains largely unexplored. This creates a critical research gap in developing fine-grained SP demand prediction methods and understanding their impact on operational planning in SP-enabled terminals.

To address these challenges, this study develops a predict-then-optimize framework for shore-power-aware berth allocation, in which SP demand is predicted from raw port call event data with different machine learning methods, and incorporated into an berth allocation model that accounts for shore power capacity constraints. This chapter makes several contributions to the field of SP demand prediction and energy-aware operational planning for SP-enabled terminals.

First, we propose a modeling method that transforms raw port call event data into a structured representation suitable for generating an hourly SP power profile. Unlike traditional approaches based on static power assumptions or aggregated berth statistics, the proposed method explicitly models the temporal evolution of SP demand by incorporating operational phases such as power ramp-up, steady-state demand periods, cargo handling with potential overlaps or gaps, and power ramp-down. This approach enables the generation of time-grained SP demand profiles that more accurately reflect real-world vessel operations.

Second, we apply and evaluate several machine-learning prediction models. In particular, Tabular Prior-data Fitted Network (TabPFN), a recently proposed tabular foundation model, is included due to its strong potential for structured tabular prediction tasks with limited training data. The models are evaluated under two feature sets representing distinct planning scenarios: a Full-Insight setting, in which detailed historical operational information is available, and an Operational-Planning setting restricted to pre-arrival variables. This distinction allows us to assess the effectiveness of SP demand prediction under limited information availability commonly encountered in practice.

Third, we integrate predicted SP demand profiles into an SP-aware berth allocation framework that explicitly accounts for SP capacity constraints. By comparing outcomes obtained under the perfect-information, machine-learning-based prediction, and statistical prediction methods, we evaluate how different demand prediction approaches affect berth allocation decisions. The results show that machine-learning-based predictions consistently outperform conventional statistical approaches, with the TabPFN-driven framework achieving the best overall performance. This predict-then-optimize framework highlights the importance of accurate, time-resolved SP demand prediction for operational planning in SP-enabled terminals.

3.2 Related work

Several reviews (Iris & Lam, 2019b; Song, 2024) have surveyed a wide range of port efficiency and decarbonization strategies, including operational improvements (Stoter et al., 2025), technology adoption, and the integration of renewable energy sources (Iris & Lam, 2021). Among these efforts, SP has received increasing attention (Abu Bakar et al., 2023; Yu et al., 2023a). In particular, growing interest has emerged in estimating the energy demand of ships at berth, primarily in the context of SP deployment, port decarbonization, and emission reduction policies. These studies differ in their methodological assumptions, data granularity, and applicability to real-time operations. A structured comparison of representative studies is provided in Table 3.1.

Several studies estimated SP demand by applying standardized load factors and ship-level technical parameters, such as gross tonnage, deadweight, or auxiliary engine capacity and calculated the energy demand with a formula. For example, Amaral et al. (2023) estimated SP using static profiles for different ship types. Similar assumptions were adopted by an anchorage-focused study (Ventikos et al., 2025), where SP needs were inferred from anchorage duration and average auxiliary engine power. Uzun et al. (2024) conducted a feasibility study on the energy and peak power demand of ships for utilizing the SP. Calculations were conducted based on the operation timings obtained from the discrete event simulation and representative ship characteristics. These methods are interpretable and simple to implement, but often at a generally aggregated level and oversimplify time-dependent operations.

More recent studies have increasingly adopted machine learning (ML) techniques to estimate ship-level or port-wide energy demand by learning empirical relationships from operational data. Okumuş et al. (2021) estimated the main and auxiliary engine power of ships based on the ship's length, gross tonnage and age using simple linear regression (LR), polynomial regression, K-nearest neighbor (KNN) regression and gradient boosting (GB) machine regression algorithms. Peng et al. (2020) used a machine learning-based method considering 15 features, including inherent ship features and external port features. Five models including LR, KNN, GB regression, random forest (RF) and backpropagation network were employed based on the energy consumption dataset of ships. Alikhani et al. (2021) employed an approach based on an artificial neural network (ANN) to forecast the hourly peak load demand and short-term electricity demand profile in a container terminal. The study by Micallef et al. (2025) presented a framework for forecasting electricity demand in port microgrids using advanced machine learning models, including RF, Least Squares Boosting Ensemble, and Gaussian Process Regression. These models were evaluated under different forecasting setups and compared against simpler baseline methods. Uyanık et al. (2022) utilized actual voyage data to predict the main engine shaft power and fuel consumption of a container ship via LR, Ridge Regression, ANN, etc. Bakar et al. (2022a) proposed a data-driven framework to forecast ship berthing duration for cold ironing applications using multiple machine learning models, providing inputs for berth allocation and port energy management. Peng et al. (2018) proposed a simulation-based method to determine the required SP power capacity by explicitly considering the stochastic arrival patterns and composition of ships in container terminals. While these ML models outperform traditional approaches in predictive accuracy, they typically output static or aggregated values (e.g., total power per call or per day) and rarely provide fine-grained time series demand profiles.

Besides forecasting SP demand, some studies incorporate shore power into port operations

Table 3.1: Comparison of related studies on shore power (SP) and port electricity (PE) demand.

Paper	Study focus		Method		Key features			
	SP	PE	ML	Formula	Ship	Oper.	Temp.	Hist.
Okumuş et al. (2021)	✓		✓		✓			
Peng et al. (2020)	✓		✓		✓	✓		
Amaral et al. (2023)	✓			✓	✓			
Alikhani et al. (2021)		✓	✓			✓	✓	✓
Micallef et al. (2025)		✓	✓			✓	✓	✓
Ventikos et al. (2025)	✓			✓	✓	✓		
Uzun et al. (2024)	✓			✓	✓	✓		
This chapter	✓		✓		✓	✓	✓	

Notes: SP = Shore Power (in some cases, also includes vessel energy), PE = Port Electricity.
ME = Machine Learning.
Ship = Ship specifications, Oper. = Operational features, Temp. = Temporal features, Hist. = Historical demand.

Table 3.2: Comparison of SP-related port operations studies.

Paper	**Scope**				**Objectives**		**Method**			
	BAP	BAQAP	SPAP	Others	Cost	Env.	MILP	MO	Metaheur.	ML
Bakar et al. (2022b)	✓				✓		✓			
He et al. (2025)		✓	✓		✓	✓	✓			
Peng et al. (2021)	✓		✓		✓	✓		✓	✓	
Zhang et al. (2025)	✓		✓		✓	✓		✓	✓	
Yu et al. (2022b)		✓	✓		✓	✓		✓	✓	
Yu et al. (2023b)		✓	✓		✓			✓	✓	
Wang et al. (2024b)		✓	✓		✓		✓			
Conte et al. (2025)				✓	✓					✓

Notes: BAP = Berth Allocation Problem, BAQAP = Berth Allocation and Quay Crane Assignment Problem, SPAP = Shore Power Allocation Problem.
Cost can include vessel waiting, operating, penalties for delay, SP installation, and usage, etc.; Env.: Environmental objectives, can include carbon emission cost and environmental benefits, etc.
MILP = Mixed Integer Linear Programming, MO = Multi-objective optimization, Metaheur. = Metaheuristic algorithms, ML=Machine Learning.

decision-making, most commonly by extending berth allocation and quayside resource planning models with shore-power assignment and capacity constraints. Compared with pure demand estimation, these works focus on how berth positions, service start times, crane deployment, and power-connection choices jointly shape both operational efficiency (e.g., waiting or delay) and sustainability outcomes (e.g., emissions reduction or electricity cost). Table 3.2 presents the studies in SP-related port operations. Bakar et al. (2022b) formulated a mixed-integer linear programming (MILP) model that integrates berth allocation with SP capacity constraints. He et al. (2025) studied an integrated berth, quay crane, and SP allocation problem under continuous berth and time settings, aiming to jointly minimize operational costs and carbon emissions. Peng et al. (2021) solved the problem of whether to allocate shore power for each berth and which berth is allocated for the stochastic arriving ship with consideration of a trade-off between economic and environmental benefits. They applied the multi-objective particle swarm optimization algorithm (MPSO) to solve the Multi-objective (MO) MILP. Zhang et al. (2025) also studied the integrated BAP and SP allocation problem and formulated an MOIP and employed the reference point-based Non-dominated Sorting Genetic Algorithm (NSGA-III). Yu et al. (2022b) investigated the joint optimization of SP usage and berth allocation and quay crane assignment (BAQAP) operations, and then extended the problem by jointly considering multiple green technologies to optimize operational efficiency and environmental performance in container terminals (Yu et al., 2023b). Wang et al. (2024b) investigated the joint optimization of berth allocation, quay crane assignment, and on-shore power supply usage in container terminals to reduce operational delay and energy-related costs. Conte et al. (2025) proposed a hybrid reinforcement learning and model predictive control framework to optimize green port operations by dynamically managing energy consumption and system-level operational decisions.

Most SP-related berth allocation and quayside operation models treat SP demand as an exogenous input, typically derived from static ship classes, fixed auxiliary engine power, and aggregated berthing durations, or they assume perfect knowledge of SP demand profiles. Consequently, the critical challenge of modeling and predicting time-resolved SP demand, based on limited pre-arrival information and raw port call records, remains underexplored. To address these gaps, this study develops a data-driven SP demand prediction framework to generate fine-grained demand profiles. The predicted demand is then integrated into an SP-aware berth allocation model, forming a predict-then-optimize paradigm to explore the impact of different prediction methods on planning performance.

3.3 Problem description and formulation

This section introduces the shore-power-aware berth allocation problem (BAP) considered in this study. A mathematical formulation is subsequently developed to model berth allocation and shore power capacity constraints in an integrated optimization framework.

3.3.1 Problem description

The introduction of shore power (SP) systems into container terminals affects the planning of port operations, especially the operations in the berth area. The berth allocation problem (BAP) is a fundamental decision-making problem in container terminal operations, which determines the assignment of vessels to berths and their service schedules over time. Traditional BAP formulations primarily focus on spatial and temporal feasibility, aiming to minimize objectives such as vessel waiting time or service delay under berth capacity constraints. However, with the introduction of SP systems in ports, vessel berthing decisions become significantly influenced by energy consumption patterns. In particular, the temporal overlap of vessel service directly determines the aggregated SP demand, thereby introducing additional SP supply capacity constraints that must be considered during planning.

Figure 3.1 illustrates the core problem addressed in this study. The berth allocation and scheduling of vessels strongly influence the temporal aggregation of SP demand profiles. The figure presents three representative scenarios.

Scenario 1: Capacity-unaware BAP. In the first scenario, berth allocation decisions are made without considering SP capacity constraints. Although each vessel has an implicit demand profile, the berth allocation problem (BAP) is solved solely based on spatial and temporal compatibility constraints. As illustrated by the red slot in the BAP figure, such decisions may lead to aggregated demand exceeding the shore power capacity limit, thereby causing infeasible or operationally risky schedules and high penalty costs.

Scenario 2: Perfect demand information. In the second scenario, the exact SP demand profile of each vessel is assumed to be known in advance. The BAP can then be formulated as an SP-aware optimization problem that explicitly enforces capacity constraints over time. While this scenario yields feasible demand profiles, it relies on perfect foresight, which is unrealistic in practical port planning contexts. Compared to Scenario 1, the total berthing time for all vessels may be longer, while the penalty cost for exceeding the capacity limit may experience a substantial decrease with a lower demand peak. The varying electricity price will also shift the peak SP demand and affect the scheduling of SP connection and usage.

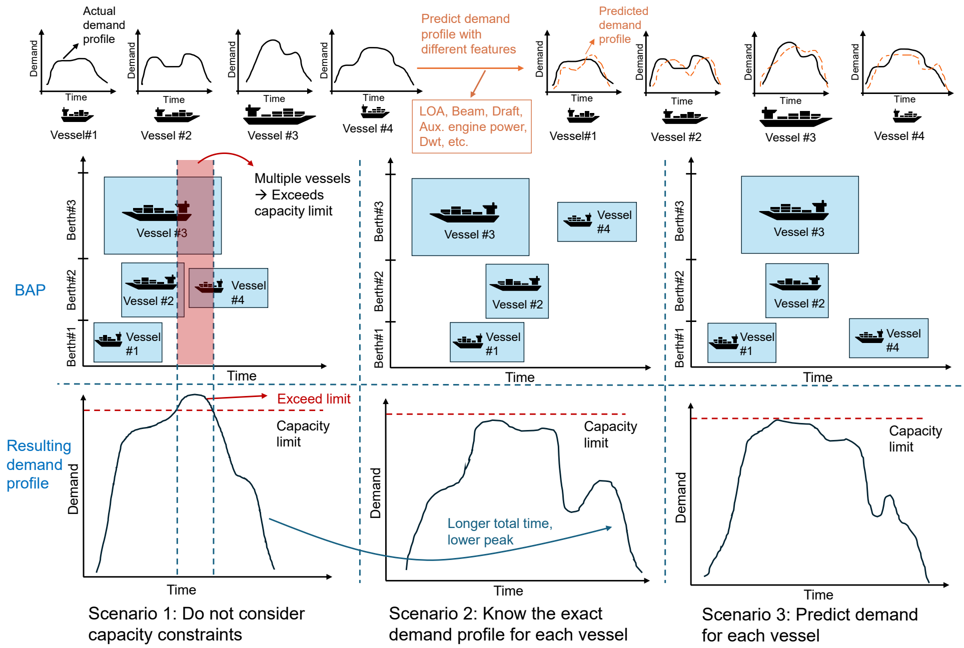

Figure 3.1: An illustrative example for the importance of fine time-grained shore power demand prediction for berth allocation plan with three scenarios

Scenario 3: Predict-then-optimize (proposed framework). In the third scenario, individual vessel demand profiles are first predicted using data-driven machine learning models based on vessel characteristics and operational features. These predicted profiles are then incorporated into an SP-aware berth allocation model. This framework enables proactive capacity management. Compared to Scenario 1, it reduces the risk of capacity violations. Compared to Scenario 2, it can approximate what happens in the real world as much as possible.

Building upon the above observations, this chapter develops an integrated framework that explicitly connects SP demand modeling, prediction, and operations planning (BAP). Specifically, we (i) model time-grained SP demand profiles from raw port call records and static vessel characteristics, (ii) apply machine learning models to predict SP demand under different information availability settings, and (iii) incorporate the predicted demand profiles into an SP-aware BAP to support energy-constrained planning decisions.

Based on this problem setting, the next subsection presents the mathematical formulation of the classical BAP model and SP-aware BAP model, where both operational constraints and SP capacity limitations are explicitly modeled.

3.3.2 Model formulation

The operational problem we study is the berth allocation problem (BAP). To demonstrate the impact of SP demand prediction on BAP, we integrate the SP capacity constraint into the classical BAP model and formulate the SP-aware BAP variant. We first consider a discrete berth allocation problem (DBAP) (Imai et al., 2001; Buhrkal et al., 2011), where the planning horizon is divided into H time slots. Each vessel is assigned to exactly one berth and starts service exactly once within its feasible start set. Service continuity is enforced through binary "in-service" variables. Building on this DBAP, we then formulate an SP-aware extension (SP-BAP).

Sets, parameters, and variables

Table 3.3 summarizes the notation used in both models. Compared with standard DBAP, SP-BAP introduces some energy-related sets, parameters and decision variables.

Discrete BAP (DBAP)

The DBAP model below determines berth assignment and vessel service schedules under discrete berth and time-slot settings:

$$\min \quad \sum_{i \in \mathcal{I}} w_i \sum_{s \in \mathcal{S}_i} (s - a_i) x_{is}, \tag{3.1}$$

$$\text{s.t.} \quad \sum_{b \in \mathcal{B}} a_{ib} = 1, \qquad \forall i \in \mathcal{I}, \tag{3.2}$$

$$\sum_{s \in \mathcal{S}_i} x_{is} = 1, \qquad \forall i \in \mathcal{I}, \tag{3.3}$$

$$w_{it} = \sum_{s \in \mathcal{S}_{it}} x_{is}, \qquad \forall i \in \mathcal{I}, \forall t \in \mathcal{T}, \tag{3.4}$$

Table 3.3: Sets, parameters, and decision variables in DBAP and SP-BAP.

Symbol	Description
Sets	
$\mathcal{I}$	Set of vessels i.
$\mathcal{B}$	Set of berths b.
$\mathcal{T}$	Set of discrete time periods t, $t \in \{1,\ldots,H\}$ (planning horizon).
$\mathcal{S}_i \subseteq \mathcal{T}$	Feasible service start periods for vessel i: $\mathcal{S}_i = \{s \in \mathcal{T} \mid s \geq a_i,\ s+p_i-1 \leq H\}$.
$\mathcal{S}_{it} \subseteq \mathcal{S}_i$	Service-start indices that make i in service at time t: $\mathcal{S}_{it} = \{s \in \mathcal{S}_i \mid s \leq t \leq s+p_i-1\}$.
$\mathcal{C}_i \subseteq \mathcal{T}$	Feasible connection start periods for vessel i: $\mathcal{C}_i = \{s \in \mathcal{T} \mid s \geq a_i,\ s+K_i-1 \leq H\}$.
$\mathcal{Z}$	Set of electrical zones z (SP-BAP only).
Parameters	
a_i	Earliest feasible period (arrival) of vessel i.
p_i	Processing/service duration of vessel i (number of slots).
H	Planning horizon length (number of periods).
l_i	Vessel length.
L_b	Berth length.
$\mathbb{I}_{ib}$	Compatibility indicator: $\mathbb{I}_{ib} = 1$ if $l_i \leq L_b$, else 0.
w_i	Waiting-time weight of vessel i.
Δ	Slot duration in hours.
c_t	Electricity price in period t (€/kWh).
$z(b)$	Berth-to-zone mapping.
C_{zt}	Zone capacity limit (kWh) in zone z at time t.
ρ	Slack penalty coefficient (€/kWh).
$P_{i,k}$	SP demand profile of vessel i at relative index $k = 1,\ldots,K_i$ (kWh), where K_i is profile length (SP-BAP only).
Decision variables	
x_{is}	$= 1$ if vessel i starts *service* at time $s \in \mathcal{S}_i$.
a_{ib}	$= 1$ if vessel i is assigned to berth b.
w_{it}	$= 1$ if vessel i is in service at time t.
o_{ibt}	$= 1$ if vessel i occupies berth b at time t.
y_{ibs}	$= 1$ if vessel i starts SP *connection* at berth b and time $s \in \mathcal{C}_i$ (SP-BAP only).
z_{it}	$= 1$ if vessel i is in SP-connection state at time t (SP-BAP only).
$\xi_{zt} \geq 0$	Nonnegative slack for zone capacity at time t.

$$\sum_{b\in\mathcal{B}} o_{ibt} = w_{it}, \qquad \forall i \in \mathcal{I}, \forall t \in \mathcal{T}, \tag{3.5}$$

$$o_{ibt} \le a_{ib}, \qquad \forall i \in \mathcal{I}, \forall b \in \mathcal{B}, \forall t \in \mathcal{T}, \tag{3.6}$$

$$\sum_{i\in\mathcal{I}} o_{ibt} \le 1, \qquad \forall b \in \mathcal{B}, \forall t \in \mathcal{T}, \tag{3.7}$$

$$a_{ib} \le \mathbb{I}_{ib}, \qquad \forall i \in \mathcal{I},\ \forall b \in \mathcal{B}, \tag{3.8}$$

$$a_{ib} \in \{0,1\},\ o_{ibt} \in \{0,1\}, \qquad \forall i \in \mathcal{I}, \forall b \in \mathcal{B}, \forall t \in \mathcal{T}, \tag{3.9}$$

$$x_{is} \in \{0,1\},\ w_{it} \in \{0,1\}, \qquad \forall i \in \mathcal{I}, \forall s \in \mathcal{S}_i, \forall t \in \mathcal{T}. \tag{3.10}$$

The objective function (3.1) minimizes the total weighted waiting time of vessels. Constraints (3.2) – (3.3) enforce a single berth assignment and a single service start for each vessel. Constraint (3.4) imposes service continuity by linking the in-service indicator w_{it} to the chosen start x_{is}. Constraints (3.5)–(3.6) ensure berth occupancy is consistent with service and only occurs at the assigned berth. Constraint (3.7) enforces the discrete berth capacity (at most one vessel per berth per time slot). Berth compatibility is enforced by bounding a_{ib} and o_{ibt} with $\mathbb{I}_{ib}$ in Constraint (3.8) (i.e., incompatible pairs have upper bound 0 in the implementation).

SP-aware DBAP (SP-BAP)

The SP-BAP extends DBAP by adding (i) a decision on when and where each vessel initiates shore-power connection, (ii) the connection-status trajectory, (iii) zone-level capacity constraints with optional soft slacks, and (iv) electricity cost under time-varying prices. All DBAP constraints (3.2)–(3.10) remain in force. We list the additional SP-related constraints and the modified objective below.

$$\sum_{b\in\mathcal{B}} \sum_{s\in\mathcal{C}_i} y_{ibs} = 1, \qquad \forall i \in \mathcal{I}, \tag{3.11}$$

$$y_{ibs} \le a_{ib}, \qquad \forall i \in \mathcal{I}, \forall b \in \mathcal{B}, \forall s \in \mathcal{C}_i, \tag{3.12}$$

$$y_{ibs} \le o_{ibs}, \qquad \forall i \in \mathcal{I}, \forall b \in \mathcal{B}, \forall s \in \mathcal{C}_i, \tag{3.13}$$

$$z_{it} = \sum_{b\in\mathcal{B}} \sum_{s\in\mathcal{C}_i:\ s\le t\le s+K_i-1} y_{ibs}, \qquad \forall i \in \mathcal{I}, \forall t \in \mathcal{T}. \tag{3.14}$$

Constraint (3.11) ensures that each vessel initiates SP connection exactly once, selecting a unique berth–time pair (b,s). Constraint (3.12) enforces spatial consistency by allowing SP connection only at the berth to which the vessel is assigned. Constraint (3.13) further requires that the vessel is physically occupying the berth at the moment when the SP connection is initiated. Finally, constraint (3.14) derives the period-by-period SP connection status z_{it} from the chosen connection start, such that the vessel remains connected for the entire duration of its SP demand profile. We then enforce temporal consistency between SP connection and berth service through the constraint below:

$$z_{it} \le w_{it}, \qquad \forall i \in \mathcal{I}, \forall t \in \mathcal{T}. \tag{3.15}$$

This constraint means a vessel can draw shore power at time t only if it is simultaneously in service at the berth. In other words, SP connection is prohibited before service starts or after service ends. As a direct consequence, the length of the SP demand profile must not exceed the service duration.

SP capacity limits are enforced at the electrical zone level. Each berth $b \in \mathcal{B}$ is assigned to exactly one zone, denoted by $z(b) \in \mathcal{Z}$. The total SP load in zone z at time t is constrained by:

$$\sum_{i \in I} \sum_{b \in \mathcal{B}:\, z(b)} \sum_{s \in C_i} P_i(t;s)\, y_{ibs} \;\le\; C_{zt} + \xi_{zt}, \qquad \forall z \in \mathcal{Z}, \forall t \in \mathcal{T}, \tag{3.16}$$

$$\xi_{zt} \ge 0, \qquad \forall z \in \mathcal{Z}, \forall t \in \mathcal{T}. \tag{3.17}$$

The term $P_i(t;s)$ denotes the SP energy drawn by vessel i at absolute time t if it initiates SP connection at time s, and is defined as:

$$P_i(t;s) = \begin{cases} P_{i,t-s+1}, & s \le t \le s + K_i - 1, \\ 0, & \text{otherwise.} \end{cases} \tag{3.18}$$

The SP-BAP objective consists of three terms: (i) waiting cost (converted to hours by Δ), (ii) energy cost computed by convolving prices with the SP profile from the chosen connection start, and (iii) penalized capacity slack. So the complete SP-BAP objective is:

$$\begin{aligned} \min \quad & \sum_{i \in I} w_i \sum_{s \in \mathcal{S}_i} (s - a_i) x_{is}\, \Delta \\ & + \sum_{i \in I} \sum_{b \in \mathcal{B}} \sum_{s \in C_i} \sum_{k=1}^{K_i} c_{s+k-1}\, P_{i,k}\, y_{ibs}\, \Delta \\ & + \rho \sum_{z \in \mathcal{Z}} \sum_{t \in \mathcal{T}} \xi_{zt}\, \Delta. \end{aligned} \tag{3.19}$$

Therefore, the complete SP-BAP model consists of the objective function (3.19) and constraints (3.2)–(3.18).

3.4 Solution methodology

This section presents a data-driven predict-then-optimize framework (Bengio et al., 2021; Vanderschueren et al., 2022) to support energy-aware port operations. Figure 3.2 illustrates the pipeline for the work. Based on the problem description, first, raw port event data and vessel technical information are collected and processed to construct port call records. Based on these records, we model the time-grained SP demand profiles. Machine learning models are then developed to predict SP demand using static vessel characteristics, operational and temporal features. The predicted demand is subsequently incorporated into an optimization model described in Section 3.3.2 for berth allocation with SP considerations.

3.4.1 Shore power (SP) modeling

With the structured port call dataset (Section 3.5.1 explains data preprocessing, how to build structured datasets and the definition of several important timestamps), we then model shore

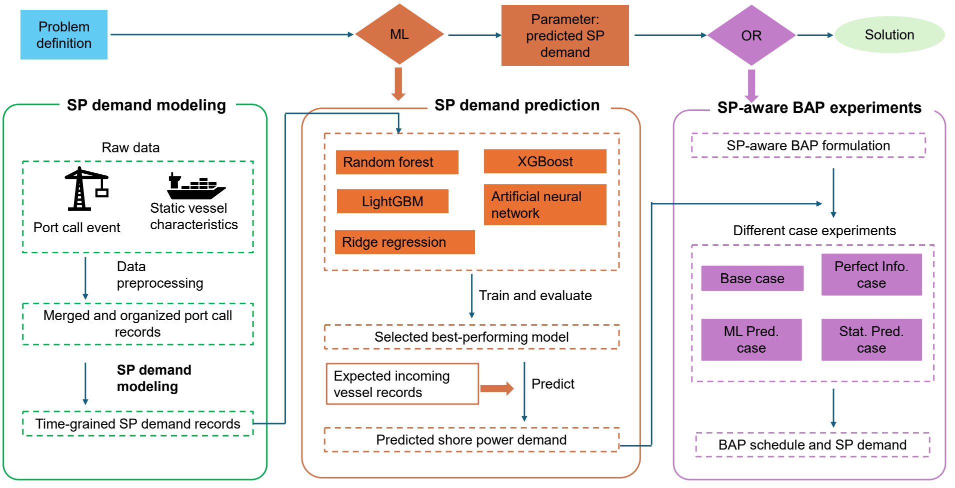

Figure 3.2: Working pipeline for the chapter

power (SP) demand at the vessel level. The modeling procedure translates operation-related timestamps and static vessel characteristics into time-grained SP demand profiles. The procedure includes the following steps.

Operation timeline segmentation and SP power assignment

A distinguishing feature of this study is the segmentation of a vessel's berthing period into multiple time blocks, each associated with a different level of SP load, reflecting realistic shifts in operational intensity. This enables a more fine-grained and behaviorally accurate estimation of SP demand compared to approaches that assume constant or aggregate loads. Typically, demand is lower during non-operational periods (e.g., while waiting to begin or after completing cargo handling), and relatively higher during active discharging and loading operations. When both discharging and loading occur simultaneously, SP demand may further increase due to the concurrent use of onboard equipment and auxiliary systems.

To reflect this temporal variability, we adopt a rule-based power estimation approach that assigns power levels according to operational states. Since SP is applied to replace auxiliary engine when the vessel is berthed at the terminal, we use different level of auxiliary engine power to model the SP power. We define three levels of SP power. In this study, low, normal, and peak power levels are set to 25%, 50%, and 75% of the vessel's rated auxiliary engine power (in eKW), respectively. The estimation of SP demand is based on the segmentation of a vessel's berthing period into operational phases. These phases are identified using timestamps related to arrival, cargo handling activities, and departure. We divide each vessel's berthing period into five stages. Figure 3.3 presents the timeline segmentation in this research with two situations: the overlap or gap period exists.

Stage 1: Pre-handling (arrival to start of cargo operations)

This initial phase is the period between the vessel's actual arrival and the beginning of discharging or loading activities. If this duration is shorter than 15 minutes, the SP power linearly increases to the low-level power (25% of the rated auxiliary engine power). For longer pre-handling periods, the first 15 minutes are set to linearly increase to the low-level power, while the remaining time uses the low-level power.

Stages 2–4: Cargo handling, including possible overlap and gap periods

This set of stages spans from the start to the end of handling operations and accounts for more complex patterns such as overlap between discharging and loading or gaps between the two.

When discharging and loading occur simultaneously (defined as "overlap"), the first 15 minutes are estimated at the normal level power (50 % of rated power), followed by a higher peak level (75 %) for the remaining overlap duration. If the overlap duration is shorter than 30 minutes, that entire overlap is treated as a single continuous handling segment under the normal-to-peak load profile described above. For overlaps longer than 30 minutes, a two-step pattern applies: the first 15 minutes at the normal level, followed by the remaining time at the low level. If a temporal gap exists between discharge and loading operations, and this gap is shorter than 30 minutes, it is treated as part of continuous handling under the normal level. For longer gaps, a two-step pattern is used: the first 15 minutes at the normal level, followed by the remaining time at the low level (25%).

The remaining periods within the total handling window that do not fall into overlap or gap are considered "regular handling" and assigned the normal-level power.

Stage 5: Post-handling (end of operations to departure)

This final phase accounts for the time of vessels at berth after cargo operations finish. If the duration from the end of handling to departure is shorter than 15 minutes, the power is linearly reduced to 0 from the low-level power over that entire period. For longer intervals, the majority of this time is treated as low-level power operation, with only the final 15 minutes

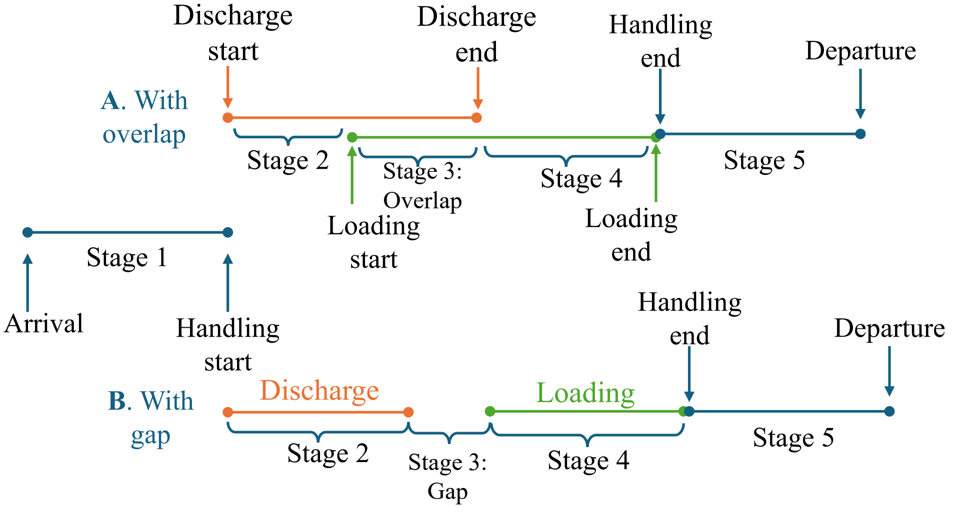

Figure 3.3: Timeline segmentation with overlap and gap

before departure set to reduce to 0 linearly.

SP demand calculation

The modeled SP demand of vessel i is then computed as

$$E_i = P_{it}\,\Delta_t, \tag{3.20}$$

where

$$\begin{aligned} t &= 1,2,\ldots,T, \quad \text{time slots,} \\ P_{it} &= \text{SP power for vessel } i \text{ in time slot } t \text{ (ekW)}, \\ \Delta_t &= \text{duration of the time slot } t \text{ (h)}. \end{aligned}$$

Once the SP power level P_{it} has been determined for each time slot based on the vessel's operational status and auxiliary engine configuration, the corresponding energy demand is calculated by multiplying the power by the duration of that time slot. By dividing the entire berthing period into discrete time intervals (usually in one hour), we obtain the estimation of (hourly) SP demand profile for each vessel.

3.4.2 Machine learning to predict SP demand

We present a framework for predicting SP demand with machine learning methods using features derived from port call and static vessel characteristics datasets. The objective is to assess how accurately the estimated SP demand profiles can be predicted under different data availability conditions, and to compare the performance of commonly used regression models.

We consider several supervised learning models in this study: Random Forest (RF), Extreme Gradient Boosting (XGBoost), LightGBM, Multi-Layer Perceptron (MLP), Tabular Prior-data Fitted Network (TabPFN) (Hollmann et al., 2025) and linear regression with ℓ_2 regularization (Ridge regression, RR). Random Forest (RF) builds an ensemble of decision trees by training each tree on a randomly sampled subset of the data and selecting a random subset of features at each node split. The final prediction is obtained by averaging the outputs of all individual trees. This method reduces variance and increases generalization, making it particularly robust to overfitting and noise. Extreme Gradient Boosting (XGBoost), in contrast, builds trees sequentially. Each tree is trained to correct the residual errors of the preceding trees by minimizing a regularized objective function using gradient descent. The model includes advanced features such as shrinkage (learning rate control), column subsampling, and regularization terms to enhance both predictive performance and generalization. LightGBM is a tree-based gradient boosting framework that builds decision trees in a leaf-wise manner, enabling efficient learning of complex non-linear relationships from structured tabular data. Random Forest, XGBoost, and LightGBM are selected because SP demand exhibits pronounced non-linearities and interaction effects across vessel characteristics, operational stages, and temporal factors. Tree-based ensemble methods are well-suited to capturing such complex relationships without requiring explicit specification of functional forms, and they have demonstrated strong performance in related demand prediction problems. We use Multi-Layer Perceptron (MLP) as a representative feed-forward artificial neural network model in this study. MLP learns non-linear input–output mappings through multiple hidden layers and non-linear activation functions, enabling it to capture complex relationships in the data without requiring explicit feature engineering. Ridge regression (RR) is also included for comparison. Although a linear model is not expected to fully capture the non-linear nature of SP demand, it provides a transparent and interpretable benchmark that reflects a commonly used parametric approach in demand modeling.

Tabular Prior-data Fitted Network (TabPFN) is a transformer-based foundation model for tabular learning. Unlike conventional machine-learning models that are trained separately for each dataset, TabPFN is pre-trained on millions of synthetically generated tabular datasets and performs prediction through in-context learning. This enables the model to transfer knowledge across tasks and directly generalize to unseen datasets. Recent studies have demonstrated that TabPFN achieves strong predictive performance on small- and medium-sized tabular datasets while requiring little or no dataset-specific hyperparameter tuning (Hollmann et al., 2025). Since the SP demand prediction considered in this study is characterized by structured tabular features and a moderate-sized dataset, TabPFN is included in this study.

To better understand the impact of different influencing factors of prediction, we conduct a feature importance analysis using SHAP (SHapley Additive exPlanations) (Lundberg & Lee, 2017). SHAP assigns each feature a contribution value for every individual prediction, based on a cooperative game-theoretic framework. SHAP values are computed by considering all possible permutations of feature inclusion, measuring the marginal effect of each feature on the prediction outcome. For tree-based models such as Random Forest and XGBoost, the SHAP TreeExplainer provides a fast and exact solution to calculate feature contributions across all samples. The global feature importance is then obtained by averaging the absolute SHAP values over the entire dataset.

3.5 Experimental study

We use the historical port call records and static vessel information to model the SP demand. To ensure the transferability of the proposed shore power (SP) demand modeling framework, experiments are conducted using data from two major container ports: the Port of Hamburg and the Port of Hong Kong.

3.5.1 Data sources

For the Port of Hamburg, we obtain port call data from the port logistics company HHLA. The HHLA COAST platform (HHLA, 2025) is an online interface offering historical port call records in the form of sailing lists, which include vessel names, arrival and departure timestamps, and start and end timestamps of cargo handling, etc. We extract port call records of the Container Terminal Altenwerder (CTA) from this platform over a continuous time window, covering March 5, 2024, to June 2, 2024. The extracted data includes seagoing vessels, feeders and barges. Each row in the dataset represents a distinct port call, which is treated as a continuous stay at the terminal. In total, the dataset includes 474 port calls from 153 distinct vessels.

For the Port of Hong Kong, we obtain data from the Hong Kong Marine Department Hong Kong Government (2025), which provides official records of ship traffic within Hong Kong water areas. We extract records within the Kwai Tsing Container Port, which is a major container port area in Hong Kong comprising multiple container terminals. The Hong Kong dataset only has vessel identifier, vessel arrival and departure times, but does not include operation-related timestamps. The extracted dataset covers a continuous time period from January 1, 2023 to August 15, 2025.

To complement the datasets for the following experiments, static vessel characteristics are retrieved from the Clarksons World Fleet Register (WFR, Clarksons Research (2025)). This database provides vessel information, including ship dimensions, capacity indicators, auxiliary engine configurations, etc. As shown in Table 3.4, port call data include vessel identification details (e.g., name, call sign) and static voyage information (e.g., ATA and ATD), whereas WFR dataset provides static dimensions such as LOA, MID BEAM, and draft.

Prior to SP demand estimation, we remove records with missing key identifiers or timestamps and duplicate rows. Port call datasets are then merged with static vessel characteristics.

Two aspects of the data used in this chapter should be highlighted for correct interpretation of the results. First, the shore power demand profiles used as prediction targets are not measured vessel-level shore power draws but are modeled from operational timestamps and assumed

Table 3.4: Overview of data availability across different data sources

Data feature	**HK port calls**	**HB port calls**	**Clarksons WFR**
Call sign	✓	✓	✓
Vessel name	✓	✓	✓
Actual arrival time (ATA)	✓	✓	
Actual departure time (ATD)	✓	✓	
Start of discharge		✓	
End of discharge		✓	
Start of loading		✓	
End of loading		✓	
Vessel length (LOA)			✓
Vessel width (MID BEAM)			✓
Draft			✓
TEU capacity			✓
Deadweight tonnage (DWT)			✓
Built year			✓
Vessel type (size)		✓	
Vessel type (purpose)			✓
Auxiliary engine Info.			✓

Notes: HK = Hong Kong; HB = Hamburg.
Vessel type (size): Seagoing vessel, feeder and barge.
Vessel type (purpose): Containership, bulk carrier, oil tank, LNG, offshore ship, special purpose ship, etc.
Auxiliary engine Info.: Auxiliary engine configuration and rated electrical power (eKw)

operational load levels, expressed as fractions of the rated auxiliary engine power (see Section 3.4.1). Second, the Hong Kong dataset does not include operation-related timestamps, and these are synthetically reconstructed from ratios of berthing duration fitted on the Hamburg dataset, as detailed in Section 3.5.2. Taken together, the numerical results in this chapter should be interpreted primarily as demonstrating the usefulness of the proposed modeling and decision-support framework — the segmentation-based shore power demand model, the machine-learning prediction pipeline, and the SP-aware berth allocation formulation — rather than as a full empirical validation of realized shore power consumption.

3.5.2 Data preprocessing

Prior to SP demand modeling, we first remove records with missing key identifiers or timestamps and duplicate rows. With the cleaned event-level datasets, a key preprocessing challenge arises for the Hong Kong case study, where vessel movements are reported as separate arrival and departure events rather than integrated vessel visits. To complete vessel stays from these disaggregated records, we construct a composite matching key by concatenating the vessel call sign and the berth identifier. Records without a valid matching key are excluded, as they cannot be reliably linked across arrival and departure event tables. Within each matching-key group, arrival and departure events are paired with chronological order.

After completing vessel visits, static vessel characteristics are merged into both port call datasets from the Clarksons WFR using the call sign as the vessel identifier. The merge restricts the following experiments to seagoing and feeder vessels for which static characteristics are available, while excluding barges that lack static characteristics. This filtering is also consistent with the scope of this study.

Since the Hong Kong dataset does not include operation-related timestamps, we then need to generate synthetic timestamps of discharge and loading activities for the Hong Kong dataset by transferring operational patterns from the Hamburg dataset. For each Hamburg port call, the total berthing duration is defined as

$$D = t^{\mathrm{ATD}} - t^{\mathrm{ATA}}, \tag{3.21}$$

where t^{ATA} and t^{ATD} denote the actual arrival and departure times, respectively. Based on observed operational timestamps, four ratios are computed:

$$r_W^{\mathrm{dis}} = \frac{t_{\mathrm{start}}^{\mathrm{dis}} - t^{\mathrm{ATA}}}{D}, \quad r_T^{\mathrm{dis}} = \frac{t_{\mathrm{end}}^{\mathrm{dis}} - t_{\mathrm{start}}^{\mathrm{dis}}}{D}, \tag{3.22}$$

$$r_W^{\mathrm{load}} = \frac{t_{\mathrm{start}}^{\mathrm{load}} - t^{\mathrm{ATA}}}{D}, \quad r_T^{\mathrm{load}} = \frac{t_{\mathrm{end}}^{\mathrm{load}} - t_{\mathrm{start}}^{\mathrm{load}}}{D}. \tag{3.23}$$

These ratios represent waiting times before discharge and loading, as well as the durations of discharge and loading, all normalized by the total berthing duration. Because these ratios vary across vessel calls but are bounded between 0 and 1, they are modeled using Beta distributions. In addition, we explicitly account for the fact that some vessel calls do not involve discharge or loading by estimating the corresponding probabilities of non-activity.

For each Hong Kong visit with observed arrival and departure times, the corresponding berthing duration D is first computed. Ratio values are then sampled from the fitted Beta distributions and converted back to absolute durations by multiplying by D. The resulting discharge and loading start and end times are reconstructed relative to the arrival time. To avoid infeasible timestamps at the boundaries of a visit, all synthesized operation times are constrained to the interval

$$\left[t^{\mathrm{ATA}} + \Delta_b,\; t^{\mathrm{ATD}} - \Delta_b\right], \tag{3.24}$$

where Δ_b denotes a minimum buffer duration set to 0.25 hours. This augmentation procedure supplements the Hong Kong dataset with operation-related timestamps, enabling subsequent SP demand modeling and prediction.

Operation-related timestamp definition

Following the data preprocessing, each vessel call is represented by a sequence of operational stages defined over its stay at the terminal. For each vessel call, we define the following timestamps and durations: Start of Handling (the earlier of discharge start or loading start), End of Handling (the later of discharge end or loading end), Overlap Start / End (the time window during which discharging and loading operations occurred simultaneously), Gap Start / End (the time window between the end of one operation (e.g., discharge) and the start of the other (e.g., loading), where neither handling process was active), Berthing duration (from actual arrival to actual departure), Waiting duration before handling (from actual arrival to start of handling), Waiting duration after handling (from end of handling to actual departure), Overlap duration (from overlap start to overlap end), Gap duration (from gap start to gap end).

With these timestamps, we then divide the timeline of each vessel berth duration into different stages using the modeling method described in Section 3.4.1 and model the SP demand.

3.5.3 Machine learning model training and evaluation

With the modeled SP demand by the method in Section 3.4.1, we then construct input features and target variables, followed by the machine learning (ML) model training and evaluation procedure.

Feature and target construction

To train ML models for hourly SP demand, we begin by defining the learning target Y and the feature set X. The prediction task is conducted at the time slot level, and one time slot represents one hour. For each vessel i and time slot t, the target variable $Y_i(t)$ is defined as the SP demand modeled in Section 3.4.1. The feature vector $X_i(t)$ consists of three categories of explanatory variables.

The first category includes temporal features derived from the vessel arrival time, such as the month of arrival, day of the week, and hour of the day. The second category comprises static vessel characteristics obtained from the WFR database, including size-related attributes and auxiliary engine power. The third category includes indicators describing the vessel's operational state at time slot t, such as whether cargo handling is ongoing and whether discharge and loading activities overlap.

To explore the influence of available information on model performance and deployment feasibility, we construct two input feature sets X. The input features are summarized as follows.

The *Full-Insight feature set* includes Arrival month, Arrival day, Arrival day of the week (i.e., Monday–Sunday), Arrival hour, LOA (length of the vessel), MID BEAM (mid-width of the vessel), Draft, DWT (deadweight tonnage), TEU, Age, Rated auxiliary engine power and some operation-related features: Slot_frac (the relative position of a time slot within a vessel's berth stay, expressed as a fraction of the total stay duration), Stay_time (the total stay time (in the number of time slots) of the vessel at the terminal), is_handling (a binary indicator equal to 1 if cargo handling operations (discharge or loading) are ongoing in the current time slot, and 0 otherwise), is_overlap (a binary indicator equal to 1 if discharge and loading activities occur simultaneously in the current time slot, and 0 otherwise) and is_gap (a binary indicator equal to 1 if the current time slot falls within an idle gap between discharge and loading activities). The *Operational-Planning feature set* includes Arrival month, Arrival day, Arrival day of the week, Arrival hour, LOA, MID BEAM, Draft, DWT, TEU, Age, Rated auxiliary engine power, Slot_frac, and Stay_time.

The *Full-Insight Feature Set* includes both static vessel characteristics and operational-related variables that are only known after the completion of a vessel call. This set represents an "offline" learning setting, in which the model is trained with complete historical knowledge. The *Operational-Planning Feature Set* includes only those features that are realistically observable prior to a vessel's arrival at berth. These include static physical vessel dimensions, auxiliary engine power, arrival time information, and berthing duration. This set imitates a "pre-arrival" scenario, aligning more closely with the restrictions of SP usage planning in real-world port operations. For linear regression models, features are standardized prior to training, while tree-based models are trained on the original feature scales.

Model training

ML models are trained separately for the Hamburg and Hong Kong datasets. Each dataset is organized at the time-slot level, where each record corresponds to a feature vector $X_i(t)$ describing vessel and operational characteristics in a given time slot and an associated target value $Y_i(t)$ representing SP demand. The datasets are split into training and test sets. We train each ML models multiple times with cross-validation. Since the Hong Kong dataset contains a sufficiently large amount of historical records, hyperparameter tuning is conducted to reduce the risk of overfitting. The large sample size allows the model to be trained and validated under multiple parameter settings while maintaining sufficient data for reliable performance evaluation.

Evaluation metrics

We evaluate model performance using different metrics. We use $\hat{Y}_i(t)$ to denote the predicted SP demand and $Y_i(t)$ the modeled demand for vessel i in time slot t, and let N denote the total number of observations in the test set.

The mean absolute error (MAE) is used to measure the average magnitude of prediction errors,

$$\mathrm{MAE} = \frac{1}{N}\sum_{i,t}\left|\hat{Y}_i(t) - Y_i(t)\right|, \tag{3.25}$$

which provides an intuitive measure of typical deviation between predicted and modeled SP demand.

The root mean squared error (RMSE) is employed to place greater emphasis on larger prediction errors:

$$\mathrm{RMSE} = \sqrt{\frac{1}{N}\sum_{i,t}\left(\hat{Y}_i(t) - Y_i(t)\right)^2}. \tag{3.26}$$

In addition, the coefficient of determination (R^2) measures the proportion of variance in the observed data that is explained by the model. It indicates how well the model predictions fit the actual data, with values closer to 1 suggesting a better fit:

$$R^2 = 1 - \frac{\sum_{i,t}\left(\hat{Y}_i(t) - Y_i(t)\right)^2}{\sum_{i,t}\left(Y_i(t) - \bar{Y}\right)^2}, \tag{3.27}$$

where $\bar{Y}$ denotes the mean value of the modeled SP demand values in the evaluation set.

Model performance comparison and analysis

Six ML models are trained and evaluated in this section: Random Forest (RF), eXtreme Gradient Boosting (XGBoost), Light Gradient Boosting Machine (LightGBM), Multi-Layer Perceptron (MLP), Tabular Prior-data Fitted Network (TabPFN) (Grinsztajn et al., 2025), and Ridge Regression (RR). For the Port of Hamburg, models are trained under two feature sets, namely the Full-Insight and Operational Planning feature sets. To mitigate the influence of randomness, each model is trained and evaluated over multiple cross-validation runs, with a different split of the dataset in each run. The results reported in Table 3.5 are the mean performance metrics averaged across these runs.

Under the *Full-Insight feature set*, which incorporates detailed operation-related indicators, all non-linear models achieve strong predictive performance. RF and XGBoost obtain the lowest MAE values, while TabPFN achieves the lowest RMSE (450.98) and the highest R^2 value (0.988), indicating superior overall predictive accuracy. LightGBM performs slightly worse, exhibiting noticeably higher MAE and RMSE values compared to RF, XGBoost, and TabPFN. The MLP also achieves competitive performance under the Full-Insight setting, outperforming LightGBM and approaching the accuracy of the best-performing models. In contrast, the RR performs substantially worse. Despite RR achieving a moderate R^2 of 0.913, its MAE and RMSE are significantly higher than those of the non-linear models. These results confirm that SP demand exhibits strong non-linear and state-dependent characteristics that cannot be adequately represented by the linear model. Non-linear models are well-suited to capture the complex temporal dynamics of SP demand when sufficient operational information is available. Under the *Operational–Planning feature set*, prediction accuracy deteriorates across all models due to the reduced availability of explanatory variables. Nevertheless, RF, XGBoost, LightGBM, and TabPFN all substantially outperform RR, maintaining R^2 values close to or above 0.89. Among these models, TabPFN achieves the highest R^2 (0.893), while RF, XGBoost, and LightGBM

Table 3.5: Prediction performance of different machine learning methods on the Hamburg and Hong Kong dataset under two feature sets

Feature set	**Model**	**MAE**	**RMSE**	R^2
HB Full-Insight	RF	259.11	491.54	0.986
	XGB	257.34	480.85	0.986
	LightGBM	322.42	572.13	0.981
	MLP	313.65	540.27	0.983
	TabPFN	261.32	450.98	0.988
	RR	903.75	1217.55	0.913
HB Operational Planning	RF	845.64	1306.26	0.884
	XGB	851.32	1337.14	0.892
	LightGBM	830.31	1339.90	0.891
	MLP	996.78	1513.08	0.861
	TabPFN	846.75	1323.40	0.893
	RR	1399.13	1946.39	0.778
HK Operational Planning	RF	882.087	1358.113	0.755
	XGB	882.891	1346.979	0.759
	LightGBM	935.364	1408.839	0.737
	MLP	950.222	1424.847	0.730
	TabPFN	913.47	1375.74	0.753
	RR	1166.053	1710.898	0.621

Notes: HB = Hamburg, HK= Hong Kong, RF = Random Forest, XGB = eXtreme Gradient Boosting, LightGBM = Light Gradient Boosting Machine, MLP = Multi-Layer Perceptron, TabPFN = Tabular Prior-data Fitted Network, RR = Ridge Regression.

obtain slightly lower prediction errors in terms of MAE or RMSE. Overall, the results indicate that tree-based ensemble methods and TabPFN are better at extracting useful predictive information from the limited feature set available during operational planning. The comparison across feature sets highlights that operational observability plays a critical role in achieving high prediction accuracy. While prediction accuracy decreases when only operational–planning information is available, tree-based ensemble methods and TabPFN remain relatively robust and consistently deliver strong predictive performance.

For the Hong Kong dataset, we use the Operational-Planning feature set for model training and evaluation. The choice is motivated by both data-related and practical considerations. The operation-related timestamps in the Hong Kong dataset (e.g., start and end times of loading and unloading) are not directly observed but synthetically generated. Although these synthetic timestamps are constructed to mimic the distribution characteristics of the Hamburg dataset, they do not fully capture the inherent interactions among operational variables observed in real port operations. From a practical port operations perspective, the information available to terminal operators at the prediction stage is limited. Features that are theoretically unknown prior to the arrival of vessels, such as the precise start and end times of cargo handling activities, are typically unavailable when SP demand prediction is required. To mitigate overfitting on the HK dataset, we conducted cross-validation-based hyperparameter tuning for RF, XGBoost, LightGBM and MLP. The resulting optimal hyperparameter configurations are summarized in Table 3.6. TabPFN is evaluated using its default configuration, as it is designed to provide strong performance without dataset-specific hyperparameter tuning.

Table 3.6: Hyperparameter tuning results for different models (HK dataset).

Model	**Hyperparameter**	**Search range**	**Selected value**
RF	n_estimators	[200, 250, 300, 350, 400, 450, 500]	400
	min_samples_split	[2, 4, 5, 6, 8, 10]	6
	min_samples_leaf	[1, 2, 3, 4]	4
	max_depth	[6, 8, 10, 12]	8
XGBoost	n_estimators	[300, 400, 500, 600, 800]	500
	learning_rate	[0.01, 0.03, 0.05, 0.1]	0.01
	max_depth	[3, 4, 5, 6, 7, 8]	3
	subsample	[0.6, 0.8, 1.0]	0.6
	gamma	[0.0, 0.1, 0.2, 0.3]	0.2
LightGBM	n_estimators	[300, 400, 500, 600, 800]	500
	learning_rate	[0.01, 0.03, 0.05, 0.1]	0.01
	num_leaves	[25, 50, 75, 100, 125]	125
	max_depth	[1, 2, 4, 6, 8, 10]	4
	min_child_samples	[10, 20, 35, 50, 75]	35
MLP	hidden_layer_sizes	[(64, 64), (128, 64), (128, 128)]	(64, 64)
	activation	[relu, tanh]	relu
	batch_size	[128, 256, 384]	128

With the tuned hyperparameters, Table 3.5 (“HK Operational planning” Part) presents the prediction outcomes. Overall, prediction accuracy under the Hong Kong dataset is noticeably lower than that observed for the Hamburg dataset, reflecting the increased difficulty of demand prediction when only limited features are available. Among the non-linear approaches, XGBoost achieves the best overall performance, obtaining the highest R^2 (0.759) and the lowest RMSE (1346.979). RF delivers nearly identical performance, with only marginally higher prediction errors. TabPFN also demonstrates competitive results, achieving an R^2 of 0.753 and prediction errors that are close to those of RF and XGBoost. LightGBM and MLP exhibit larger prediction errors and lower explanatory power. These results suggest that, under restricted feature information, more complex boosting or neural network models do not necessarily translate into superior performance. In contrast, RR exhibits the weakest performance, with the highest MAE (1166.053), the largest RMSE (1710.898), and the lowest R^2 (0.621). This confirms that under limited feature availability, the linear model is less capable of capturing the non-linear and state-dependent characteristics of SP demand.

Compared with the Hamburg results, consistent patterns emerge: First, non-linear methods systematically outperform linear models across both ports. RF, XGBoost, and TabPFN consistently form the group of best-performing models, indicating their stronger capability to extract predictive information from limited operational features. Third, all ML models achieve lower prediction accuracy on the Hong Kong dataset than on the Hamburg dataset, which may stem from differences in data characteristics. In contrast to Hamburg, where operation-related timestamps are directly observed, the Hong Kong operation-related features are synthetically constructed, potentially introducing additional noise into the dataset. These findings further support the suitability of RF, XGBoost, and TabPFN for SP demand prediction in practical planning environments.

Feature importance analysis

As explained in Section 3.4.2, we apply SHAP to analyze feature importance. The XGBoost model is selected for feature importance analysis due to its consistently competitive predictive performance across the experiments. For each setting, global importance is computed as the mean absolute SHAP value across all samples.

Figure 3.4 presents the SHAP feature importance analysis result for the XGBoost model trained on the Hamburg dataset when we use the full-insight feature set. The auxiliary engine `rated_power` ("aux_power" in the figure) clearly dominates all other features, indicating that the installed auxiliary capacity is the primary determinant of SP demand. This result is physically intuitive, as rated power directly constrains the maximum electrical energy consumption during port stays. Beyond `rated_power`, several operation-related features contribute substantially. In particular, `is_overlap` ("load/disc_overlap" in the figure) and `is_handling` ("cargo_handling" in the figure) rank among the most influential variables, highlighting the importance of overlapping operations and active cargo handling periods. These features capture real-time operational dynamics that strongly affect SP demand. Static vessel characteristics, represented by `beam_mid`, also exhibit a contribution, suggesting that vessel size influences SP demand beyond the rated auxiliary engine power. In contrast, arrival-time-related variables (e.g., arrival hour, day, and month) play only a minor role when rich operational information is available.

When the input features are restricted to the operational-planning feature set, the importance structure changes noticeably, as illustrated in Figure 3.5. Although `rated_power` remains the most influential feature, operational state variables such as `is_overlap` and `is_handling` are no longer available. Consequently, the model relies more heavily on static vessel characteristics. In this setting, `slot_fraction` becomes the second most important feature, exhibiting both positive and negative contributions across observations. Vessel size-related attributes, including `beam_mid`, `TEU`, and `DWT`, also show increased importance compared to the full-insight case. Temporal variables related to vessel arrival (e.g., `arrival_day`, `arrival_hour`, and `arrival_month`) remain clustered around zero SHAP values, suggesting that they provide little additional explanatory power in this setting. Overall, the results highlight that, when real-time operational indicators are unavailable, the model shifts its reliance toward a combination of vessel characteristics, while still capturing non-linear demand patterns through features such as `slot_fraction`.

Figure 3.6 shows the SHAP feature importance analysis results for the XGBoost model trained on the Hong Kong dataset using the operational-planning feature set. A similar pattern to the Hamburg case is observed. Again, `rated_power` is the most influential factor, followed

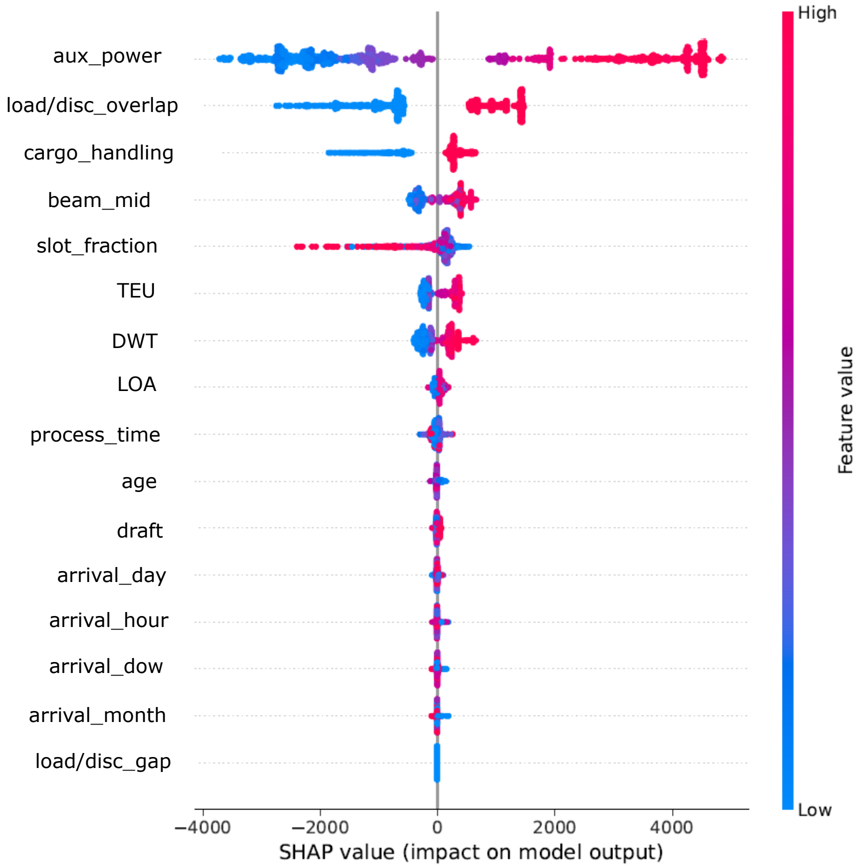

Figure 3.4: SHAP feature importance analysis for the XGBoost model trained on the Hamburg dataset using the full-insight feature set

by `slot_fraction`, confirming the central role of installed auxiliary capacity and the temporal position of a vessel within its port call for SP demand prediction. However, the contribution of secondary features is noticeably weaker than in the Hamburg dataset. Most vessel characteristics and temporal variables exhibit very small SHAP values, indicating limited additional explanatory power. This concentration of importance on a small subset of features reflects the more limited information content of the Hong Kong dataset. The model relies primarily on rated power and non-operational features, which is consistent with the comparatively lower predictive performance observed for the Hong Kong dataset.

3.5.4 SP-aware BAP experiments

To quantify how SP demand prediction affects berth allocation decision, we compare four different planning cases that differ only in the information used to construct the SP demand profiles. The four cases considered are Base Case, Perfect Information (Perfect Info.) Case,

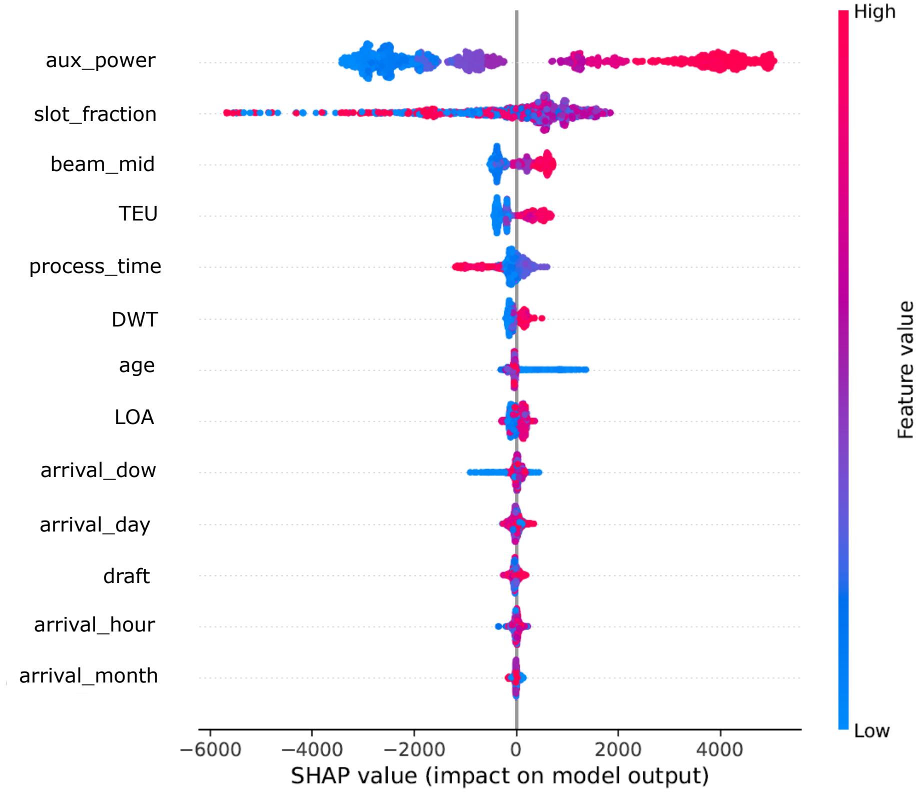

Figure 3.5: SHAP feature importance analysis for the XGBoost model trained on the Hamburg dataset using the operational-planning feature set

Machine-learning-based Prediction (ML Pred.) Case, and Statistical Prediction (Stat. Pred.) Case.

Base Case. In the Base Case, berth allocation and vessel scheduling are determined by solving the standard discrete BAP (DBAP) without considering SP-related constraints or energy costs. Given the resulting berth assignments and vessel scheduling, combining the provided SP demand profile, we calculate the associated energy and penalty costs. The total cost is obtained by summing up the waiting cost from the DBAP solution, the energy and penalty costs. This case reflects the baseline planning in which berth allocation decisions are made independently of detailed energy considerations.

Perfect Information (Perfect Info.) Case. In the Perfect Information Case, vessel-specific SP demand profiles are assumed to be known exactly in advance and are fully incorporated into the SP-aware BAP optimization. This case represents an ideal benchmark, providing a cost value under complete and accurate demand information, and serves as a reference against which prediction approaches can be evaluated.

Machine-Learning-Based Prediction (ML Pred.) Case. SP demand profiles are generated

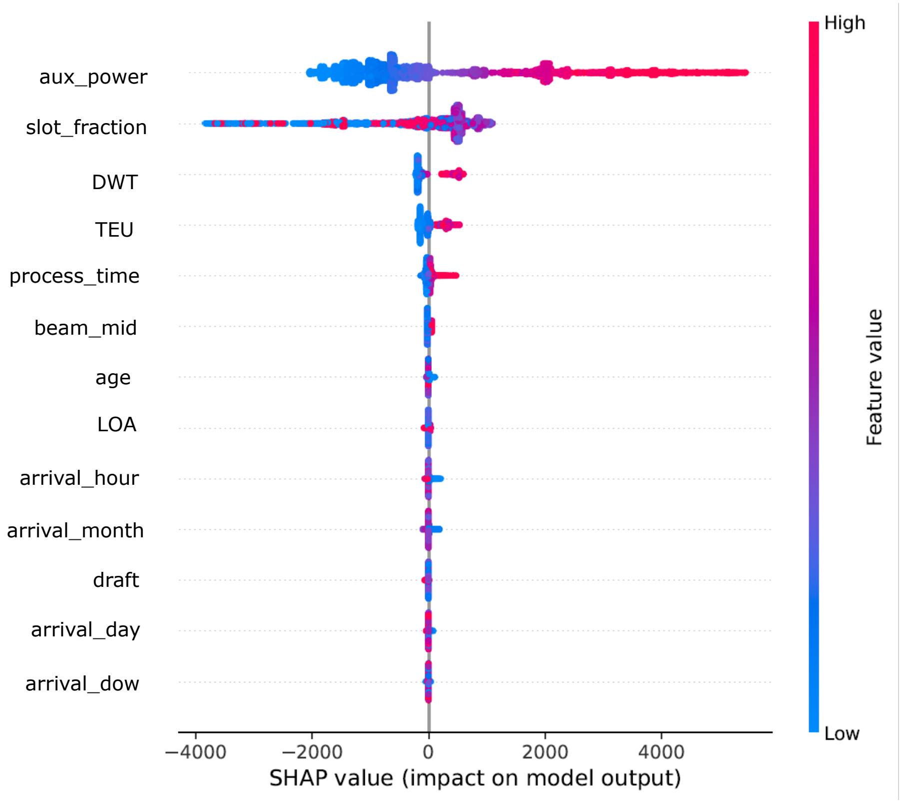

Figure 3.6: SHAP feature importance analysis for the XGBoost model trained on the Hong Kong dataset using the operational-planning feature set

using the machine-learning prediction framework (RF, XGBoost, LightGBM, MLP, TabPFN), based on information available prior to vessel arrival using the operational-planning feature set. This case reflects a data-driven planning scenario.

Statistical-Based Prediction (Stat. Pred.) Case. SP demand is estimated using a simple, intuitive statistical method. This case represents a low-complexity substitute for ML-based prediction methods. In the Stat.-based prediction case, SP demand profiles are generated using a classical time-series forecasting approach, the Holt–Winters exponential smoothing method. It is adopted as a representative statistical baseline because of its simplicity, robustness, and widespread use in short-term operational forecasting (Rumbe et al., 2024; Tjøstheim, 2025). It provides an intuitive benchmark that reflects how SP demand might be estimated in practice when limited information is available. The method captures level and trend components in historical SP demand data and produces smoothed demand trajectories without relying on vessel-specific explanatory variables. Only historical SP observations prior to the planning horizon are used, making this approach computationally lightweight.

All SP-aware BAP experiments are conducted using historical data from the Port of Hong Kong. It is selected because of its large data volume, which allows for statistically meaningful evaluation. The considered terminal consists of 4 berths, all connected to a single electrical zone with a shared SP capacity constraint. The experiments have two sets. Each set consists of vessel call records extracted from a consecutive multi-day time window. Specifically, Set 1 covers a three-day period from 2025-08-04 to 2025-08-07 and includes 18 vessel calls. Set 2 corresponds to a five-day period from 2025-08-04 to 2025-08-09 and involves 31 vessel calls. Tables 3.7 and 3.8 present the cost comparison results for Set 1 and Set 2 based on realized costs, i.e., all solutions are evaluated under the true SP demand. We first solve the SP-BAP model and get the solution for vessel schedule and berth allocation, and then calculate the corresponding energy and penalty costs with the realized SP demand. In both tables, percentage values quantify the deviation from a chosen benchmark rather than absolute cost reductions. In particular, comparisons with the Perfect Info. case indicate how closely a prediction-based approach approximates the ideal planning outcome under complete demand information. This provides a consistent and fair comparison across different prediction approaches.

Table 3.7: Cost comparison for Set 1 under different prediction methods (with realized cost).

Method	**Waiting cost**	**Energy cost**	**Penalty cost**	**Total realized cost**	**Gap to Perfect Info. (%)**
Perfect information	30,420.00	217,147.10	0.00	247,567.10	0.00
Base case (no prediction)	13,320.00	229,811.63	18,143.74	261,275.37	5.54
Random Forest (RF)	20,160.00	220,006.90	18,143.74	258,310.63	4.34
XGBoost	20,160.00	220,006.90	18,143.74	258,310.63	4.34
LightGBM	20,160.00	220,006.90	18,143.74	258,310.63	4.34
Multi-Layer Perceptron (MLP)	20,520.00	219,554.49	18,143.74	258,218.23	4.30
TabPFN	21,780.00	219,406.94	16,508.30	257,695.24	4.09
Holt–Winters ES	13,320.00	229,811.63	18,143.74	261,275.37	5.54

Notes: ES = Exponential Smoothing

Table 3.8: Cost comparison for Set 2 under different prediction methods (with realized cost).

Method	**Waiting cost**	**Energy cost**	**Penalty cost**	**Total realized cost**	**Gap to Perfect Info. (%)**
Perfect information	54,180.00	385,400.71	0.00	439,580.71	0.00
Base case (no prediction)	34,380.00	392,734.49	170,981.45	598,095.94	36.06
Random Forest (RF)	41,760.00	386,895.30	58,856.91	487,512.21	10.90
XGBoost	38,880.00	387,103.84	106,545.18	532,529.02	21.14
LightGBM	40,320.00	387,071.57	77,954.64	505,346.21	14.96
Multi-Layer Perceptron (MLP)	40,860.00	389,575.87	29,600.31	460,036.18	4.65
TabPFN	44,819.99	389,271.93	17,742.77	451,834.69	2.79
Holt–Winters ES	36,540.00	390,360.58	176,998.38	603,898.95	37.38

Notes: ES = Exponential Smoothing

For Set 1 (Table 3.7), the Perfect Info. case achieves the lowest total cost, serving as an ideal benchmark. The Base case and the Holt–Winters exponential smoothing (ES) approach yield identical results, both showing a gap of 5.54% relative to the Perfect Information case. This indicates that the statistical method fails to provide useful guidance for decision-making and leads to the same scheduling outcome as the case without prediction. All ML-based approaches (RF, XGBoost, LightGBM, MLP, and TabPFN) reduce the total realized cost compared to the Base case, achieving gaps between 4.09% and 4.34%. RF, XGBoost, and LightGBM produce identical realized costs, while MLP achieves a slightly lower total cost. Among all methods, TabPFN delivers the best performance, with the lowest total realized cost and a gap of only 4.09% relative to the Perfect Information benchmark. The improvement is mainly attributable to a reduction in realized penalty costs, indicating that the demand estimates generated by TabPFN lead to scheduling decisions that are slightly more effective in mitigating SP capacity violations. Nevertheless, the overall differences among ML-based approaches remain relatively small, suggesting that for Set 1 the solution quality is primarily determined by the availability of reasonably accurate demand estimates rather than by the specific prediction model adopted.

For Set 2 (Table 3.8), the impact of incorporating SP demand information becomes more pronounced. In the Base case, ignoring SP constraints results in substantial capacity violations, leading to extremely high penalty costs and a total cost that is 36.06% higher than the Perfect Information benchmark. In contrast, all ML-based approaches significantly reduce penalty costs and total cost by incorporating demand predictions into the optimization process. Compared to Set 1, the differences among ML-based methods become more substantial in Set 2. Among them, TabPFN achieves the best performance, with a gap of only 2.79% relative to the Perfect Information case. The model yields the lowest realized penalty cost among all prediction approaches, indicating that its demand prediction enables more effective capacity-aware berth allocation decisions. MLP also performs well, achieving a gap of 4.65% and ranking second among all methods. RF and LightGBM provide moderate performance, while XGBoost exhibits a larger deviation from the benchmark, mainly due to higher realized penalty costs. The statistical approach (Holt–Winters ES) again performs poorly, resulting in the highest total cost and a gap of 37.38%. This is even worse than the Base case, indicating that inaccurate demand prediction may mislead the optimization process and lead to inferior operational outcomes.

Overall, the results demonstrate that ML-based SP demand prediction provides a reliable basis for integrated berth allocation and energy planning, consistently producing solutions close to the Perfect Information benchmark. In contrast, statistical methods that fail to capture demand variability may not only provide limited benefits but can also degrade performance under realistic demand conditions.

While the tables present cost outcomes, Figure 3.7 - 3.10 provide additional insights into the temporal pattern of SP demand. Figures 3.7 and 3.9 illustrate aggregated terminal-level SP demand profiles for all vessels in the planning horizon in Set 1 and Set 2. Each figure compares the Base case, Perfect Info. case, ML Pred. case, and Stat. Pred. case against the capacity limit. We choose the TabPFN model to represent ML method in Figure 3.7 and Figure 3.9.

As shown in Figure 3.7, the SP demand lines obtained in Perfect Info. and ML Pred. case exhibit similar temporal patterns throughout the planning horizon. Both curves closely track each other and remain largely aligned with the capacity constraint, with only limited excursions beyond the threshold. This visual proximity is consistent with the cost results in Table 3.7, where the ML-based solution yields a total cost close to the Perfect Info. benchmark. The Stat.-based

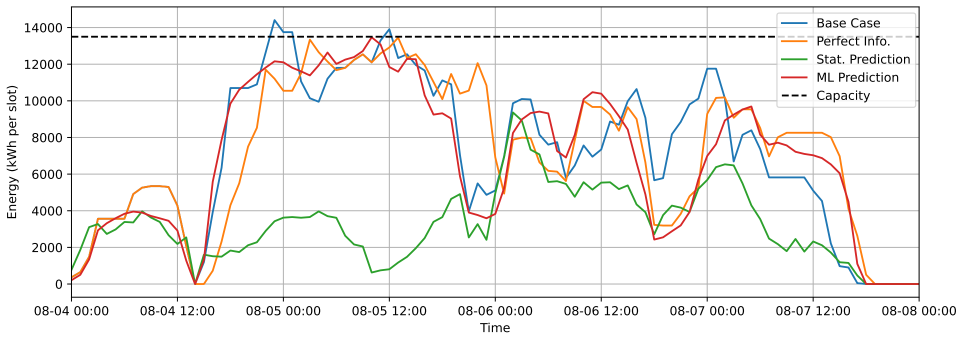

Figure 3.7: Aggregated terminal-level SP demand profiles for Set 1 (2025-08-04 to 2025-08-07), comparing the Base Case (without SP consideration), Perfect Info. Case, ML Pred. Case (with TabPFN method) and Stat. Pred. Case against the zone capacity limit

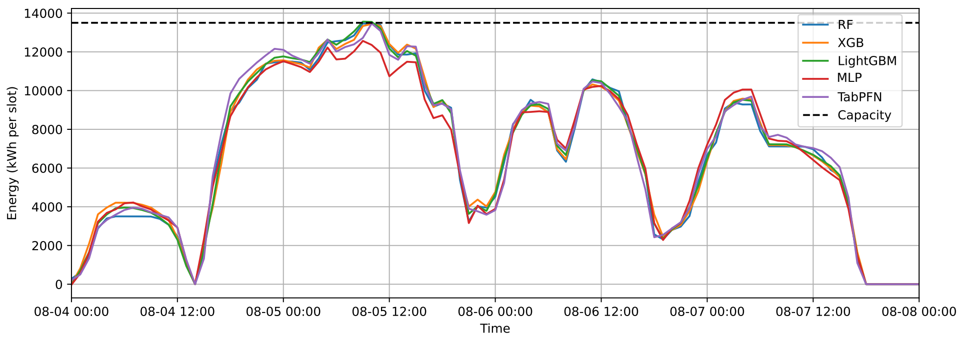

Figure 3.8: Aggregated terminal-level SP demand profiles for Set 1 (2025-08-04 to 2025-08-07), comparing different machine learning prediction methods including Random Forest, XGBoost, LightGBM, MLP and TabPFN

SP demand profile exhibits considerably lower values, reflecting a systematic underprediction of SP demand. By contrast, the Base Case, which ignores SP considerations during optimization, shows more pronounced and irregular peaks, explaining the presence of non-negligible penalty costs observed in Table 3.7.

Figure 3.9 depicts a larger-scale test instance with more vessel calls. In this setting, the Base Case profile sometimes exceeds the zone capacity limit, resulting in severe violations and high penalty costs. This behavior directly corresponds to the dominant penalty cost component presented in the result of the Base Case in Table 3.8. Both the Perfect Info. and ML-based profiles substantially reduce the violation by reshaping SP demand over time. Notably, the ML-based profile closely follows the Perfect Info. trajectory across most of the horizon. This strong temporal alignment explains why the ML-based solution differs from the Perfect Info. benchmark by only a small gap in total cost. Again, the Stat.-based profile displays significantly lower demand levels. This profile remains well below the capacity limit, and the suppressed values do not reflect realistic SP demand patterns. Across both sets, the figures reinforce the conclusion drawn from the cost tables: ML-based SP demand prediction consistently produces

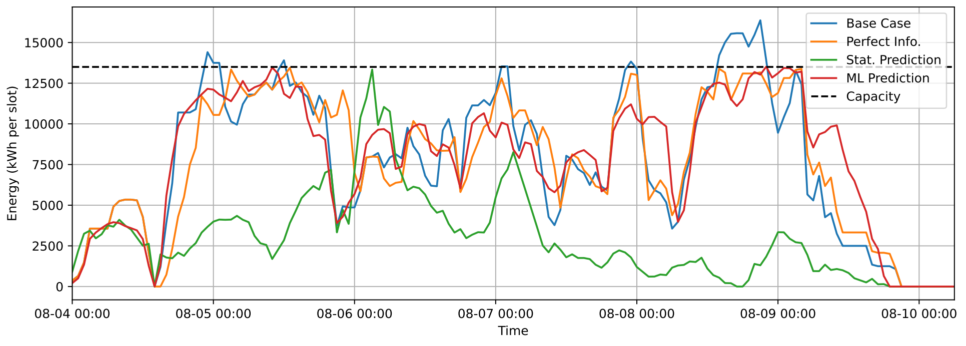

Figure 3.9: Aggregated terminal-level SP demand profiles for Set 2 (2025-08-04 to 2025-08-09), comparing the Base Case (without SP consideration), Perfect Info. Case (with TabPFN method), ML Pred. Case and Stat. Pred. Case against the zone capacity limit

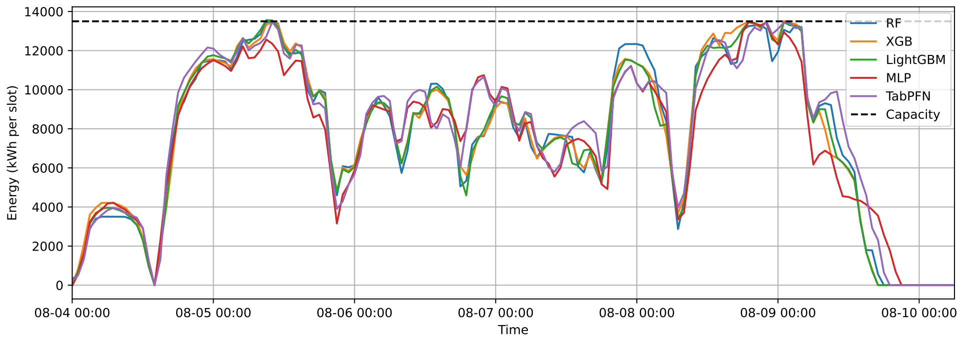

Figure 3.10: Aggregated terminal-level SP demand profiles for Set 2 (2025-08-04 to 2025-08-09), comparing different machine learning prediction methods including Random Forest, XGBoost, LightGBM, MLP and TabPFN

demand trajectories that are closest to those obtained under perfect information, which is critical for capacity feasibility and penalty avoidance.

Figure 3.8 illustrates the SP demand profiles obtained from the BAP solution when driven by five different machine-learning predictors, namely RF, XGBoost, LightGBM, MLP and TabPFN. Despite the methodological differences among these models, the resulting SP demand profiles exhibit a high degree of structural similarity. All ML-based profiles identify the same high-demand periods, with peak loads occurring at nearly identical time slots. This indicates that, in Set 1, the temporal structure of SP demand is dominated by the underlying berth allocation and operational constraints. The differences among ML models are limited to minor local variations around peak and transition periods. Figure 3.10 presents the corresponding comparison for Set 2. Similar to Set 1, all ML-based profiles in Set 2 display strong temporal alignment, with major demand peaks appearing in the same periods across these models. This confirms that the temporal structure of SP demand remains relatively robust to the choice of ML predictor.

Compared with Set 1, the inter-model differences are more pronounced, particularly around peak-demand periods and near the end of the planning horizon, where the resulting demand profiles exhibit more noticeable divergence.

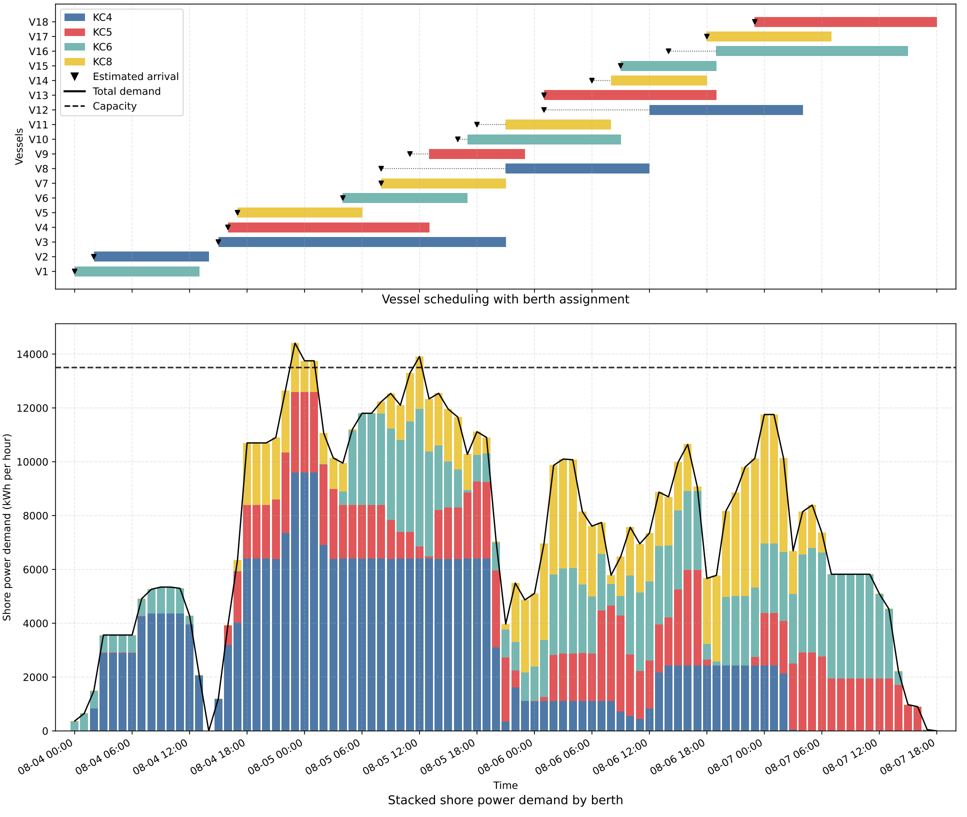

Figure 3.11: Vessel scheduling and stacked shore power demand profile for Set 1 in Base Case.

Figures 3.11 – 3.14 illustrate the vessel scheduling with berth allocation and the corresponding stacked shore power demand profiles under four different cases in Set 1. Each figure contains two parts: the upper part shows the berth allocation and vessel schedule, while the lower part depicts the stacked SP demand by berth over time. The stacked berth-level profiles form the aggregated SP demand curve, which is shown as the black line in the lower parts of Figure 3.11 - 3.14 and summarized in Figure 3.7. The aggregated demand is simply the sum of SP demand across all vessels at each time step.

In general, vessels are scheduled sequentially according to their estimated arrival times. In the Base Case, the scheduling pattern is determined without prediction of future SP demand. As a result, vessel service periods tend to cluster in certain time windows where berth resources are available, producing several periods with a high concentration of simultaneous operations. These clusters later translate into peaks in the SP demand profile. The Perfect Info. Case, where the operator has full knowledge of the actual SP demand profiles, exhibits higher vessel delays compared to the Base Case, as some service times are postponed to better align berth

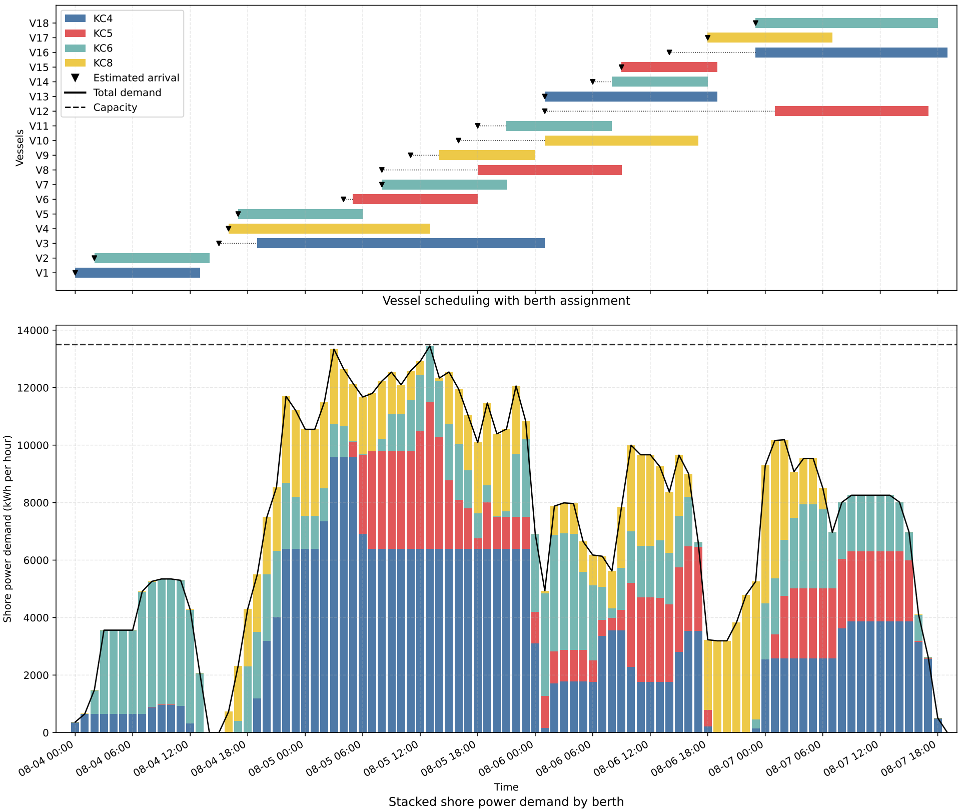

Figure 3.12: Vessel scheduling and stacked shore power demand profile for Set 1 in Perfect Info. Case.

allocation with the SP capacity constraints. The ML Pred. Case shows a scheduling pattern that closely resembles the Perfect Info. Case. The predicted SP demand profiles capture the temporal characteristics of actual demand reasonably well. The operator is able to make scheduling plans similar to those achieved with perfect information. In contrast, the Stat. Prediction Case displays more noticeable deviations in scheduling decisions. Since the statistical model prediction are less precise, the optimizer cannot fully anticipate future demand, leading to scheduling patterns that are somewhat closer to the Base Case than to the Perfect Info. Case.

In addition to the difference in vessel scheduling, the berth allocation results also vary across the four cases. Except for some large vessels that can only be accommodated by longer berths, the length requirements of most vessels can be satisfied by multiple berths. For instance, all four berths are capable of accommodating vessels V1 and V2 in terms of length constraints. Therefore, these vessels can in principle be assigned to any of the available berths. In the Base Case, vessels V1 and V2 are assigned to berths KC4 and KC6, respectively, whereas in the ML Prediction Case, they are allocated to KC4 and KC5.

The stacked SP demand profiles directly reflect the vessel scheduling outcomes. Each colored segment in the stacked bars corresponds to the SP demand of vessels assigned to a specific berth.

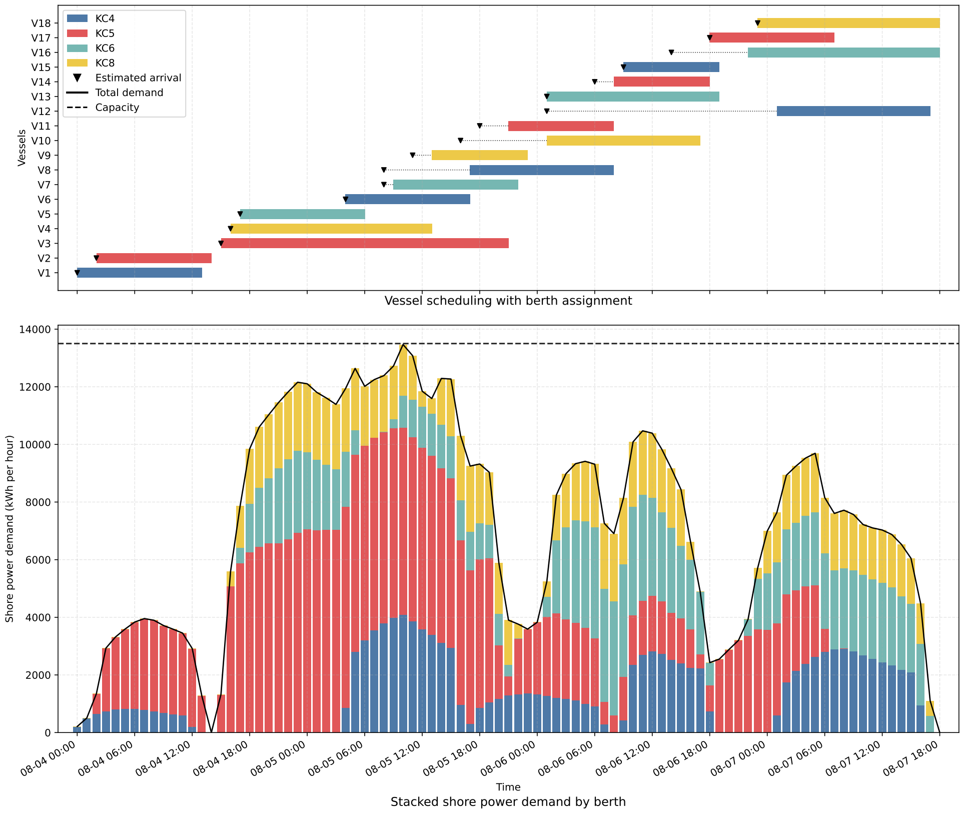

Figure 3.13: Vessel scheduling and stacked shore power demand profile for Set 1 in ML Prediction Case (TabPFN in this case).

The total height of the stacked bars represents the aggregated shore power demand at each time step. As can be observed from Figures 3.11, 3.12, and 3.13, demand peaks typically correspond to time windows when multiple vessels are simultaneously connected to shore power. These peaks arise when service periods of different vessels overlap across multiple berths. For example, during the time window from 08-04 15:00 to 08-05 21:00, three vessels (V3, V4 and V5) come to the terminal at the beginning, so the demand rise sharply. Three to four berths are occupied during this time period, and V3 has a high demand for shore power, the total demand remains at a high level.

A comparison of the four cases also highlights the impact of scheduling adjustments on demand shifting. Compared with the Base Case (Figure 3.11), the Perfect Info. Case (Figure 3.12) and the ML Pred. Case (Figure 3.13) exhibit more coordinated scheduling decisions. In these cases, the operator shifts vessel service start times or berth assignments to lower SP loads during peak hours, thereby reducing the simultaneous operation of high-power vessels and producing a smoother aggregated demand curve. For example, vessels V3 and V6 start their service slightly later in the Perfect Info. Case than in the Base Case. This adjustment reduces the overlap of high SP demand with other vessels, thereby allowing the peak demand to remain

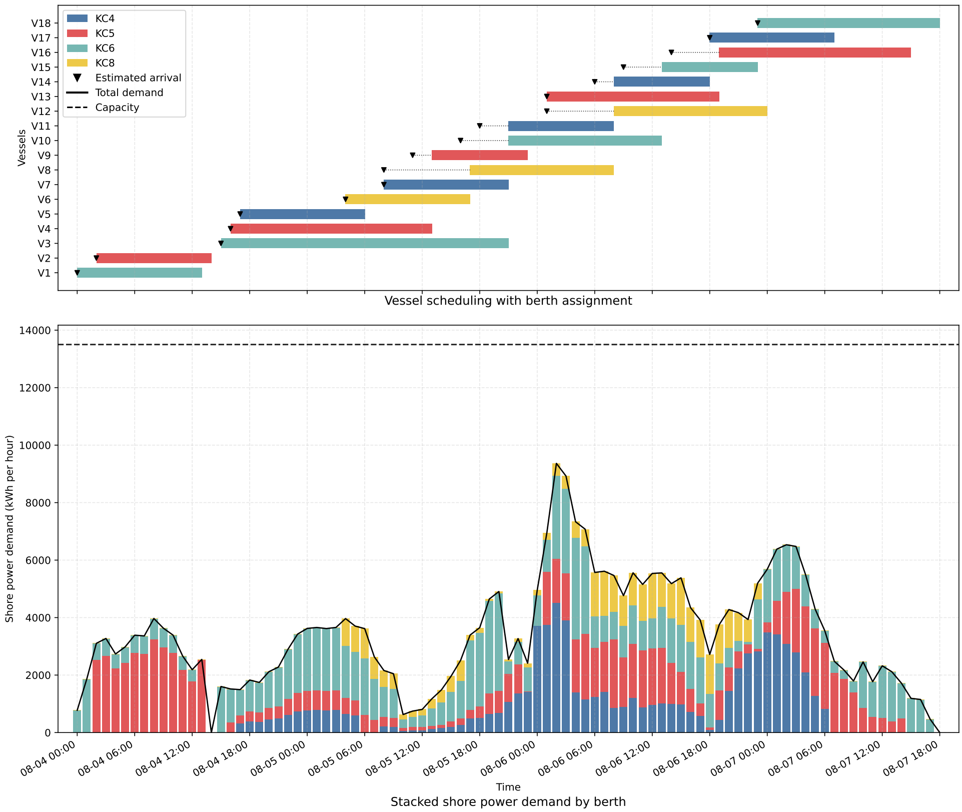

Figure 3.14: Vessel scheduling and stacked shore power demand profile for Set 1 in Stat. Prediction Case.

below the capacity limit and avoiding potential penalty costs. The dashed horizontal line in the demand profiles represents the SP capacity limit. With more accurate demand information available, the scheduling decisions in the Perfect Info. and ML Prediction Cases tend to keep the aggregated demand closer to but below this threshold, indicating that the available SP capacity is effectively utilized while avoiding excessive peaks.

Overall, the figures demonstrate that vessel scheduling and SP demand profiles are strongly coupled. Scheduling decisions determine when vessels connect to shore power, which directly shapes the aggregated energy demand curve. Conversely, accurate demand prediction enables more informed scheduling, leading to more stable load profiles and more efficient utilization of SP capacity. These results highlight the potential benefits of integrating machine learning-based demand forecasting with berth allocation optimization, particularly in ports where SP capacity constraints play a significant role in operational planning.

3.6 Managerial insights

We summarize some managerial insights derived from the SP demand prediction experiments and the integrated SP-aware berth allocation optimization. The insights highlight practical implications for terminal operators and port energy planners.

- Integrating SP demand into berth planning is essential to avoid hidden energy risks. The experiments demonstrate that berth allocation decisions made without explicitly considering SP demand can lead to exceeding the capacity limit. In the Base Case, ignoring SP during optimization results in pronounced demand peaks and severe penalty costs once SP capacity constraints are enforced. This implies that traditional berth planning approaches may conceal significant energy-related risks, which become visible after schedules are fixed. Explicitly integrating SP demand into berth allocation decisions is therefore crucial for avoiding high energy costs resulting from energy peak demand (even significantly exceeding the capacity limit).

- ML-based SP prediction enables near-ideal planning performance in both cost and schedule structure. The ML-based prediction approach provides the demand parameters for the SP-BAP model to get berth allocations and vessel schedules that closely resemble those obtained under perfect information. The ML-based SP demand forecasting allows near-ideal planning quality to be achieved in practice, narrowing the gap between realistic operations and perfect-information benchmarks.

- TabPFN and tree-based ensemble models have better performance in predicting SP demand. The comparative results across different ML models indicate that TabPFN and tree-based ensemble methods, particularly XGBoost, deliver more accurate SP demand forecasts and lead to planning outcomes that are closer to the Perfect Info. benchmark in both cost and scheduling structure. In contrast, simpler models tend to produce less reliable demand prediction (e.g., Ridge Regression and statistical methods), which result in less optimal berth allocation and vessel scheduling decisions (e.g., statistical methods).

- Best predictive accuracy does not necessarily translate into the best planning performance. The comparative results reveal that the ML model achieving the highest predictive accuracy is not always the one that yields the best outcomes when embedded in the optimization model. For instance, although XGBoost generally demonstrates better performance in SP demand prediction for the Port of Hamburg under the operational-planning feature set, its integration into the optimization framework does not lead to the most cost-efficient or operationally effective solutions. Instead, the TabPFN model produces better planning outcomes. This discrepancy highlights that the prediction accuracy of the model and its integration into the optimization framework both play critical roles in decision-support contexts. These findings suggest substantial potential for future research on the joint design of prediction models and operational decision-making frameworks.

- The performance of ML prediction methods depends strongly on feature availability. The results demonstrate that the predictive performance of ML models is sensitive to the set of available input features. When richer feature sets are used, including detailed operational-related information, all models achieve improved prediction accuracy. However, under realistic operational-planning conditions, where certain features are unavailable prior to vessel arrival, the performance of all models deteriorates, although tree-based methods remain relatively more robust.

- SP-aware BAP influences vessel scheduling and shifts the peak SP load. The comparison across the four cases shows that SP-aware planning under the ML prediction method redistributes vessel assignments across berths, which is more consistent with the Perfect Info. benchmark. This redistribution reduces the excessive concentration of high-demand calls on specific berths and mitigates the formation of long waiting tails for individual vessels. SP-aware berth planning can be viewed as a tool not only for energy feasibility, but also for balancing service load and improving schedule fairness across vessels.

3.7 Conclusions

With the growing push for stricter regulations on maritime emissions, terminals increasingly require accurate, time-grained predictions of shore power (SP) demand to support infrastructure planning and operational control. Existing prediction methods often lack the temporal granularity and interpretability for practical deployment. Shore power demand constitutes a critical component of terminal operations, particularly at the berth level where capacity constraints directly interact with operational decisions. Aggregated or coarse-grained demand predictions are insufficient, as inaccurate representations of temporal demand may result in capacity violations or infeasible schedules.

This chapter addresses RQ 2 and RQ 3. This chapter introduce a berth allocation problem that accounts for shore power capacity constraints and develop several prediction methods trained on real-world data from the cases of Hamburg and Hong Kong to enable berth allocation decisions that anticipate shore power demand and respect grid capacity constraints on the land side.

We first model segmented shore power demand profiles that capture the temporal evolution of vessel energy demand during different operational phases by reconstructing the historical port call records. We then establish two feature sets: one incorporating complete historical data (Full-Insight set) and one restricted to pre-arrival observable variables (Operational-Planning set). Several machine-learning medels are evaluated, including Random Forest, XGBoost, LightGBM, Multi-Layer Perceptron (MLP), and Tabular Prior-data Fitted Network (TabPFN). As a recently proposed tabular foundation model, TabPFN demonstrates strong performance for structured tabular prediction tasks with moderate data availability.

The results show that TabPFN and tree-based ensemble models achieve high accuracy under the Full-Insight set, while maintaining effective performance under limited information availability in the Operational-Planning set, yielding around 35% better performance relative to berth allocations based on common estimation approaches. Feature importance analysis using SHAP reveals that auxiliary engine power, vessel dimensions, and berthing durations are the most influential factors shaping shore power demand. The predicted shore power demand profiles are then integrated into a shore-power-aware berth allocation framework to assess their impact. Comparative experiments show that ML-based demand prediction outperforms conventional statistical approaches, with the TabPFN-driven framework achieving the best overall performance and producing berth allocation plans that closely approximate the perfect-information benchmark. These findings highlight the importance of accurate, time-grained shore power demand prediction for operational decision-making in SP-enabled terminals. Overall, this work presents a replicable framework that transforms raw port call event data into operationally relevant shore power demand profiles and integrates the resulting predictions into port operational optimization. Beyond the specific application of shore power, the proposed framework demonstrates the broader potential of coupling energy demand prediction with operational decision-making to support the transition toward more sustainable and energy-aware port operations.

Chapter 4

Dual-Fuel Vessel Operations under Fuel Supply Uncertainty

In Chapter 3, we explore the modeling and prediction of shore power demand, and investigate its integration into port operations. This chapter extends the research scope from energy-aware port operations to low-carbon shipping network operations, with a particular focus on fuel management and operational planning (i.e., bunkering in this chapter) for dual-fuel liner shipping services under uncertain fuel supply conditions. This chapter addresses RQ 4: How to optimize sailing speed, fuel choice, and bunkering decisions for dual-fuel vessels considering fuel supply uncertainty from ports?

This chapter is structured as follows: Section 4.1 introduces the background and the operational challenges caused by uncertain fuel supply. Section 4.2 reviews the related literature. Section 4.3 describes the integrated sailing speed, bunkering, and fuel choice problem and models it with the deterministic, chance-constrained, and distributionally robust chance-constrained formulations. Section 4.4 presents numerical experiments followed by managerial insights in Section 4.5. Finally, the conclusions are summarized in Section 4.6.

Part of this chapter is submitted as a journal paper: Tang, X., P. He, Ç. Iris, F. Schulte (2026a) Dual-Fuel Vessel Operations under Fuel Supply Uncertainty: Robust Planning and Scenario Analysis

4.1 Introduction

Maritime transportation is the backbone of global trade, carrying more than 80% of worldwide cargo transportation. However, the shipping industry is also a significant contributor to global greenhouse gas emissions and environmental pollution. To accelerate maritime decarbonization, the International Maritime Organization (IMO) and regional authorities have introduced increasingly stringent emission reduction targets and carbon-related regulations. Consequently, shipping companies are under growing pressure to reduce carbon emissions while maintaining operational efficiency and economic competitiveness.

In response to growing decarbonization pressure, major shipping companies and regional feeder operators are increasingly investing in dual-fuel vessels as part of their fleet transition strategies (Li et al., 2025). These vessels typically combine a conventional marine fuel with an alternative fuel, among which liquefied natural gas (LNG) and methanol are two prominent options. LNG benefits from relatively mature bunkering infrastructure, whereas methanol is attracting growing attention because of its potential to support lower-emission shipping. By enabling vessels to switch between fuels during voyages, dual-fuel technology provides greater flexibility in balancing fuel availability, operational cost, and environmental performance.

However, the operation of dual–fuel vessels remains challenging because alternative–fuel bunkering facilities and supply capacity are unevenly distributed across ports. To support the operation of alternative–fueled ships, some regions or countries are developing bunkering stations. For instance, the European region has developed one of the world's most advanced alternative-fuel bunkering networks, supported by environmental regulations and continued investments in port infrastructure. Nevertheless, the maturity of this infrastructure differs across fuels and ports. LNG bunkering services are relatively well established at several major European ports, whereas methanol bunkering networks are still developing. Moreover, alternative-fuel infrastructure and supply capacity tend to be concentrated at major hub ports, while smaller regional ports may provide fewer bunkering options and more limited supply.

In addition to infrastructure limitations, fuel supply uncertainty has become another critical challenge for low-carbon shipping operations. The availability of alternative fuels may vary significantly across ports due to different reasons, such as infrastructure limitations, production capacity fluctuations and transportation disruptions. Under such uncertain environments, deterministic planning approaches may lead to infeasible bunkering strategies, fuel shortages, or excessive operational costs. Therefore, developing robust optimization approaches capable of handling fuel supply uncertainty is essential for supporting reliable and cost–effective maritime decarbonization. Additionally, compared with traditional single–fuel vessels, dual–fuel ships require simultaneous decisions regarding fuel selection, bunkering quantity, fuel inventory management, and sailing speed across multiple ports and voyage legs. These decisions become even more challenging when low-carbon fuels such as methanol are not widely available throughout the shipping network.

Although existing studies have investigated sailing speed optimization, bunkering strategies, and fuel switching problems, several important research gaps remain. First, most existing studies focus on fuel price uncertainty (Wang et al., 2018; He et al., 2026). While related distributionally robust approaches have recently been extended to dual-fuel liner services (He et al., 2026), limited attention has been paid to uncertain fuel supply availability, particularly for emerging alternative fuels such as methanol. Current studies on dual-fuel shipping operations often assume fixed fuel availability at ports (Li et al., 2025), which may not accurately reflect the practical challenges faced by shipping companies during the transition toward low-carbon fuels. Second, the integrated optimization of sailing speed, fuel switching, and bunkering decisions under uncertain fuel supply conditions remains insufficiently explored in the literature. Moreover, the probability distribution of port-level fuel supply is often difficult to estimate reliably because historical observations may be limited, particularly for emerging alternative fuels. This creates a need for uncertainty-aware methods that can remain reliable when the assumed supply distribution is imperfectly specified.

To address these gaps, this chapter investigates how sailing speed, fuel bunkering, and fuel switching can be coordinated for dual-fuel liner services under uncertain port-level fuel supply. We propose modeling approaches, scenario analysis, and managerial and policy implications for robust dual-fuel liner operations. Three aspects in particular extend the state of the art of dual-vessel operations: port-level fuel supply uncertainty, the interaction between station coverage and alternative-fuel pricing, and a counterfactual-upper-bound characterization of how vessel and network capacity shape achievable methanol uptake.

This chapter makes several contributions. First, this chapter extends the integrated planning of dual-fuel liner services by explicitly incorporating uncertain port-level fuel supply into sailing speed, bunkering, and fuel-switching decisions. Unlike studies that treat fuel availability as a fixed port attribute, this chapter distinguishes between whether a fuel is available at a port and how much of that fuel can actually be supplied. It thereby captures how supply uncertainty affects bunkering quantities, onboard fuel inventories, voyage-leg fuel choices, sailing speeds, and schedule performance across interconnected liner services.

Second, this chapter develops and compares deterministic, chance-constrained programming (CCP), and distributionally robust chance-constrained (DRCC) models. Since the true distribution of port-level fuel supply is usually unknown and the historical data may be limited, the estimated distribution may not accurately represent future supply conditions. The DRCC model therefore employs a Wasserstein ambiguity set to account for uncertainty in the underlying fuel supply distribution, which is reformulated as a tractable model. The three models are further evaluated in terms of planned operating costs and out-of-sample feasibility.

Third, computational experiments based on a real-world feeder liner service network provide practical insights into the adoption of alternative fuel. The comparison between MGO–LNG and MGO–Methanol operations shows how fuel characteristics and infrastructure maturity affect the cost and reliability of dual-fuel operations under supply uncertainty. Further experiments on methanol uptake compare realized fuel-mix shares against a counterfactual upper bound, that is, the share attainable if methanol were free, holding infrastructure and operational constraints fixed. The comparison shows that bunkering–station coverage determines what is achievable (the upper bound rises from 33% at 2 ports to 84% at 11 in the studied network), while price competitiveness determines how close operators reach it. Neither instrument substitutes for the other, and coordinated action on both is needed to move methanol from a marginal to a dominant fuel in the mix.

4.2 Related work

This section reviews the relevant literature from individual speed and bunkering decisions to integrated operational planning, followed by studies addressing uncertainty in this topic. Table 4.1 summarizes representative studies closely related to the main research scope of this chapter, focusing on the integration of sailing speed, bunkering, fuel switching, and uncertainty considerations.

Table 4.1: Comparison of representative studies on speed, bunkering, and fuel decisions

Study	Speed	Bunkering	Fuel switching	Alternative fuel	Uncertainty source
Fagerholt et al. (2010)	✓	–	–	–	–
Zhen et al. (2017)	–	✓	–	–	Fuel consumption and bunkering prices
Wang & Meng (2015)	✓	✓	–	–	Operational uncertainty
Liu et al. (2019)	✓	✓	–	–	Transport demand
Wu et al. (2024)	–	✓	✓	✓	Fuel prices
He et al. (2024)	✓	✓	–	✓	–
Zhao et al. (2025)	✓	✓	✓	✓	–
Wu et al. (2023)	✓	–	✓	✓	Fuel prices
He et al. (2026)	✓	✓	✓	✓	Fuel prices
This chapter	✓	✓	✓	✓	Port-level fuel supply

Sailing speed optimization has long been recognized as an effective operational measure for reducing fuel consumption, operating costs, and emissions. Early studies mainly focused on sailing speed optimization for conventional shipping operations. For example, Fagerholt et al. (2010) proposed a nonlinear optimization model for tramp shipping services, where fuel consumption was modeled as a nonlinear function of sailing speed. Similarly, Norstad et al. (2011) incorporated sailing speed decisions into a tramp ship routing and scheduling problem and developed a heuristic solution approach. Psaraftis & Kontovas (2014) further analyzed the trade-offs among fuel consumption, freight rates, and inventory costs in ship speed optimization problems. As environmental regulations became increasingly stringent, researchers gradually began incorporating emission-related considerations into operational planning problems. For instance, Fagerholt et al. (2015) investigated the joint optimization of vessel routes and sailing speeds under Emission Control Area (ECA) regulations using a mixed-integer programming framework.

At the same time, fuel bunkering decisions also attracted increasing attention in the literature. Meng et al. (2015) studied the joint routing and bunkering problem for tramp ships under fixed sailing speeds, while Zhen et al. (2017) developed a dynamic programming approach for optimal bunkering policies in liner shipping operations. More recently, Omholt-Jensen et al. (2025) examined a tramp ship routing and scheduling problem with bunker optimization and proposed a matheuristic solution method based on path flow formulations. Extending bunker planning to dual-fuel vessels, Wu et al. (2024) developed a multistage stochastic programming model for the refueling of LNG–low–sulfur–fuel–oil dual–fuel liner ships under Carbon Intensity Indicator requirements and carbon taxation. The model considers port–specific fuel availability and fuel price fluctuations and illustrates how relative fuel prices and LNG availability influence the refueling mix. Nevertheless, this stream of literature primarily concentrates on fuel procurement and inventory management, with sailing speed, fuel switching, and network–wide operational interactions receiving relatively limited consideration.

Given the close relationship between speed-dependent fuel consumption and fuel procurement, a growing body of research has jointly optimized sailing speed and bunkering decisions. Wang & Meng (2015) formulated an integrated liner shipping problem involving sailing speed and bunker management as a mixed-integer nonlinear programming model. Aydin et al. (2017) investigated speed and bunkering optimization under uncertain service times and port time windows. Liu et al. (2019) further incorporated transport demand uncertainty into liner ship speed and bunkering optimization and solved the resulting stochastic model using the Sample Average Approximation (SAA) method. These studies show that optimizing speed and bunkering decisions simultaneously can better capture the impact of sailing decisions on fuel consumption, bunker inventory, and procurement costs.

More recent studies have expanded the scope of integrated optimization by combining speed and bunkering with route selection, fleet deployment, engine choice, and alternative-fuel adoption. He et al. (2024) investigated the joint optimization of routes, sailing speeds, and bunkering strategies for LNG-fueled tramp ships. For container liner shipping, Zhao et al. (2025) jointly optimized heterogeneous fleet deployment, sailing speed, and fuel bunkering within a bi-objective framework that balances operating costs and carbon emissions. Their study considered multiple conventional and alternative propulsion systems and highlighted the role of dual-fuel vessels in balancing economic and environmental objectives. At a more strategic level, Wu et al. (2023) studied the selection of multi-fuel engines under fuel price uncertainty. Their model jointly determines engine type, fleet deployment, fuel selection, and sailing speed, thereby demonstrating that the value of multi-fuel capability depends on both long-term investment decisions and the flexibility to switch fuels in response to changing prices. Similarly, Wang & Iris (2025) developed a two-stage stochastic programming model for fleet transition under uncertainty, jointly considering alternative-fuel selection, fleet deployment, purchasing, chartering, and retrofitting decisions. Zhou et al. (2026) proposed a predict-then-optimize framework that integrates fuel-consumption prediction with long-term decisions on slow steaming, maintenance, fuel switching, and vessel retrofitting. More recently, Peng et al. (2026) developed a two-stage stochastic optimization framework for the long-term transition of container-ship power systems. The framework jointly considers technology selection, capacity configuration, retrofit timing, and energy-use strategies under uncertainty in technology costs, fuel prices, and auxiliary-energy substitution rates. These studies provide important insights into alternative-fuel technology adoption and long-term fleet transition. However, their focus is primarily strategic, whereas the operational coordination of sailing speed, bunkering quantities, and fuel switching across multiple liner services remains less explored.

The reliability of the integrated planning is strongly affected by uncertainties in operating conditions, market conditions, and fuel availability. Existing studies have considered uncertain service times and port time windows (Aydin et al., 2017), transport demand (Liu et al., 2019), fuel consumption and bunkering prices (Zhen et al., 2017), and fuel price fluctuations (Wu et al., 2024; He et al., 2026). At the strategic level, fuel price uncertainty has also been incorporated into multi-fuel engine selection (Wu et al., 2023), while Peng et al. (2026) considered multiple sources of techno-economic uncertainty in long–term ship power–system transition planning. These studies have employed stochastic programming, robust optimization, and scenario–based approaches to improve decisions under uncertain operating and market conditions. Despite these advances, uncertainty in the supply of alternative fuels available at bunkering ports has received comparatively limited attention. Most existing studies either assume that the required fuel is fully available at designated bunkering ports or represent fuel availability as a deterministic binary condition. This assumption can be restrictive for emerging alternative fuels such as LNG and methanol, whose bunkering networks and supply systems are still developing. To address these gaps, this chapter investigates the integrated operation of dual–fuel liner services under uncertain port–level fuel supply and, through comparative experiments, evaluates the cost, emission, and out-of-sample reliability implications of alternative decision-making approaches across different fuel and supply conditions.

4.3 Problem definition and model formulation

This section defines the joint sailing speed, fuel-bunkering, and fuel-switching problem under uncertain port fuel supply. It first introduces the shipping network, describes the problem and then presents the deterministic, chance–constrained, and distributionally robust chance–constrained formulations.

4.3.1 Problem description

This chapter investigates a joint bunkering, fuel choice, and sailing speed optimization problem for dual-fuel liner shipping services under uncertain port fuel supply. Figure 4.1 depicts a liner shipping network with dual-fuel vessels. The network consists of a set of shipping routes, where each route consists of a predefined sequence of port calls and sailing legs between consecutive ports. The ports in this shipping network provide bunkering service for the vessels, with some ports supplying conventional marine fuels (e.g., MGO) and some ports supplying alternative low-carbon fuels (e.g., LNG or methanol). At present, the availability of low-carbon fuels is still limited. With the ongoing transition toward maritime decarbonization, the number of ports providing alternative fuels is expected to gradually increase in the future. The vessel deployed on each route is equipped with dual-fuel propulsion systems and can operate using either conventional marine fuel oil or alternative fuel. Unlike conventional single-fuel vessels, dual-fuel ships provide operational flexibility by allowing fuel switching during voyages, thereby enabling operators to balance fuel costs, emission costs, and fuel availability constraints. For each sailing leg, the operator determines the sailing speed and the fuel type used during navigation. Different sailing speeds lead to different voyage durations and fuel consumption levels, thereby influencing both operating costs and schedule reliability. At each port, the operator may decide whether to bunker fuel and determine the corresponding bunkering quantity for each available fuel type. However, not all ports provide all fuel types, and the available fuel supply at ports may be limited. Furthermore, the fuel inventory carried onboard is constrained by fuel tank capacities

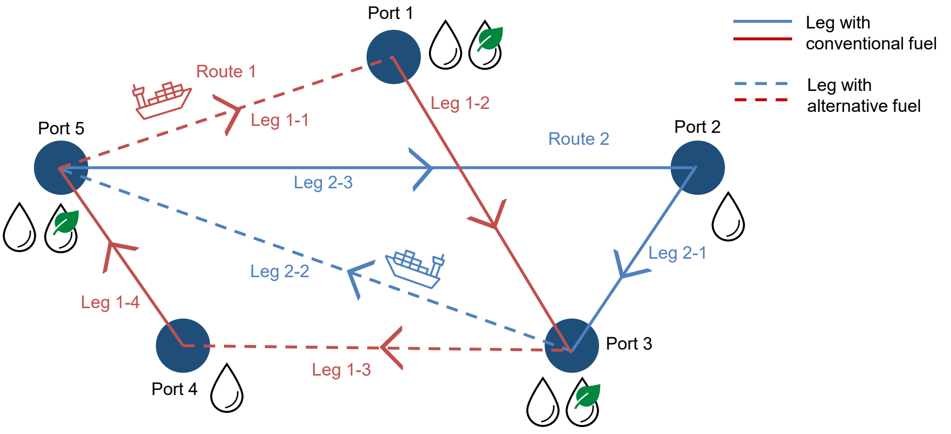

Figure 4.1: Illustrative example of a liner shipping network with duo-fuel vessels

and minimum safety fuel requirements. This chapter considers uncertainty in port fuel supply availability. In practice, the amount of fuel that can be supplied at a port may fluctuate due to different reasons, such as disruptions in fuel logistics and infrastructure limitations. As a result, the planned bunkering quantity may not always be fully satisfied in real operations.

Specifically, the shipping network consists of a set of routes $\mathcal{R}$. Each route $r \in \mathcal{R}$ contains an ordered set of port visits $\mathcal{P}^r$, and a corresponding set of sailing legs $\mathcal{L}^r$ connecting consecutive ports. The operator needs to simultaneously determine the sailing speed on each sailing leg, the fuel type used on each leg, the bunkering ports and bunkering quantities, and the onboard fuel inventory evolution throughout the voyage. The objective is to minimize the total operating cost of the liner service, including bunkering costs, carbon emission costs, and delay penalty costs, while satisfying operational, fuel inventory, and uncertain fuel supply constraints. The resulting problem is formulated as a mixed-integer optimization model. To address fuel supply uncertainty, a distributionally robust chance-constrained (DRCC) model based on Wasserstein ambiguity sets is further developed, which guarantees solution robustness against distributional ambiguity in fuel supply realizations.

To facilitate the modeling, we make the following assumptions:

(1) Each shipping route is operated by a single vessel. The sailing time required to complete a shipping route is approximately one week, so assigning one vessel is generally consistent with practical liner shipping operations;

(2) The influence of environmental conditions, including wind, waves, and ocean currents, on vessel fuel consumption is neglected;

(3) Auxiliary engines consume the same fuel type as the main propulsion engine;

(4) The durations of mooring, cargo loading, and cargo unloading are assumed to be deterministic and fixed, without considering variations caused by factors such as port congestion;

(5) Fuel bunkering is allowed after cargo loading and unloading operations have been completed. The bunkering duration depends on both the refueling quantity and the bunkering

Table 4.2: Sets for the multi-route network MILP model

Notations	Descriptions
$\mathcal{R}$	Set of shipping routes in the network
$\mathcal{P}$	Set of physical ports in the network (unique, no repetition)
$\mathcal{N}^r$	Ordered set of port calls (visits) on route $r \in \mathcal{R}$; the same physical port may appear multiple times via different visits
$\mathcal{L}^r$	Set of visit-legs between consecutive visits on route r: $\mathcal{L}^r = \{(n, n+1) \mid n \in \mathcal{N}^r, n+1 \in \mathcal{N}^r\}$
$\mathcal{V}$	Set of alternative speeds
$\mathcal{V}^{r,n}$	Set of feasible speeds for visit-leg $(n, n+1) \in \mathcal{L}^r$
$\mathcal{F}$	Set of fuel types
$\mathcal{F}^i$	Set of fuels that can be bunkered at physical port $i \in \mathcal{P}$

rate. In addition, for operational safety reasons, the preparation and disconnection procedures of the fueling equipment before and after bunkering cannot be performed simultaneously with cargo handling activities. Therefore, each bunkering operation includes an additional fixed setup time (He et al., 2026).

All parameters and variables necessary for building mathematical models are listed in Tables 4.2, 4.3, and 4.4.

4.3.2 Deterministic model

Building on the above description and parameter definitions, a deterministic mathematical model is developed to optimize sailing speeds, fuel switching, and refueling strategies for liner services, as follows:

$$\begin{aligned} \min \quad \sum_{r \in \mathcal{R}} \Bigg(& \sum_{n \in \mathcal{N}^r} \sum_{f \in \mathcal{F}} p_{\pi_{r,n} f}\, b_f^{r,n} + \sum_{n \in \mathcal{N}^r} \gamma_{r,n} \psi_{r,n} \\ & + \sum_{(n,n+1) \in \mathcal{L}^r} \sum_{v \in \mathcal{V}^{r,n}} \sum_{f \in \mathcal{F}} \eta \phi_f (\Delta_{vf} + \delta_f)\, t_v^{r,n} x_{vf}^{r,n} \alpha_{r,n} \Bigg). \end{aligned} \tag{4.1}$$

$$\sum_{v \in \mathcal{V}^{r,n}} \sum_{f \in \mathcal{F}} x_{vf}^{r,n} = 1, \quad \forall r \in \mathcal{R},\ \forall (n, n+1) \in \mathcal{L}^r. \tag{4.2}$$

$$q_f^{r,n} \geq q_{rf}^{lb}, \quad \forall r \in \mathcal{R},\ \forall n \in \mathcal{N}^r,\ \forall f \in \mathcal{F}. \tag{4.3}$$

$$b_f^{r,n} = 0, \quad \forall r \in \mathcal{R},\ \forall n \in \mathcal{N}^r,\ \forall f \in \mathcal{F} \setminus \mathcal{F}_{\pi_{r,n}}. \tag{4.4}$$

$$q_f^{r,n} + b_f^{r,n} \leq q_{rf}^{ub}, \quad \forall r \in \mathcal{R},\ \forall n \in \mathcal{N}^r,\ \forall f \in \mathcal{F}. \tag{4.5}$$

Table 4.3: Parameters for the multi-route network MILP model

Notations	Descriptions
$\pi_{r,n}$	Mapping from visit (r,n) to the corresponding physical port in $\mathcal{P}$
Δ_{vf}	Main engine fuel consumption rate (mt/h) at speed v using fuel f
δ_f	Auxiliary engine fuel consumption rate (mt/h) using fuel f
p_{if}	Average bunker price of fuel f at physical port $i \in \mathcal{P}$
ϕ_f	Carbon emission factor of fuel f
$t_v^{r,n}$	Sailing time (h) of leg $(n,n+1) \in \mathcal{L}^r$ on route r at speed v
q_{rf}^{ub}	Fuel tank capacity upper bound of vessel on route r for fuel f
q_{rf}^{lb}	Minimum residual fuel volume upon arrival of vessel on route r for fuel f
$\tau_{r,n}$	Loading and unloading time (h) at visit port n of route r
θ_{if}	Bunkering speed (mt/h) for fuel f at physical port i
$\gamma_{r,n}$	Delay penalty (USD/h) at visit port n of route r
$eta_{r,n}$	Earliest start berthing time at visit port n of route r
λ	Setup time (h) for refueling (incurred per bunkering operation)
η	Carbon emission cost per ton of CO_2
$\alpha_{r,n}$	Coefficient indicating whether the corresponding leg $(n,n+1)$ is within (100%) or from/to Europe (50%)
S_f^i	Available supply of fuel f at physical port i during the planning horizon
M	A sufficiently large constant for linking constraints

$$q_f^{r,n+1} = q_f^{r,n} + b_f^{r,n} - \sum_{v \in \mathcal{V}^{r,n}} \left(\Delta_{vf} + \delta_f\right) t_v^{r,n} x_{vf}^{r,n}, \quad \forall r \in \mathcal{R},\ \forall (n,n+1) \in \mathcal{L}^r,\ \forall f \in \mathcal{F}. \tag{4.6}$$

$$M \zeta_f^{r,n} \geq b_f^{r,n}, \quad \forall r \in \mathcal{R},\ \forall n \in \mathcal{N}^r,\ \forall f \in \mathcal{F}_{\pi_{r,n}}. \tag{4.7}$$

$$d_{r,n} \ \geq\ a_{r,n} + \tau_{r,n} + \sum_{f \in \mathcal{F}_{\pi_{r,n}}} \frac{b_f^{r,n}}{\theta_{\pi_{r,n} f}} + \lambda \sum_{f \in \mathcal{F}_{\pi_{r,n}}} \zeta_f^{r,n}, \quad \forall r \in \mathcal{R},\ \forall n \in \mathcal{N}^r. \tag{4.8}$$

$$a_{r,n} \geq eta_{r,n}, \quad \forall r \in \mathcal{R},\ \forall n \in \mathcal{N}^r. \tag{4.9}$$

$$d_{r,n} + \sum_{v \in \mathcal{V}^{r,n}} \sum_{f \in \mathcal{F}} t_v^{r,n} x_{vf}^{r,n} \leq a_{r,n+1}, \quad \forall r \in \mathcal{R},\ \forall (n,n+1) \in \mathcal{L}^r. \tag{4.10}$$

$$\psi_{r,n} \geq a_{r,n} - eta_{r,n}, \quad \forall r \in \mathcal{R},\ \forall n \in \mathcal{N}^r. \tag{4.11}$$

$$\sum_{r \in \mathcal{R}} \sum_{n \in \mathcal{N}^r:\ \pi_{r,n} = i} b_f^{r,n} \leq S_f^i, \quad \forall i \in \mathcal{P},\ \forall f \in \mathcal{F}. \tag{4.12}$$

Table 4.4: Decision variables for the multi-route network MILP model

Notations	Descriptions
$x_{vf}^{r,n} \in \{0,1\}$	1 if the vessel on route r sails visit-leg $(n,n+1) \in \mathcal{L}^r$ at speed v using fuel f; 0 otherwise
$\zeta_f^{r,n} \in \{0,1\}$	1 if the vessel on route r bunkers fuel f at visit port n
$a_{r,n} \geq 0$	Arrival time (h) of the vessel on route r at visit port n
$d_{r,n} \geq 0$	Departure time (h) of the vessel on route r at visit port n
$\psi_{r,n} \geq 0$	Arrival delay time (h) of the vessel on route r at visit port n
$b_f^{r,n} \geq 0$	Amount of fuel f bunkered on route r at visit port n
$q_f^{r,n} \geq 0$	Amount of remaining fuel f upon arrival of the vessel on route r at visit port n
$\chi_{if} \in \mathbb{R}$	Auxiliary variable for the distributionally robust chance–constrained model reformulation
$\varpi_{if,k} \geq 0$	Auxiliary variable for the distributionally robust chance–constrained model reformulation, $k = 1,\ldots,N$, N is the nunmber of instances for the possible realizations of the uncertain parameter
$l_{if,k} \in \{0,1\}$	Auxiliary variable for the distributionally robust chance–constrained model reformulation

$$x_{vf}^{r,n} \in \{0,1\},\ \forall r \in \mathcal{R},\ \forall (n,n+1) \in \mathcal{L}^r,\ \forall v \in \mathcal{V}^{r,n},\ \forall f \in \mathcal{F}. \tag{4.13}$$

$$\zeta_f^{r,n} \in \{0,1\},\ \forall r \in \mathcal{R},\ \forall n \in \mathcal{N}^r,\ \forall f \in \mathcal{F}. \tag{4.14}$$

$$b_f^{r,n} \geq 0,\ \forall r \in \mathcal{R},\ \forall n \in \mathcal{N}^r,\ \forall f \in \mathcal{F}. \tag{4.15}$$

$$q_f^{r,n} \geq 0,\ \forall r \in \mathcal{R},\ \forall n \in \mathcal{N}^r,\ \forall f \in \mathcal{F}. \tag{4.16}$$

$$a_{r,n} \geq 0,\ d_{r,n} \geq 0,\ \psi_{r,n} \geq 0,\ \forall r \in \mathcal{R},\ \forall n \in \mathcal{N}^r. \tag{4.17}$$

The objective function (4.1) minimizes the total operational cost over all routes, including three components: (i) bunkering costs at ports, (ii) delay penalties incurred when the actual berthing time exceeds the latest allowable time window, and (iii) sailing-related CO_2 emission costs. Since vessels are assumed to use onshore power supply (OPS) while berthed, no fuel is consumed during port stays and therefore no port-time fuel or emission cost is included in the objective. Constraint (4.2) ensures that each leg is sailed using exactly one speed–fuel combination. The binary variable $x_{vf}^{r,n}$ enforces a discrete operational choice, meaning that fuel switching can only occur at visit leg boundaries. Constraint (4.3) guarantees that the remaining onboard fuel upon arrival at each port call never falls below a predefined safety stock level. Constraint (4.4) enforces port fuel availability by preventing bunkering of fuels that are not supplied at the corresponding port. Constraint (4.5) limits the sum of the remaining fuel and bunkered fuel so that the onboard fuel inventory does not exceed the tank capacity. Constraint (4.6) describes the fuel balance along each sailing leg. Specifically, the remaining fuel at the next port equals the previous inventory plus the bunkered amount minus the fuel consumption during sailing. Because OPS is adopted at berth, no auxiliary-engine fuel consumption is deducted during port stays, which allows a unified balance equation for all fuel types. Constraint (4.7) links the continuous bunkering amount with the binary bunkering decision through a big-M formulation, ensuring that fuel can only be bunkered if the corresponding indicator is activated. Constraint (4.8) determines the departure time from each port call. They incorporate the arrival time, handling time, and additional setup time required when bunkering takes place. Constraint (4.9) requires that the actual arrival time should not be earlier than the earliest start berthing time. Constraint (4.10) propagates the sailing time between consecutive ports, thereby defining the arrival time at the next port. Constraint (4.11) calculates the arrival delay relative to the latest allowable berthing time, which contributes to the delay penalty in the objective function. Constraint (4.12) models the shared supply-side limitation at each physical port by restricting the total bunkering demand aggregated across all services. This coupling constraint captures competition for limited port fuel resources and links otherwise independent service operations. Finally, constraints (4.13)–(4.17) define the domains of all decision variables, including binary sailing and bunkering decisions and continuous fuel inventory and time variables.

The objective function (4.1) minimizes the total operational cost over all routes, including three components: (i) bunkering costs at ports, (ii) delay penalties incurred when the actual berthing time exceeds the latest allowable time window, and (iii) sailing-related CO_2 emission costs. Since vessels are assumed to use shore power (SP) while berthed, no fuel is consumed during port stays and therefore no port-time fuel or emission cost is included in the objective. Constraint (4.2) ensures that each leg is sailed using exactly one speed–fuel combination. Unlike the original proportional formulation, the binary variable $x_{vf}^{r,n}$ enforces a discrete operational choice, meaning that fuel switching can only occur at leg boundaries. Constraint (4.3) guarantees that the remaining onboard fuel upon arrival at each port call never falls below a predefined safety stock level. Constraint (4.4) enforces port fuel availability by preventing bunkering of fuels that are not supplied at the corresponding port. Constraint (4.5) limits the sum of the remaining fuel and bunkered fuel so that the onboard fuel inventory does not exceed the tank capacity. Constraint (4.6) describes the fuel balance along each sailing leg. Specifically, the remaining fuel at the next port equals the previous inventory plus the bunkered amount minus the fuel consumption during sailing. Because OPS is adopted at berth, no auxiliary-engine fuel consumption is deducted during port stays, which allows a unified balance equation for all fuel types. Constraint (4.7) links the continuous bunkering amount with the binary bunkering decision through a big-M formulation, ensuring that fuel can only be bunkered if the corresponding indicator is activated. Constraint (4.8) determines the departure time from each port call. They incorporate the arrival time, handling time, and additional setup time required when bunkering takes place. Constraint (4.9) requires that the actual arrival time should not be earlier than the earliest start berthing time. Constraint (4.10) propagates the sailing time between consecutive ports, thereby defining the arrival time at the next port. Constraint (4.11) calculates the arrival delay relative to the latest allowable berthing time, which contributes to the delay penalty in the objective function. Constraint (4.12) models the shared supply-side limitation at each physical port by restricting the total bunkering demand aggregated across all services. This coupling constraint captures competition for limited port fuel resources and links otherwise independent service operations.

Finally, constraints (4.13)–(4.17) define the domains of all decision variables, including binary sailing and bunkering decisions and continuous fuel inventory and time variables.

4.3.3 Chance-constrained programming (CCP) Model

To balance operational reliability with economic efficiency under uncertain port fuel supply, we first adopt an individual chance-constrained programming (CCP) approach. Specifically, for each physical port $i \in \mathcal{P}$ and fuel type $f \in \mathcal{F}$, we require that the probability of the aggregated bunkering demand not exceeding the realized supply is no less than a prescribed confidence level $1 - \varepsilon_{if}$.

Let $\tilde{S}^i_f$ denote the available supply of fuel f at physical port i during the planning horizon. Define the aggregated bunkering demand at (i, f) as

$$D_{if}(\boldsymbol{b}) := \sum_{r \in \mathcal{R}} \sum_{n \in \mathcal{N}^r:\ \pi_{r,n} = i} b^{r,n}_f, \quad \forall i \in \mathcal{P},\ \forall f \in \mathcal{F}, \tag{4.18}$$

and then the deterministic port supply constraint (4.12) can be reformulated as the following individual chance constraint:

$$\mathbb{P}\Big(D_{if}(\boldsymbol{b}) \leq \tilde{S}^i_f\Big) \geq 1 - \varepsilon_{if}, \quad \forall i \in \mathcal{P},\ \forall f \in \mathcal{F}, \tag{4.19}$$

where $\varepsilon_{if} \in (0, 1)$ is the risk tolerance level specified by the shipping operator. Constraint (4.19) ensures that the fuel demand at each port is met with high probability. Because the probability distribution of the uncertain fuel supply $\tilde{S}^i_f$ is generally unavailable and may not follow any standard parametric distribution, deriving a tractable deterministic equivalent formulation is difficult. Therefore, the Sample Average Approximation (SAA) approach is adopted to solve the model.

Solving the CCP model via the SAA method

To solve the chance-constrained programming model with uncertain port fuel supply, the Sample Average Approximation (SAA) method is employed. Assume that for each physical port $i \in \mathcal{P}$ and fuel type $f \in \mathcal{F}$, we obtain N historical or simulated samples of the uncertain fuel supply, denoted by $\tilde{S}^i_{f,1}, \tilde{S}^i_{f,2}, \ldots, \tilde{S}^i_{f,N}$.

The original individual chance constraint (4.19) can then be approximated by the following sample average formulation:

$$\frac{1}{N} \sum_{k=1}^{N} \mathbb{I}\left[D_{if}(\boldsymbol{b}) \leq \tilde{S}^i_{f,k}\right] \geq 1 - \varepsilon_{if}, \quad \forall i \in \mathcal{P},\ \forall f \in \mathcal{F}, \tag{4.20}$$

where $\mathbb{I}[\cdot]$ denotes the indicator function, which equals 1 if the condition inside is satisfied and 0 otherwise.

Since the indicator function is nonlinear and non-convex, we introduce a binary auxiliary variable $z_{ifk} \in \{0, 1\}$ such that

$$z_{ifk} = \begin{cases} 1, & \text{if } D_{if}(\boldsymbol{b}) \leq \tilde{S}^i_{f,k}, \\ 0, & \text{otherwise}, \end{cases} \quad \forall i \in \mathcal{P},\ \forall f \in \mathcal{F},\ \forall k = 1, \ldots, N. \tag{4.21}$$

Using a sufficiently large constant M_{if}, the above condition can be linearized as

$$D_{if}(\boldsymbol{b}) \leq \tilde{S}^i_{f,k} + M_{if}(1 - z_{ifk}), \quad \forall i \in \mathcal{P},\, \forall f \in \mathcal{F},\, \forall k = 1, \ldots, N. \tag{4.22}$$

Accordingly, the chance constraint can be reformulated as

$$\frac{1}{N}\sum_{k=1}^{N} z_{ifk} \geq 1 - \varepsilon_{if}, \quad \forall i \in \mathcal{P},\, \forall f \in \mathcal{F}. \tag{4.23}$$

The CCP model can therefore be reformulated as a mixed-integer linear programming (MILP) model consisting of the objective function (4.1), constraints (4.2)–(4.11), (4.13)–(4.17), together with constraints (4.22)–(4.23).

4.3.4 Distributionally robust chance-constrained (DRCC) model

To hedge against distributional ambiguity, we employ a distributionally robust optimization (DRO) framework and construct a Wasserstein-distance-based ambiguity set around the empirical distribution inferred from historical supply observations.

For each (i, f), suppose that N historical realizations of the supply are available, denoted by $\{\hat{S}^i_{f,1}, \ldots, \hat{S}^i_{f,N}\}$. The corresponding empirical distribution is defined as

$$\hat{\mathbb{P}}_{if,N} := \frac{1}{N}\sum_{k=1}^{N} \delta_{\hat{S}^i_{f,k}}, \tag{4.24}$$

where $\delta_{\hat{S}^i_{f,k}}$ is the Dirac measure concentrated at $\hat{S}^i_{f,k}$. We then define the (individual) Wasserstein ambiguity set as a ball of radius $\rho_{if} \geq 0$ centered at $\hat{\mathbb{P}}_{if,N}$:

$$\mathcal{U}_{if}(\rho_{if}) := \left\{\mathbb{Q} \in \mathcal{M}(\Xi_{if}) \,:\, d_W(\mathbb{Q}, \hat{\mathbb{P}}_{if,N}) \leq \rho_{if}\right\}, \quad \forall i \in \mathcal{P},\, \forall f \in \mathcal{F}, \tag{4.25}$$

where $\mathcal{M}(\Xi_{if})$ denotes the set of all probability distributions defined on $\Xi_{if} \subseteq \mathbb{R}$, and Ξ_{if} represents the set of all possible realizations of the uncertain fuel supply $\tilde{S}^i_f$. and $d_W(\cdot,\cdot)$ denotes the Wasserstein distance (under a chosen ground metric) (Mohajerin Esfahani & Kuhn, 2018; Gao & Kleywegt, 2023).

The individual distributionally robust chance constraint (DRCC) requires that constraint (4.19) holds for all distributions within $\mathcal{U}_{if}(\rho_{if})$:

$$\inf_{\mathbb{Q} \in \mathcal{U}_{if}(\rho_{if})} \mathbb{Q}\Big(D_{if}(\boldsymbol{b}) \leq \tilde{S}^i_f\Big) \geq 1 - \varepsilon_{if}, \quad \forall i \in \mathcal{P},\, \forall f \in \mathcal{F}. \tag{4.26}$$

By utilizing the Wasserstein ball, the model accounts for plausible supply distributions that are close to the historical empirical distribution but may generate supply outcomes not explicitly observed in the data, thereby achieving a flexible trade-off between robustness and performance (Gao & Kleywegt, 2023; He et al., 2026).

Tractable Reformulation of DRCC model

We next derive a tractable deterministic reformulation of constraint (4.26) following the data-driven reformulation techniques (Chen et al., 2024) for Wasserstein-based chance constraints. For a fixed (i,f), define the *safe set* and *unsafe set* as:

$$\mathcal{S}_{if}(\boldsymbol{b}) := \{s \in \mathbb{R} : \ s \geq D_{if}(\boldsymbol{b})\}, \qquad \bar{\mathcal{S}}_{if}(\boldsymbol{b}) := \{s \in \mathbb{R} : \ s < D_{if}(\boldsymbol{b})\}, \tag{4.27}$$

then constraint (4.26) is equivalent to requiring that the worst-case violation probability is bounded by ε_{if}:

$$\sup_{\mathbb{Q} \in \mathcal{U}_{if}(\rho_{if})} \mathbb{Q}\left(\tilde{S}^i_f \in \bar{\mathcal{S}}_{if}(\boldsymbol{b})\right) \leq \varepsilon_{if}. \tag{4.28}$$

Step 1: Distance to the unsafe set Since $\tilde{S}^i_f$ is one-dimensional, the unsafe set corresponds to the open half-line $(-\infty, D_{if}(\boldsymbol{b}))$. The distance from sample $\hat{S}^i_{f,k}$ to the unsafe set is defined as

$$\operatorname{dist}\left(\hat{S}^i_{f,k}, \bar{\mathcal{S}}_{if}(\boldsymbol{b})\right) = \inf_{s < D_{if}(\boldsymbol{b})} \left|\hat{S}^i_{f,k} - s\right|. \tag{4.29}$$

If $\hat{S}^i_{f,k} < D_{if}(\boldsymbol{b})$, the sample already belongs to the unsafe set, and therefore the distance equals zero. Otherwise, if $\hat{S}^i_{f,k} \geq D_{if}(\boldsymbol{b})$, the closest point in the unsafe set is arbitrarily close to the boundary point $D_{if}(\boldsymbol{b})$, yielding

$$\operatorname{dist}\left(\hat{S}^i_{f,k}, \bar{\mathcal{S}}_{if}(\boldsymbol{b})\right) = \hat{S}^i_{f,k} - D_{if}(\boldsymbol{b}). \tag{4.30}$$

Combining the above two cases gives

$$\operatorname{dist}\left(\hat{S}^i_{f,k}, \bar{\mathcal{S}}_{if}(\boldsymbol{b})\right) = \left(\hat{S}^i_{f,k} - D_{if}(\boldsymbol{b})\right)_+, \qquad (x)_+ := \max\{x, 0\}. \tag{4.31}$$

Step 2: εN-smallest distances and LP lifting For each sample $k = 1, \ldots, N$, we define

$$r_{if,k} := \operatorname{dist}\left(\hat{S}^i_{f,k}, \bar{\mathcal{S}}_{if}(\boldsymbol{b})\right), \tag{4.32}$$

and let

$$r_{if,1} \leq r_{if,2} \leq \cdots \leq r_{if,N} \tag{4.33}$$

denote the ordered distances. According to Theorem 2 in Chen et al. (2024), constraint (4.28) is equivalent to

$$\frac{1}{N} \sum_{k=1}^{\varepsilon_{if} N} r_{if,(k)} \geq \rho_{if}. \tag{4.34}$$

Constraint (4.34) indicates that the DRCC is satisfied if and only if the average of the $\varepsilon_{if} N$ smallest distances from the empirical samples to the unsafe set is no smaller than the Wasserstein radius ρ_{if}.

To avoid explicitly sorting the distances, we employ the following lifting representation. First, we introduce the lemma from the work of He et al. (2026) below:

Lemma 4.1 *Let $\{r_1, r_2, \ldots, r_N\}$ be a set of real numbers sorted in ascending order. For any $\varepsilon \in (0,1)$ such that $\varepsilon N \in \mathbb{Z}_+$, the sum of the εN smallest elements is equivalent to the optimal value of the following linear programming problem:*

$$\max_{\chi,\varpi} \quad \varepsilon N\chi - \sum_{k=1}^{N} \varpi_k \tag{4.35}$$

$$\text{s.t.} \quad r_k \geq \chi - \varpi_k, \quad k = 1, \ldots, N, \tag{4.36}$$

$$\varpi_k \geq 0, \quad \chi \text{ is free.} \tag{4.37}$$

□

Proof of Lemma 4.1.

The sum of the εN smallest elements in the set $\{r_1, r_2, \ldots, r_N\}$ can be represented by the following linear programming model:

$$\min_{x} \quad \sum_{k=1}^{N} r_k x_k \tag{4.38}$$

$$\text{s.t.} \quad \sum_{k=1}^{N} x_k = \varepsilon N, \tag{4.39}$$

$$x_k \in [0,1], \forall k \in \{1, 2, ..., N\} \quad k = 1, \ldots, N. \tag{4.40}$$

The dual formulation of (4.38)–(4.40) is given by

$$\max_{\chi,\varpi} \quad \varepsilon N\chi - \sum_{k=1}^{N} \varpi_k \tag{4.41}$$

$$\text{s.t.} \quad r_k \geq \chi - \varpi_k, \quad k = 1, \ldots, N, \tag{4.42}$$

$$\varpi_k \geq 0, \quad \chi \text{ is free.} \tag{4.43}$$

By the strong duality theorem of linear programming, the optimal objective values of the primal and dual problems are equal. Therefore, the sum of the εN smallest elements is equivalent to the optimal value of (4.41)–(4.43). This completes the proof.

Applying Lemma 4.1 to (4.34) yields the following equivalent reformulation:

$$\varepsilon_{if} N\chi_{if} - \sum_{k=1}^{N} \varpi_{if,k} \geq \rho_{if} N, \quad \forall i \in \mathcal{P}, \forall f \in \mathcal{F}, \tag{4.44}$$

with

$$\text{dist}\Big(\hat{S}^i_{f,k}, \bar{S}_{if}(\boldsymbol{b})\Big) \geq \chi_{if} - \varpi_{if,k}, \quad \forall i \in \mathcal{P}, \forall f \in \mathcal{F}, \forall k = 1, \ldots, N, \tag{4.45}$$

and

$$\varpi_{if,k} \geq 0, \quad \chi_{if} \text{ is free}, \quad \forall i \in \mathcal{P}, \forall f \in \mathcal{F}, \forall k = 1, \ldots, N. \tag{4.46}$$

We then substitute (4.31) into (4.45) and yield

$$\left(\hat{S}^i_{f,k} - D_{if}(\boldsymbol{b})\right)_+ \geq \chi_{if} - \varpi_{if,k}, \quad \forall i \in \mathcal{P}, \forall f \in \mathcal{F}, \forall k = 1, \ldots, N. \tag{4.47}$$

Step 3: Exact MIP reformulation of the positive-part function Constraint (4.47) can be represented exactly via a standard big-M mixed-integer formulation. Introduce binary variables $l_{if,k} \in \{0,1\}$ and a sufficiently large constant M_{if}:

$$\hat{S}^{i}_{f,k} - D_{if}(\boldsymbol{b}) + M_{if} l_{if,k} \geq \chi_{if} - \varpi_{if,k}, \qquad \forall i \in \mathcal{P},\ \forall f \in \mathcal{F},\ \forall k = 1,\ldots,N, \tag{4.48}$$

$$M_{if}(1 - l_{if,k}) \geq \chi_{if} - \varpi_{if,k}, \qquad \forall i \in \mathcal{P},\ \forall f \in \mathcal{F},\ \forall k = 1,\ldots,N, \tag{4.49}$$

$$l_{if,k} \in \{0,1\}, \qquad \forall i \in \mathcal{P},\ \forall f \in \mathcal{F},\ \forall k = 1,\ldots,N. \tag{4.50}$$

Replacing the deterministic port supply constraint (4.12) by (4.44), (4.46) and (4.48)–(4.50) yields a tractable mixed-integer programming model. So the full reformulation of DRCC model consists of the objective function (4.1), constraints (4.2)–(4.11), (4.13)–(4.17), (4.44), (4.46), and (4.48)–(4.50). Depending on the choice of the ground metric in the Wasserstein distance, the resulting model can be cast as an MILP and can be solved using off-the-shelf solvers such as CPLEX or Gurobi.

4.4 Experimental studies

This section presents numerical experiments to evaluate the effectiveness and robustness of the proposed optimization models under uncertain fuel supply conditions. The experiments are designed to analyze the computational performance of the proposed approaches, compare the deterministic, CCP (with SAA method), and DRCC models, and investigate the impacts of key parameters such as carbon emission cost. In addition, future methanol uptake scenarios are further examined to evaluate the potential impacts of alternative fuel infrastructure expansion and methanol price reduction.

4.4.1 Test instances

The experimental shipping network consists of four short-sea liner services operating in Northern and Western Europe as shown in Figure 4.5, namely Finland Express 1 (FI1), Baltic Bridge Express (BBX), Iberia Europe Service (IBC), and Poland Shuttle (PLS). The network covers major container ports in the North Sea, Baltic Sea, and Iberian regions, including Rotterdam, Antwerp, Helsinki, Gdańsk, Hamburg, Lisbon, and Leixões. The corresponding port of call and sailing distances are obtained from the official service schedules published by Ocean Network Express (ONE). To capture operational flexibility, each sailing leg is associated with a minimum and maximum sailing speed. The constructed network is subsequently used to investigate how uncertainty in fuel supply affects operational performance and the performance of different models.

We consider three representative marine fuels, namely Marine Gas Oil (MGO), Liquefied Natural Gas (LNG), and methanol in the experiments. These fuels represent conventional fossil fuel, transitional low-carbon fuel, and alternative clean fuel pathways in maritime transportation. The corresponding fuel parameters are summarized in Table 4.6. Among the considered fuels, LNG provides the highest calorific value, while methanol has a significantly lower energy density, resulting in higher fuel consumption for the same sailing distance. The fuel-specific CO_2 emission factors are further incorporated into the carbon emission cost calculation in optimization models. In the current scenario, among the 12 ports included in the network, 11 ports are assumed to provide MGO bunkering services, while LNG is available at 7 ports. In contrast, due to the still limited adoption of methanol in the maritime industry, methanol bunkering infrastructure is assumed to be available at only 2 ports in the network. This setting reflects the current transitional stage of maritime decarbonization, where conventional fuels remain widely accessible, whereas alternative low-carbon fuels are still constrained by limited bunkering coverage.

The penalty cost for delays at each port is set at 10,000 EUR per hour. The bunkering setup time is 0.5 hours. The basic emission cost is 75 EUR per ton. Sailing speeds are discretized into intervals of 0.1 knots. We create 150 sets of in-sample data and 150 sets of out-of-sample test data. The parameters ρ and ε are set to 0.1 and 0.05, respectively.

4.4.2 Impact of fuel supply uncertainty on operational costs

To evaluate the impact of fuel supply uncertainty on operational decisions, the deterministic model, CCP model (with SAA method), and DRCC model are compared under different numbers of in-sample uncertainty sets. Two dual-fuel scenarios are considered, namely MGO–LNG and MGO–Methanol. The deterministic model serves as the baseline case without uncertainty consideration, while CCP+SAA and DRCC explicitly incorporate uncertain fuel supply information into the optimization framework. Table 4.7 presents the corresponding objective values under different model settings. For the chance-constrained and distributionally robust models, the

Table 4.5: Shipping routes used in the numerical experiments

Route code	Port of call	Number of port of calls	Number of visit legs
FI1	Antwerp (ANR) → Rotterdam (RTM) → Helsinki (HEL) → Kotka (KTK) → Antwerp (ANR)	5	4
BBX	Rotterdam (RTM) → Gdańsk (GDN) → Klaipėda (KLJ) → Riga (RIX) → Gdańsk (GDN) → Rotterdam (RTM)	6	5
IBC	Leixões (LEI) → Lisbon (LIS) → Southampton (SOU) → Bremerhaven (BRV) → Rotterdam (RTM) → Leixões (LEI)	6	5
PLS	Bremerhaven (BRV) → Hamburg (HAM) → Gdansk (GDN) → Bremerhaven (BRV)	4	3

Table 4.6: Parameters of fuels

Fuel	**Fuel type**	**CO_2 emission (g CO_2/ g fuel)**	**Calorific values (MJ/t)**
MGO	Conventional fuel	3.206	42,700
LNG	Low-carbon fuel	2.750	50,000
Methanol	Alternative clean fuel	1.375	19,900

number of in-sample uncertainty sets is varied from 50 to 150 to examine the stability of the solutions under different sample sizes.

The results show that the deterministic model consistently achieves the lowest objective value in both fuel scenarios, since it ignores fuel supply uncertainty and optimizes decisions solely based on nominal parameter values. Once uncertainty is incorporated through CCP and DRCC formulations, the objective values increase due to the additional robustness requirements imposed on bunkering and sailing decisions.

For the MGO–LNG scenario, both CCP and DRCC models produce relatively stable objective values as the number of in-sample sets increases from 50 to 150. The DRCC model consistently yields slightly higher costs than CCP, reflecting the conservative nature of distributionally robust optimization under Wasserstein ambiguity sets. A similar trend can be observed in the MGO–Methanol scenario, although the increase in objective value becomes significantly more pronounced. Compared with the MGO–LNG case, the methanol-based scenario exhibits higher total costs for both CCP and DRCC models. This is mainly because methanol has a lower calorific value and more limited bunkering availability in the considered network, resulting in higher fuel consumption and reduced operational flexibility. Moreover, the cost gap between CCP and DRCC becomes larger in the MGO–Methanol scenario, indicating that fuel supply uncertainty has a stronger impact when alternative fuel infrastructure remains insufficiently developed.

In addition, the influence of the number of in-sample sets is more noticeable in the MGO–Methanol scenario. For the CCP model, increasing the number of in-sample sets from 50 to 100 slightly reduces the objective value, while the result remains relatively stable afterward. By contrast, the DRCC model shows a gradual increase in objective value as the number of in-sample sets increases from 50 to 150. Overall, the results demonstrate that the proposed DRCC model can effectively capture uncertainty-induced operational risks.

Table 4.7: Computational performance of different models

Model	MGO–LNG		MGO–Methanol	
	Number of in-sample sets	Objective Value	Number of in-sample sets	Objective Value
Deterministic model	–	2,117,846.55	–	2,252,119.51
CCP+SAA	50	2,136,120.73	50	2,370,721.92
	100	2,134,410.26	100	2,355,524.09
	150	2,135,605.54	150	2,356,805.60
DRCC	50	2,140,332.54	50	2,404,306.45
	100	2,139,931.22	100	2,425,486.47
	150	2,140,164.10	150	2,430,343.52

4.4.3 Reliability of operational plans under fuel supply uncertainty

To further evaluate the robustness of the obtained solutions under uncertainty realizations, out-of-sample tests are conducted for both CCP and DRCC models. The probability of satisfying the chance constraints under different numbers of in-sample tests is reported for the MGO–LNG and MGO–Methanol scenarios, respectively.

Figure 4.2 illustrates the out-of-sample performance for the MGO–LNG scenario. The DRCC model consistently achieves significantly higher feasibility probabilities than the CCP model across all sample sizes. Specifically, the CCP model achieves feasibility probabilities of approximately 69%, 58%, and 69% when the number of in-sample sets equals 50, 100, and 150, respectively. In contrast, the DRCC model maintains substantially higher feasibility levels of around 86%–88% for all cases. These results indicate that the DRCC model provides considerably stronger robustness against fuel supply uncertainty. Moreover, the feasibility performance of DRCC remains highly stable as the number of in-sample sets increases, suggesting that the Wasserstein-based ambiguity set can effectively hedge against distributional uncertainty even with limited training samples. By comparison, the CCP model exhibits larger fluctuations in out-of-sample feasibility, implying that solutions obtained purely from empirical sample approximations may suffer from weaker generalization ability under unseen uncertainty realizations.

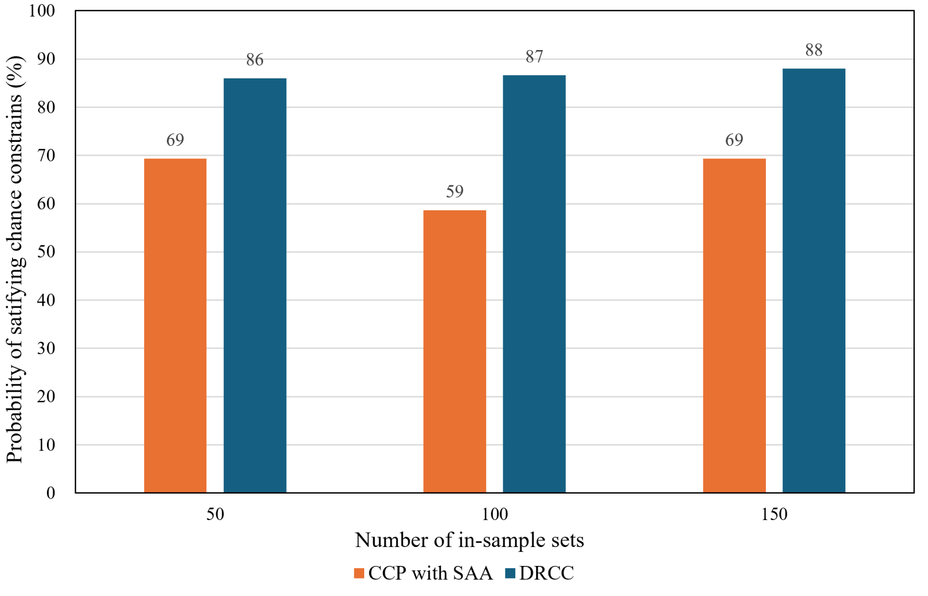

Figure 4.2: Out-of-sample feasibility performance for the MGO–LNG scenario

Figure 4.3 presents the corresponding out-of-sample results for the MGO–Methanol scenario. Compared with the MGO–LNG case, the overall feasibility levels become lower for both models, reflecting the more challenging operational environment caused by limited methanol bunkering infrastructure and lower fuel energy density. For the CCP model, the feasibility probabilities are approximately 62%, 51%, and 57% under 50, 100, and 150 in-sample sets, respectively. By

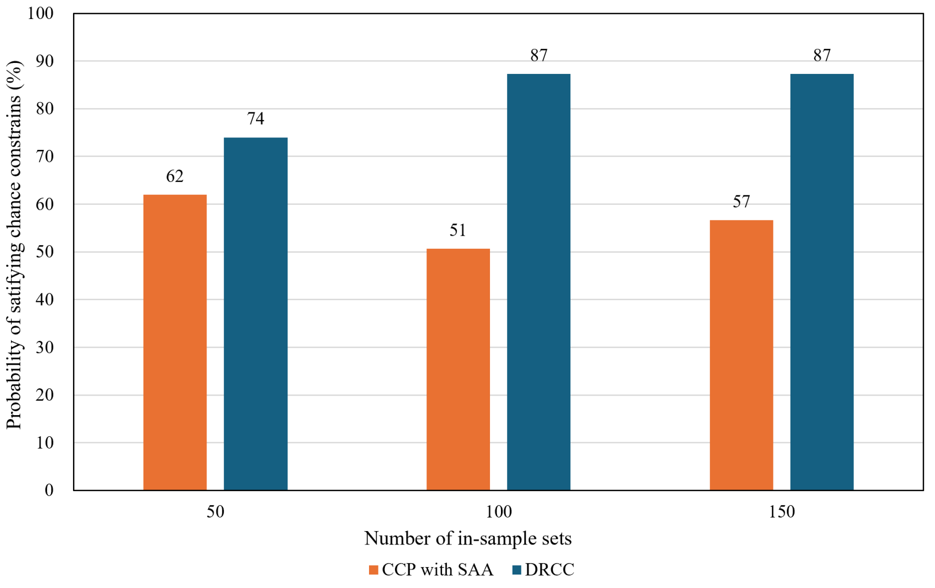

Figure 4.3: Out-of-sample feasibility performance for the MGO–Methanol scenario

contrast, the DRCC model achieves substantially higher feasibility probabilities of approximately 74%, 87%, and 87%. The improvement becomes particularly significant when the number of in-sample sets increases from 50 to 100, indicating that the DRCC model can better utilize additional uncertainty information to construct more reliable robust solutions.

Overall, the out-of-sample results demonstrate that the proposed DRCC framework significantly improves operational robustness compared with the CCP framework with SAA approach, especially in alternative-fuel scenarios with insufficient bunkering coverage. Although the DRCC model leads to higher operational costs, as shown in Table 4.7, it substantially enhances the probability of satisfying fuel supply chance constraints under unseen uncertainty realizations. This highlights the practical importance of incorporating distributionally robust optimization into maritime fuel planning problems under uncertain fuel supply conditions.

4.4.4 Impact of carbon pricing on operational decisions

To investigate the influence of environmental regulation intensity on operational decisions, a sensitivity analysis is conducted with respect to the carbon emission cost parameter η for the MGO–LNG scenario. The carbon emission cost varies from 30 to 150 EUR/t CO_2 (30, 45, 60, 75, 90, 105, 120, 135, 150 EUR/t), and the corresponding changes in operational cost components and total emissions are analyzed.

Figure 4.4 illustrates the variation of bunkering cost, delay cost, emission cost, and total cost under different carbon emission cost levels. As expected, the emission cost increases significantly with the increase of η, since higher carbon prices directly penalize fuel-related emissions. Consequently, the total operational cost also exhibits a clear upward trend as the carbon emission cost increases. By contrast, the bunkering cost remains relatively stable across different carbon price levels, indicating that the fuel bunkering strategy changes only moderately within the considered range of carbon prices. Similarly, the delay cost fluctuates only slightly, suggesting that the vessel scheduling decisions remain relatively stable. Overall, the results indicate that the increase in total cost is mainly driven by the growing emission-related penalties rather than substantial changes in bunkering or scheduling costs.

Figure 4.5 presents the corresponding changes in total carbon emissions. Overall, carbon emissions gradually decrease as carbon prices increase, indicating that stronger carbon pricing provides effective incentives for shipping companies to adopt cleaner operational strategies. The reduction in emissions is achieved through adjustments in fuel usage and sailing decisions while maintaining relatively stable bunkering and scheduling costs. A slight increase in emissions can be observed when the carbon price increases from 105 to 120 EUR/t CO_2. This reflects a localized adjustment in the optimal operational strategy, where changes in bunkering locations or sailing decisions temporarily offset part of the emission reduction benefit. Nevertheless, the overall trend remains clear, with higher carbon prices leading to lower network-wide carbon emissions.

Overall, the results demonstrate that carbon pricing can promote lower–emission shipping operations while maintaining relatively stable operational performance. Although higher carbon prices inevitably increase total operating costs, they also provide economic incentives for cleaner fuel utilization and more energy–efficient operations. These findings suggest that carbon pricing can serve as an effective policy instrument for supporting the transition toward low–carbon

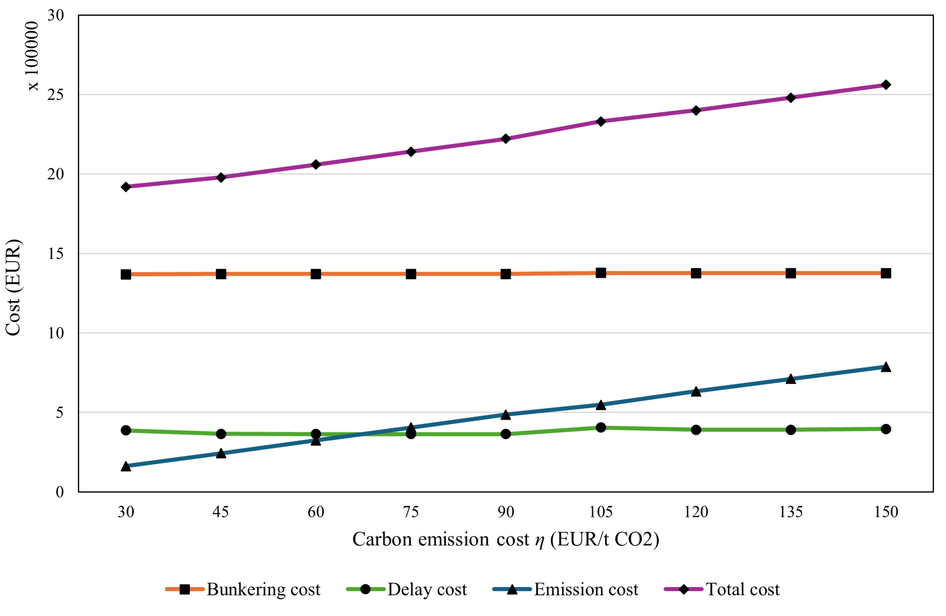

Figure 4.4: Sensitivity analysis of costs under different carbon emission cost levels for the MGO–LNG scenario

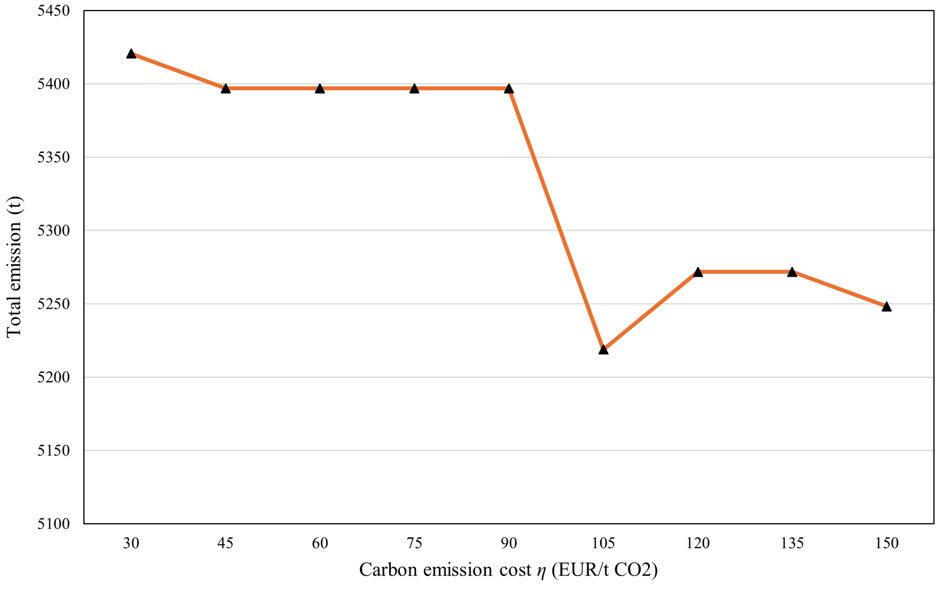

Figure 4.5: Sensitivity analysis of total carbon emissions under different carbon emission cost levels for the MGO–LNG scenario

maritime transport while preserving the operational efficiency of liner shipping services.

4.4.5 Methanol uptake

To examine how the future development of methanol may affect fuel–switching decisions and emission performance, several sets of experiments are conducted for the MGO–Methanol configuration under a carbon emission cost of 150 EUR/t. Experiments investigate the effect of progressively expanding methanol availability across the port network, and the effect of reducing the methanol price. For the supply expansion experiments, a methanol price reduction of approximately 20%, 40%, and 60% relative to the original price is applied to all supply scenarios. The number of ports supplying methanol increases progressively from 2 out of 12 ports in the base case to 5, 8, and 11 ports in the three expanded supply scenarios. The price reduction set looks into the effect of methanol price reductions under a developed supply network (11 out of 12 ports can provide methanol bunkering service). These experiments use the original methanol price as the reference case and consider reductions of approximately 20%, 40%, and 60%.

Before examining the detailed bunkering and fuel consumption patterns under different methanol supply scenarios, Figure 4.6 provides an overview of the share of methanol in total fuel use. The bars report the proportions of methanol in total MGO–Methanol consumption and bunkering when the methanol price is reduced by 60%. The horizontal lines indicate the corresponding counterfactual upper bounds under an extreme idealized condition in which the methanol price is assumed to be zero. These bounds represent the maximum economically attainable methanol shares under the given availability of methanol supply, while the other operational and technical constraints remain unchanged.

As the number of methanol-supplying ports increases from 2 to 5, 8, and 11, the upper bound rises from 32.8% to 62.7%, 73.4%, and 83.7%, respectively, while the realized consumption share under the 60% price reduction follows a similar pattern, increasing from 31.5% to 58.9%, 72.9%, and 83.2%. This demonstrates that broader supply coverage can substantially increase the feasible use of methanol when its price is sufficiently competitive. Moreover, the observed shares are already close to their counterfactual upper bounds, particularly in the scenarios with 8 and 11 supplying ports. This suggests that, at a 60% price reduction, the methanol shares are very close to the upper bound, indicating that the potential for further methanol adoption through price reductions has been largely exploited at this price level. The remaining restriction may be associated with the spatial availability of methanol supply and other operational constraints. Moreover, expanding methanol supply from 2 to 5 ports leads to a substantial increase in both the upper bound and the realized methanol shares. Although both measures continue to increase as methanol becomes available at more ports, the gains from further expansion to 8 and 11 ports are comparatively smaller, suggesting diminishing marginal benefits from broader supply coverage. The upper bound remains around 84%, rather than reaching 100%, because tank-capacity limits, minimum safety-stock requirements, and the spatial structure of voyage legs still require some use of MGO.

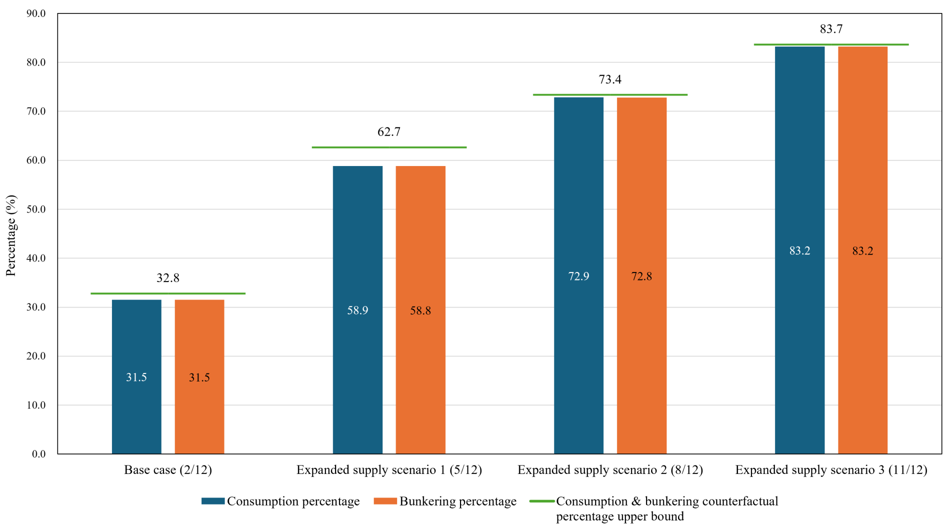

Figure 4.6: Methanol shares in total fuel consumption and bunkering under 60% price reduction and their counterfactual upper bound.

Figure 4.7 presents the effect of expanding methanol supply when its price is reduced by approximately 20%. Expanding methanol availability from 2 to 5 ports changes the optimal fuel strategy: methanol consumption increases from 322.17 t to 430.26 t, while MGO consumption decreases from 1553.95 t to 1503.21 t. Methanol bunkering increases from 364.82 t to 487.22 t, whereas MGO bunkering decreases from 1761.30 t to 1704.25 t. This adjustment also leads to a modest reduction in carbon emissions. However, further expansion from 5 to 8 and subsequently

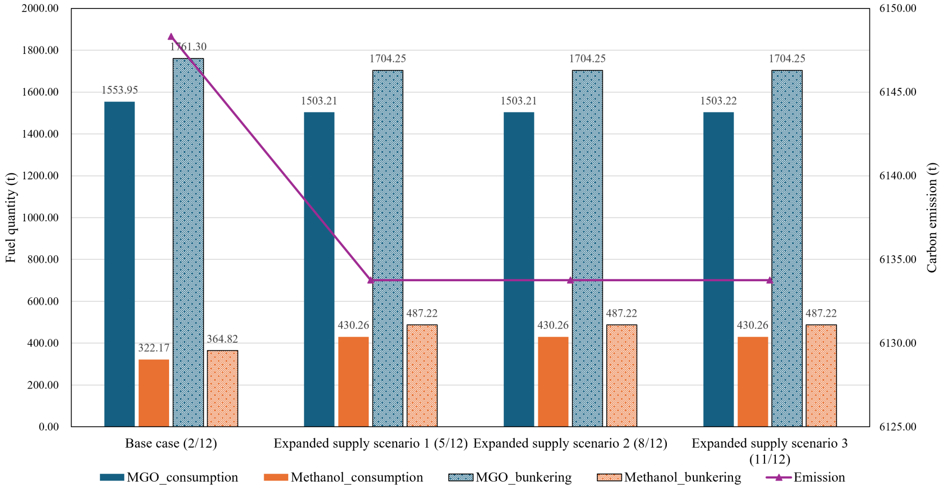

Figure 4.7: Consumption and bunkering quantity of different fuels and carbon emissions in scenarios of supply expansion for methanol fuel under the price level of 20% reduction.

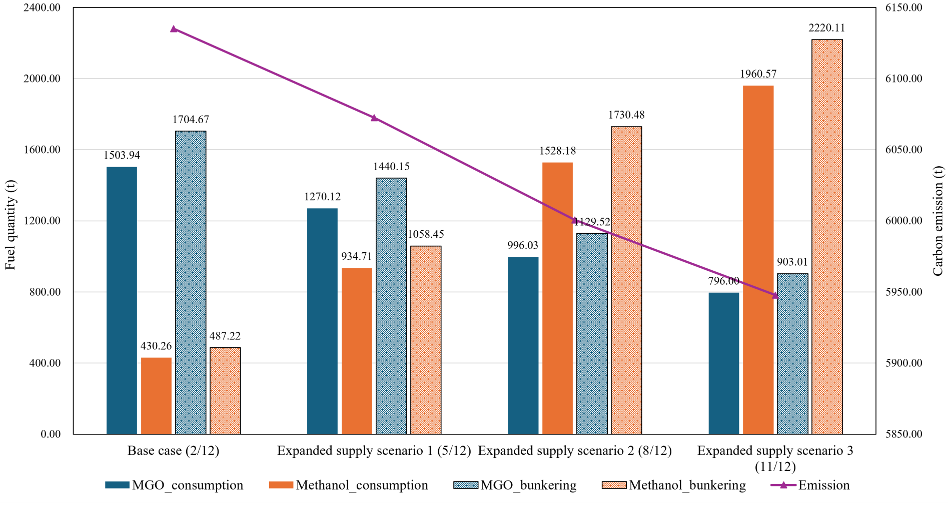

Figure 4.8: Consumption and bunkering quantity of different fuels and carbon emissions in scenarios of supply expansion for methanol fuel under the price level of 40% reduction.

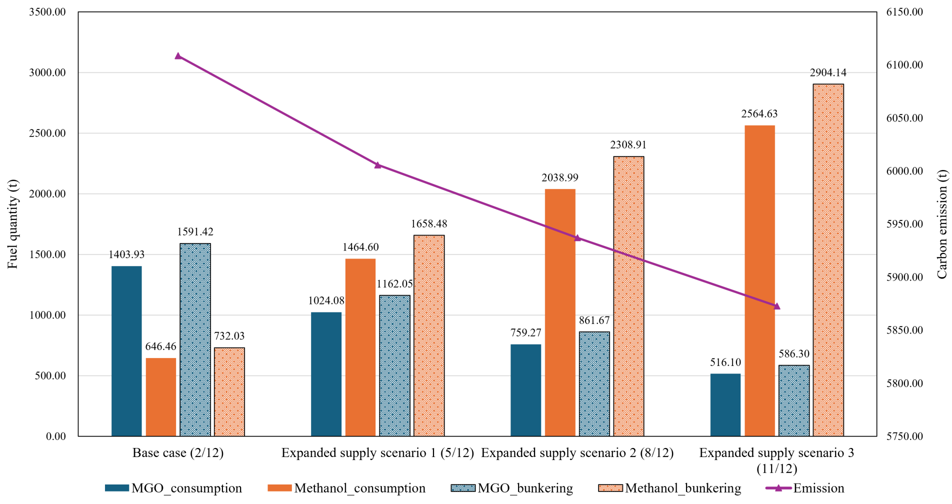

Figure 4.9: Consumption and bunkering quantity of different fuels and carbon emissions in scenarios of supply expansion for methanol fuel under the price level of 60% reduction.

11 methanol-supplying ports produces almost no additional change. Thus, at the 20% price-reduction level, supply expansion exhibits a clear saturation effect after methanol becomes available at five strategically located ports. The results also indicate that supply expansion alone is insufficient to induce extensive fuel switching when methanol remains relatively expensive.

Figure 4.8 shows the response to supply expansion becomes substantially stronger when the methanol price is reduced by approximately 40%. As the number of methanol-supplying ports increases from 2 to 5, 8, and 11, methanol consumption rises continuously from 430.26 t to 1960.57 t. At the same time, MGO consumption decreases from 1503.94 t to 796.00 t. The bunkering decisions follow the same pattern: methanol bunkering increases from 487.22 t to 2220.11 t, whereas MGO bunkering decreases from 1704.67 t to 903.01 t. Unlike the saturation observed under the 20% price reduction, each stage of infrastructure expansion produces additional fuel switching and emission reductions under the 40% price reduction. Methanol consumption exceeds MGO consumption when the supply network expands to 8 ports, indicating that a sufficiently competitive methanol price enables additional supply locations to alter the optimal fuel mix substantially. Therefore, at this price level, infrastructure availability remains an active constraint, and expanding the supply network generates sustained operational and environmental benefits.

Figure 4.9 shows that the effect of supply expansion is even more pronounced when the methanol price is reduced by approximately 60%. Methanol consumption increases from 646.46 t in the 2-port base case to 2564.63 t as its availability expands to 11 ports. Conversely, MGO consumption decreases from 1403.93 t to 516.10 t. Methanol bunkering rises from 732.03 t to 2904.14 t, while MGO bunkering declines from 1591.42 t to 586.30 t. At this price level, methanol consumption already exceeds MGO consumption after the supply network expands from 2 to 5 ports, and the dominance of methanol strengthens with every subsequent expansion. Carbon emissions also decrease consistently as additional methanol-supplying ports are introduced. These results indicate a strong complementarity between fuel affordability and infrastructure availability: once methanol becomes highly price-competitive, limited port availability restricts its adoption, while supply expansion unlocks increasingly extensive substitution of MGO by methanol.

A comparison of Figures 4.7–4.9 demonstrates that the value of supply expansion is conditional on the methanol price. Under the 20% price reduction, increasing the network beyond 5 supplying ports provides almost no additional benefit. Under the 40% and 60% price reductions, however, methanol use increases and MGO use and carbon emissions decrease at every stage of expansion. Moreover, the transition to methanol-dominated operation occurs earlier when the price reduction is larger: it occurs at 8 supplying ports under the 40% reduction but already at 5 supplying ports under the 60% reduction. Hence, infrastructure development and price reductions act as complementary measures. Supply expansion creates opportunities to bunker and use methanol, while price competitiveness determines whether those opportunities are incorporated into the optimal operational strategy.

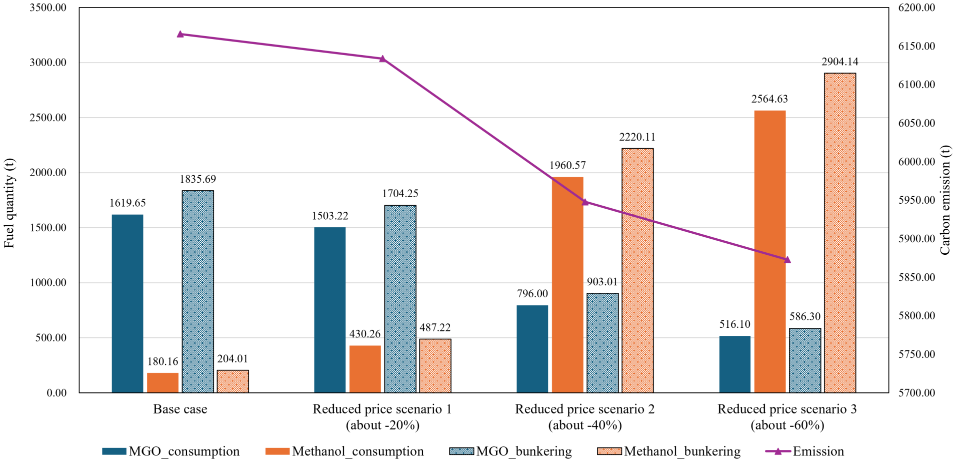

Figure 4.10: Consumption and bunkering quantity of different fuels and carbon emissions in scenarios of price reduction for methanol fuel.

Figure 4.10 further investigates the influence of methanol price reductions of approximately 20%, 40%, and 60%. A moderate price reduction of approximately 20% causes only a limited adjustment in the fuel mix. Compared with the base case, MGO consumption decreases from 1619.65 t to 1503.22 t, while methanol consumption increases from 180.16 t to 430.26 t. The corresponding bunkering quantities change from 1835.69 t to 1704.25 t for MGO and from 204.01 t to 487.22 t for methanol. This suggests that, at this price level, methanol becomes more attractive but does not yet replace MGO as the principal fuel. A more substantial transition occurs when the methanol price is reduced by approximately 40%. Methanol consumption rises sharply to 1960.57 t, while MGO consumption falls to 796.00 t. Methanol bunkering consequently increases to 2220.11 t, compared with 903.01 t for MGO. Under the approximately 60% price reduction scenario, fuel switching becomes even more pronounced: methanol consumption and bunkering reach 2564.63 t and 2904.14 t, respectively. The larger mass of methanol consumed should be interpreted in light of its lower energy density relative to MGO; a greater mass of methanol is required to provide an equivalent amount of propulsion energy. Nevertheless, the results clearly demonstrate a large-scale shift in the optimal fuel mix toward methanol.

Carbon emissions decrease progressively as the methanol price falls, but the reduction is nonlinear. The approximately 20% price reduction produces only a small emission improvement, consistent with the limited change in the fuel mix. By contrast, the approximately 40% price reduction results in a pronounced decline in emissions as methanol becomes the dominant fuel by mass. A further price reduction to approximately 60% lowers emissions to about 5875 t, compared with approximately 6175 t in the base case. This corresponds to an emission reduction of about 4.8%. The emission reduction is smaller in percentage terms than the increase in methanol consumption because methanol has a substantially lower energy density, and its environmental benefit must therefore be evaluated together with the amount required to meet vessel energy demand.

Overall, the experiments show that infrastructure availability and fuel price are mutually reinforcing determinants of methanol adoption. Expanding the supply network removes spatial bunkering constraints, but its effect is limited when methanol remains relatively expensive. Conversely, as methanol becomes more cost-competitive, restricted availability becomes an increasingly important barrier, and each stage of supply expansion facilitates additional substitution of MGO and further emission reductions. The results therefore suggest that limited, strategically targeted infrastructure development may be sufficient under moderate price improvements, whereas broad supply-network expansion becomes valuable when substantial cost reductions make large-scale methanol use economically attractive. Coordinated improvements in both availability and affordability are consequently required to achieve extensive methanol adoption.

4.5 Managerial insights

We summarize some managerial insights derived from the proposed model and computational experiments. The insights highlight practical implications for shipping companies, port operators, and policymakers in supporting robust fuel planning under uncertain fuel supply conditions.

- Fuel supply uncertainty should be incorporated into bunkering and scheduling planning. Plans based only on expected fuel availability may become infeasible when actual port supply deviates from forecasts. For the MGO–LNG case, the DRCC approach increases out–of–sample feasibility from approximately 58%–69% under CCP to approximately 86%–88%. Although this reliability requires moderately higher planned costs, it reduces the risks of fuel shortages, emergency bunkering, and voyage disruptions. Such uncertainty-aware planning is particularly important for emerging fuels with limited supply networks.
- The value of (distributionally) robust planning becomes more pronounced when alternative-fuel supply networks remain limited. Alternative fuels with limited bunkering coverage provide fewer opportunities to adjust bunkering plans when actual fuel supply deviates from expectations. Compared with LNG, the smaller methanol supply network therefore exposes vessel operations to greater risks of fuel shortages and voyage infeasibility. The improved out–of–sample feasibility achieved by the DRCC model demonstrates the importance of explicitly accounting for supply uncertainty. Shipping companies should consider not only fuel availability along a route but also the redundancy of alternative supply locations, while

ports and fuel suppliers should prioritize network resilience when planning new bunkering facilities.

- Closing the cost gap between alternative fuel and conventional fuel requires coordinated fuel supply expansion and fuel price reduction. The cost gap generally refers to the overall economic difference between using methanol and conventional fuels, including not only the difference in fuel purchase prices but also the other operational costs, emission costs, and additional costs arising from infrastructure and corresponding services. In our experiments, the counterfactual upper bound on the methanol share (i.e., the share achievable if methanol were free) rises from 33% with 2 bunkering ports to 63%, 73%, and 84% with 5, 8, and 11 ports, and is never 100% because tank capacities and voyage geometry require some MGO use. These results indicate that additional bunkering stations make methanol economically attractive, while price reductions allow vessels to use this advantage more extensively. To narrow the cost gap, fuel producers, port operators, and shipping companies could jointly develop strategically located bunkering stations, establish long-term fuel supply agreements, and increase production and distribution capacity. Policy support, such as production incentives, infrastructure co-financing, and carbon-based measures, could further improve methanol's competitiveness and reduce the investment risk during the early stage of deployment.

- Expanding the number of methanol bunkering stations is essential for unlocking alternative-fuel uptake once methanol becomes sufficiently price-competitive. In our experiments, under the 60% methanol price reduction, increasing the number of supplying ports from 2 to 5 raises the methanol consumption share from 31.5% to 58.9%, making methanol the dominant fuel by mass. Further expansion to 8 and 11 ports increases this share to 72.9% and 83.2%, respectively. These results show that limited station coverage remains a major barrier even when the fuel price is attractive. Port operators and policymakers should therefore expand the bunkering network in phases, initially prioritizing strategically located stations and subsequently extending coverage as methanol demand grows.

- Price reductions are critical for enabling large-scale methanol adoption, but their marginal effect eventually becomes limited by infrastructure and operational constraints. In our experiments, with 11 supplying ports, reducing the methanol price by 40% increases its consumption from 180.16 t in the reference case to 1960.57 t, while a 60% reduction raises it further to 2564.63 t and lowers carbon emissions by approximately 4.8%. At the 60% reduction level, however, the realized methanol shares are already close to their counterfactual zero-price upper bounds, suggesting that further price reductions alone would provide limited additional uptake without addressing the remaining spatial and operational barriers.

- Carbon pricing can encourage emission reductions but is more effective when supported by competitive and accessible alternative fuels. The sensitivity analysis shows that higher carbon emission costs generally encourage lower-emission operational decisions without substantially affecting delay costs or service schedules, although they increase total operating costs. Meanwhile, the methanol development scenarios show that expanding supply alone has limited marginal effects once strategically important ports are covered, whereas sufficient price reductions lead to more substantial fuel switching. These findings suggest that carbon pricing should be combined with targeted infrastructure development and measures that improve the price competitiveness of alternative fuels.

4.6 Conclusions

Dual–fuel vessels are increasingly introduced as an important measure to support the decarbonization of maritime shipping. However, the transition toward low–carbon marine fuels creates new operational challenges for liner shipping. Although LNG and methanol provide potential alternatives to conventional marine fuels, their adoption is constrained by limited bunkering coverage, uncertain port fuel supply, and insufficient price competitiveness. Moreover, the close interactions among sailing speed, bunkering, and fuel-switching decisions make it difficult for shipping companies to balance operating costs, emissions, and supply reliability.

This chapter addresses RQ 4. In this chapter, we investigate the integrated planning of dual-fuel liner services under uncertain fuel supply. We develop deterministic, chance-constrained programming (CCP), and distributionally robust chance-constrained (DRCC) models to jointly optimize sailing speed, bunkering quantities and locations, and fuel switching. Since the true distribution of port–level fuel supply is usually unknown and the available data is limited, the DRCC model uses a Wasserstein ambiguity set to consider a range of probability distributions around the empirical distribution. We conduct computational experiments based on a real-world feeder liner service network for both MGO–LNG and MGO–Methanol configurations.

The results demonstrate that explicitly accounting for fuel supply uncertainty is essential for reliable operational planning. Although deterministic and CCP solutions generally incur lower planned costs, they are more likely to become infeasible when realized fuel supplies deviate from expectations. The DRCC approach substantially improves out–of–sample feasibility at the expense of moderately higher operating costs. For the MGO–LNG configuration, it increases the feasibility rate from approximately 58%–69% under CCP to approximately 86%–88%.

We also conduct experiments looking into the methanol uptake scenarios. The results show that supply availability and price competitiveness jointly determine the extent of methanol adoption. With a 20% price reduction, expanding methanol supply from 2 to 5 ports changes the optimal fuel strategy, whereas further expansion to 8 or 11 ports provides almost no additional benefit. When methanol becomes sufficiently price-competitive, increasing the number of bunkering stations plays a stronger role. Under the 60% price reduction, expanding supply from 2 to 5 ports increases the methanol consumption share from 31.5% to 58.9%, while further expansion to 8 and 11 ports raises it to 72.9% and 83.2%, respectively. These realized shares sit close to the counterfactual upper bounds attainable if methanol were free (63% at 5 ports, 84% at 11), which are set by bunkering-station coverage and never reach 100% because tank capacities and voyage geometry require some MGO use. This shows that broader station coverage is necessary to unlock further methanol uptake once its price becomes attractive.

Price reduction also has a strong influence on the overall scale of methanol adoption. A reduction of approximately 20% produces only a moderate adjustment in the fuel mix, whereas a reduction of approximately 40% results in a pronounced shift toward methanol. When the price is reduced by 60%, the methanol consumption shares are already close to their counterfactual upper bounds under the idealized zero-price condition. This indicates that the potential to promote further methanol use through price reductions has been largely exploited at this price level, leaving supply availability and other operational constraints as the main barriers to additional adoption. The carbon cost analysis further shows that higher emission costs generally encourage lower-emission decisions without substantially changing service schedules, although their effectiveness depends on the availability and price competitiveness of alternative fuels.

Overall, reliable and lower-emission dual-fuel operations require sailing speed, bunkering, and fuel-switching decisions to be coordinated under supply uncertainty. The findings further indicate that closing the cost gap between alternative fuel (methanol in this chapter) and conventional fuel requires coordinated fuel supply expansion and fuel price reduction. Bunkering–station coverage determines what is achievable, and price competitiveness determines how close operators get to it. Initially prioritizing strategically located bunkering facilities can improve the effectiveness of infrastructure investment, while broader network expansion becomes justified once fuel prices are competitive enough to make the added coverage usable. The proposed framework therefore provides practical decision support for shipping companies, ports, and policymakers seeking to balance economic performance, emission reduction, and operational reliability during the maritime fuel transition.

Chapter 5

Conclusions and Future Research

This thesis investigates energy-aware operational planning and optimization for future low-carbon port and maritime transportation systems under uncertainty, covering stochastic terminal energy management, shore power demand prediction and integration, and robust dual-fuel vessel operation optimization. This chapter concludes the thesis. The research questions in Chapter 1 are answered in Section 5.1. Section 5.2 provides future research directions.

5.1 Conclusions

This thesis addresses the main research question "How can energy-aware operations planning be designed across port and maritime systems to support decarbonization objectives under uncertainty?". The main research question is decomposed into 4 sub-research questions and are addressed in Chapters 2–4.

5.1.1 Answers to sub-research questions

We summarize answers to these sub-questions as follows:

RQ 1: *How can terminal-level energy management and port operations be optimized under uncertain electricity prices and vessel arrival patterns?*

In Chapter 2, we propose a two-stage stochastic mixed-integer programming model to optimize container terminal operations planning and demand-responsive energy management. Operations considered in this model include vessel scheduling at berths, temperature control of refrigerated containers, and allocation of handling capacity of quay cranes, yard cranes, and automated guided vehicles to serve each vessel. Various scenarios for vessel arrival times and electricity prices are explored, representing the uncertainty of energy demand and supply, respectively. We solve the proposed model by developing a dedicated progressive hedging algorithm. Computational experiments based on a case study of the Altenwerder container terminal in Hamburg are conducted. The results suggest potential cost savings of 5.9 % on average with a single energy price based on a long-term contract and 13.2 % when applying varying real-time electricity prices based on wholesale market rates. The results also reveal clear demand-response behavior, where flexible loads are shifted toward periods with lower electricity prices. These findings underscore the substantial potential of demand response strategies for (electrified) container terminal operations.

RQ 2: *How to model shore power demand and predict it with raw vessel port call data?*

In Chapter 3, we propose a data-driven predict-then-optimize framework that constructs fine-grained SP demand profiles directly from raw vessel port call records and static vessel characteristics. The method first segments the berthing process into multiple operational stages, including pre-handling, cargo handling, overlap/gap periods, and post-handling, and assigns different shore power levels according to operational intensity. The time-grained shore power demand is then calculated by multiplying shore power and time duration of different stages. Machine learning models, including Random Forest (RF), XGBoost, LightGBM, Multilayer Perceptron (one typical model of Artificial Neural Network), Tabular Prior-data Fitted Network (TabPFN), and Ridge Regression, are then trained under both Full-Insight (with complete historical data) and Operational-Planning feature settings (with data restricted to pre-arrival observable variables). Results show that TabPFN and tree-based ensemble models achieve the best predictive performance, with XGBoost and RF obtaining R^2 values up to 0.986 under the Full-Insight setting while maintaining robust performance under limited pre-arrival information.

RQ 3: *How does SP demand modeling and prediction influence berth allocation decisions and terminal shore power profiles?*

In Chapter 3, the predicted shore power demand profiles are integrated into a shore power-aware berth allocation problem (SP-BAP) to evaluate their operational impacts. Experimental results demonstrate that ignoring shore power demand during berth planning can lead to severe peak-load violations and high penalty costs, while machine learning (ML)-based predictions generate scheduling outcomes close to the Perfect Information benchmark. In larger-scale experiments, the Base Case without the consideration of shore power produces total costs 36.06% higher than the Perfect Information case due to excessive shore power capacity violations, whereas ML-based approaches significantly reduce both penalty costs and peak demand. The best-performing ML-based BAP solution yields an objective value with a deviation of only approximately 3% from the Perfect Information benchmark. The results further show that SP-aware scheduling adjusts terminal demand profiles by shifting vessel service times and berth assignments, improving shore power capacity utilization and operational feasibility.

RQ 4: *How to optimize sailing speed, fuel choice, and bunkering decisions for dual-fuel vessels considering fuel supply uncertainty from ports?*

Chapter 4 develops an integrated optimization framework for dual-fuel liner shipping operations under uncertain fuel supply conditions. A deterministic mixed-integer optimization model is first formulated to jointly optimize sailing speed selection, fuel switching behavior, and bunkering decisions while considering fuel inventory, operational schedules, and fuel supply constraints. To explicitly address fuel supply uncertainty, the model is further extended into a chance-constrained programming (CCP) model and a distributionally robust chance-constrained (DRCC) model based on Wasserstein ambiguity sets. Computational experiments for both MGO-LNG and MGO-Methanol scenarios demonstrate that the proposed DRCC approach achieves significantly higher out-of-sample feasibility and operational robustness than deterministic and CCP-SAA approaches under uncertain fuel supply conditions. The results further show that expanding methanol bunkering infrastructure and reducing methanol prices substantially increase methanol usage and reduce total carbon emissions. Overall, the findings demonstrate the importance of robust optimization and coordinated fuel management for supporting reliable and low-carbon dual-fuel shipping operations under uncertain future fuel environments.

5.1.2 Answers to the main research question

The main research question is: *How can energy-aware operations planning be designed across port and maritime systems to support decarbonization objectives under uncertainty?*

At the port level, this thesis investigates stochastic energy management and operational planning for electrified container terminals under uncertain electricity prices and vessel arrival patterns. In addition, a predict-then-optimize framework is proposed to estimate and predict fine-grained shore power demand from raw vessel port call data and integrate the predicted demand into berth allocation decisions. The results demonstrate that energy-aware operational planning can effectively reduce operational costs, improve shore power utilization, and mitigate peak electricity demand under uncertain operational environments.

At the maritime network level, this thesis further investigates the joint optimization of sailing speed, fuel switching, and bunkering decisions for dual-fuel liner shipping services under uncertain fuel supply conditions. A distributionally robust optimization framework based on Wasserstein ambiguity sets is developed to improve operational robustness against uncertain alternative fuel availability. The results show that robust fuel management and coordinated operational planning can significantly improve out-of-sample feasibility while supporting emission reduction objectives.

From the uncertainty modeling perspective, this thesis incorporates different types of uncertainty using stochastic optimization, distributionally robust optimization, and machine learning approaches. In port operations, scenario-based stochastic programming is employed to capture uncertain electricity prices and vessel arrival patterns. For shore power demand uncertainty, machine learning models are developed to learn complex operational patterns from raw vessel port call data and generate fine-grained demand predictions for operational planning. In maritime bunkering planning, fuel supply uncertainty is addressed through chance-constrained and Wasserstein-based distributionally robust optimization formulations that explicitly account for ambiguity in fuel supply distributions. These approaches enable the proposed frameworks to generate solutions that remain reliable, adaptive, and economically efficient under uncertain future operational and energy conditions.

Overall, this thesis demonstrates that integrating energy-related considerations into operational planning, together with prediction and optimization approaches, can effectively improve the economic efficiency, operational reliability, and environmental performance of future port and maritime transportation systems.

Read together, the three technical chapters form a layered decomposition of a single decarbonization-oriented planning problem across scales. At the terminal scale, Chapter 2 shows that treating electricity as an uncertain, dispatchable input rather than a fixed cost item unlocks demand-response savings on the order of 13 percent. At the berth scale, Chapter 3 shows that treating shore power demand as a learnable, decision-relevant quantity rather than an exogenous input meaningfully improves berth allocation decisions and reduces capacity violations. At the network scale, Chapter 4 shows that treating alternative fuel supply at ports as an ambiguous rather than known distribution substantially improves out-of-sample feasibility of dual-fuel bunkering plans. In each case, moving from a deterministic, add-on treatment of energy to a stochastic or distributionally robust, co-equal treatment of energy shifts the operating point — cost, reliability, or emissions — in a materially favorable direction.

5.1.3 Implications for practice

Taken together, the three chapters provide several implications for port operators, shipping companies, energy providers, infrastructure planners, and policymakers. The following insights translate the main findings of this thesis into broader recommendations for energy-aware and lower-emission port and shipping operations.

1. **Integrating energy considerations into core operational planning.**

   The analysis in this thesis suggests that energy should be treated as a core operational decision dimension rather than as a fixed input or a constraint checked after operational plans have been determined. At container terminals, electricity procurement and energy use should be coordinated with equipment schedules and vessel-handling activities; at the berth level, shore power demand should be considered when assigning vessels to berths and time windows; and at the shipping-network level, sailing speed, bunkering quantities, and fuel choice should be planned jointly. Considering these decisions separately can produce schedules that appear operationally feasible but become costly or unreliable once electricity capacity, shore power demand, or fuel availability is taken into account. Port and shipping companies should therefore embed energy-related information and objectives directly into their operational planning systems.

2. **Treating uncertainty management as a foundation for operational reliability.**

   Practitioners should evaluate operational plans not only according to their expected costs under assumed conditions but also according to their performance when energy demand, prices, and supply deviate from forecasts. In the experiments of terminal operation and energy management, ignoring uncertainty in energy demand and supply resulted in costs that were up to approximately 20% higher, demonstrating the financial consequences of relying on deterministic assumptions. At the shipping-network level, the distributionally robust approach achieved out-of-sample feasibility rates of approximately 86–88%, compared with about 58–69% for the chance-constrained sample-average approach in the MGO–LNG experiments. These findings indicate that uncertainty-aware planning can require a higher planned cost, but provides substantially greater protection against costly rescheduling, energy imbalances, capacity violations, or infeasible bunkering plans. Such robustness should therefore be regarded as an operational reliability investment.

3. **Considering downstream decision performance when evaluating predictive models.**

   The evaluation and selection of predictive models can consider both predictive accuracy and their effects on downstream decisions, with the relative importance of these criteria depending on the intended application. When predictions are used independently for monitoring or forecasting, conventional accuracy measures may provide the main basis for model selection. When predictions are used as inputs to an optimization model, downstream operational performance provides an important complementary criterion. In the shore power experiments, XGBoost achieved the highest predictive accuracy in the case of the Port of Hamburg, whereas the TabPFN and MLP produced better downstream berth-planning outcomes, demonstrating that the most accurate model does not necessarily generate the most effective operational decisions. Practitioners may therefore benefit from evaluating predictive models within the complete prediction-and-optimization pipeline rather than relying exclusively on predictive accuracy.

4. **Exploiting operational flexibility before—and alongside—capital-intensive investment.**

   The analysis suggests that port and shipping operators can obtain meaningful energy and cost improvements by making better use of existing operational flexibility. In the experiments of terminal operations and energy management, hourly-price-aware optimization reduced costs by up to 13.2% without requiring additional investment in energy storage or on-site renewable generation. Similar flexibility can be obtained by redistributing shore power demand across berths and time periods or by coordinating sailing speed, fuel choice, and bunkering decisions across a liner service. However, optimization shifts and manages demand peaks rather than eliminating the underlying physical constraints, and it cannot compensate indefinitely for insufficient grid, shore power, or bunkering capacity. Operational optimization should therefore be used both to capture near-term savings and to reveal the residual bottlenecks for which physical investment is genuinely required.

5. **Using operational evidence to guide strategic energy-infrastructure expansion.**

   Infrastructure planning should be informed by operational demand patterns and network effects rather than by uniform expansion targets alone. For shore power, planners should consider when and where vessel schedules produce simultaneous demand peaks, because aggregate energy demand can conceal local and time-specific capacity constraints. For dual-fuel vessel operations, the experiments indicate that increasing methanol supply ports can substantially change the optimal fuel strategy, whereas the incremental value of further expansion depends strongly on methanol's price competitiveness and the existing network configuration. This suggests that early infrastructure investments should prioritize locations that remove binding operational bottlenecks and provide access across multiple services. Optimization-based scenario analysis can support this process by identifying where additional capacity or supply coverage produces the greatest improvement in feasibility, fuel uptake, or system performance.

6. **Aligning decision authority, cost responsibility, and benefit allocation.**

   The implementation of energy-aware planning depends not only on its technical potential but also on how decision authority, costs, and benefits are distributed among the actors involved. Terminal operators and port authorities should identify which actor bears electricity-purchase and imbalance costs, which actor controls flexible loads and operational schedules, and which actor ultimately captures the resulting savings. Where these responsibilities are divided among terminal operators, shipping lines, energy suppliers, balance-responsible parties, and terminal customers, the actor required to change its operations may have insufficient financial incentive to do so. Contractual arrangements such as flexibility payments, shared-savings agreements, and capacity-sharing mechanisms may therefore be needed to align individual incentives with system-level benefits. The business case for energy-aware planning should consequently be assessed from the perspective of each participating actor rather than solely in terms of total system cost savings.

7. **Combining infrastructure, market incentives, and carbon policy to support maritime decarbonization.**

   The transition towards lower-emission port and shipping operations requires a coordinated combination of infrastructure provision, energy and fuel pricing, and carbon policy. The methanol experiments show that bunkering coverage determines the operational upper bound on methanol use, while price competitiveness largely determines how closely shipping operators approach that bound. Under the 11-port setting, for example, a 60% methanol price reduction brings the realized methanol share close to the structural upper bound of approximately 84%. Carbon pricing can further encourage a shift towards fuels with lower operational emissions without materially changing liner schedules, but it cannot independently resolve limited fuel availability or a large price gap between conventional and alternative fuels. Policymakers, ports, fuel suppliers, and shipping companies should therefore coordinate strategically located infrastructure investment with measures that improve alternative-fuel affordability and reward emissions reductions, rather than relying on any single intervention.

5.2 Future research directions

Although this thesis proposes an optimization and prediction framework for energy-aware port and shipping under uncertainty, many challenges remain regarding the coordination of operational planning, energy management, uncertainty modeling, and intelligent decision-making in future decarbonized maritime systems. The following future research directions are discussed from both chapter-specific and broader system-level perspectives.

5.2.1 Research extensions directly related to the thesis chapters

The following research directions are closely connected to the methodologies and problem investigated in Chapters 2–4, and may serve as direct extensions of the proposed models and frameworks:

1. **Extension of stochastic energy management models for electrified terminals.**

   Future research may extend the stochastic energy management framework developed in Chapter 2 by incorporating additional uncertainty sources, such as renewable energy generation variability and equipment failures. Moreover, rolling-horizon optimization and real-time rescheduling approaches could be investigated to improve the adaptability of terminal operations under dynamically changing operational conditions. Future studies may also consider larger-scale terminal systems with multiple interconnected terminals, distributed energy resources, and integrated smart grid interactions.

2. **Improved shore power demand prediction and integrated berth planning.**

Future research may further improve shore power demand prediction in Chapter 3 by incorporating richer operational information, real-time vessel tracking data, weather conditions, and temporal learning models capable of capturing dynamic operational patterns. Future studies may also investigate real-time prediction and dynamic rescheduling approaches that continuously update operational decisions according to newly observed port conditions and vessel operation states. Furthermore, future work may incorporate grid-side constraints and dynamic electricity pricing to study the joint interaction between terminal operations, shore power demand, and port energy systems, thereby supporting more holistic energy-aware port planning. In parallel, direct validation of the predicted shore power demand profiles against measured vessel-level shore power consumption data would strengthen the empirical grounding of the framework proposed in Chapter 3.

3. **Advanced robust optimization for fuel planning under uncertainty.**

   Future research may extend the proposed DRCC framework in Chapter 4 by considering additional uncertainty sources, such as fuel price volatility, carbon pricing uncertainty, fuel infrastructure disruptions, and evolving environmental regulations. Multi-stage stochastic optimization or adaptive robust optimization approaches may further improve the representation of sequential operational decisions over long-term liner service planning horizons. In addition, future studies may investigate more detailed fuel supply network interactions, including fuel storage capacity planning, fuel distribution scheduling, and coordination among multiple bunkering ports. Future research may also integrate prediction to better evaluate the long-term operational feasibility and adoption of cleaner marine fuels such as methanol.

5.2.2 Broader future research directions for decarbonized maritime systems

Beyond the chapter-specific extensions discussed above, several broader research directions may further support the long-term development of integrated, low-carbon, and intelligent maritime transportation systems:

1. **Integration of machine learning and optimization.**

   This thesis applies a predict-then-optimize framework, where machine learning models first predict shore power demand and the predicted results are then used in optimization models. However, the prediction model with the highest forecasting accuracy does not necessarily produce the best optimization outcomes. This suggests that minimizing prediction error alone may not directly improve operational decision-making performance. Therefore, future research may further explore tighter integration between prediction and optimization, such as predict-and-optimize frameworks, decision-focused learning, end-to-end learning and optimization frameworks, adaptive prediction models, or reinforcement learning approaches that dynamically update operational decisions according to newly observed data and system states.

2. **Expansion toward multi-energy and integrated energy systems.**

   Future port and maritime systems are expected to involve increasingly complex interactions among electricity systems, shore power infrastructure, renewable energy generation, battery storage, and alternative marine fuels. For example, future smart ports may integrate shore power systems with smart grids, renewable energy sources such as wind and solar power, and local battery storage systems to improve energy flexibility and reduce carbon emissions. At the same time, ports are also expected to interact more actively with external energy systems, such as regional electricity grids and energy markets, through electricity purchasing, demand response, and energy exchange mechanisms. Future research may therefore explore integrated multi-energy management frameworks that jointly optimize port operations, smart grid interactions, renewable energy utilization, energy storage scheduling, external energy exchange, and fuel management across interconnected port and shipping systems.

3. **Extension toward broader alternative fuel and energy services in ports.**

   While this thesis mainly focuses on bunkering decisions for LNG and methanol dual-fuel vessels, future research may extend the scope to broader fuel- and energy-related services in port and maritime systems. For example, ports may need to jointly plan alternative fuel bunkering, fuel storage capacity, fuel distribution facilities, and shore-side energy services for vessels. Beyond deciding where and how much fuel to bunker, future studies could investigate how ports allocate limited fuel supply among different vessels, how fuel delivery schedules interact with berth allocation and vessel turnaround time, and how alternative fuel infrastructure should be deployed across port networks. In addition, the coordination between marine fuel supply, shore power provision, and port energy management could be further explored to support integrated low-carbon energy services for future shipping.

4. **System-level coordination for net-zero maritime transportation.**

   Future maritime decarbonization requires coordination among multiple stakeholders and interconnected systems, including shipping companies, ports, fuel suppliers, energy providers, terminal operators, and policymakers. Although ports play a critical role in supporting low-carbon shipping through shore power services and alternative fuel infrastructure, they represent only one component of the broader net-zero maritime transportation system. Future research may therefore investigate system-level planning frameworks that jointly consider shipping networks, port infrastructure, external energy systems, fuel supply chains, and regulatory policies. In addition, the interactions among different components, such as vessel operations, port energy management, renewable energy integration, and fuel production and distribution systems, should be further explored to support the coordinated transition toward fully decarbonized maritime transportation systems.

Bibliography

Abu Bakar, N. N., N. Bazmohammadi, J. C. Vasquez, J. M. Guerrero (2023) Electrification of onshore power systems in maritime transportation towards decarbonization of ports: A review of the cold ironing technology, *Renewable and Sustainable Energy Reviews*, 178, p. 113243.

Alamoush, A. S., F. Ballini, A. I. Ölçer (2020) Ports' technical and operational measures to reduce greenhouse gas emission and improve energy efficiency: A review, *Marine Pollution Bulletin*, 160, p. 111508.

Alikhani, P., L. B. Tjernberg, L. Astner, P. Donnerstal (2021) Forecasting the electrical demand at the port of gävle container terminal, in: *11th IEEE PES Innovative Smart Grid Technologies Europe, ISGT Europe 2021*, Institute of Electrical and Electronics Engineers Inc., Espoo, Finland, pp. 1–6.

Alzahrani, A., I. Petri, Y. Rezgui, A. Ghoroghi (2021) Decarbonisation of seaports: A review and directions for future research, *Energy Strategy Reviews*, 38, p. 100727.

Amaral, M., N. Amaro, P. Arsénio (2023) Methodology for assessing power needs for onshore power supply in maritime ports, *Sustainability*, 15(24), p. 16670.

Aydin, N., H. Lee, S. A. Mansouri (2017) Speed optimization and bunkering in liner shipping in the presence of uncertain service times and time windows at ports, *European Journal of Operational Research*, 259(1), pp. 143–154.

Bakar, N. N. A., N. Bazmohammadi, H. Çimen, T. Uyanik, J. C. Vasquez, J. M. Guerrero (2022a) Data-driven ship berthing forecasting for cold ironing in maritime transportation, *Applied Energy*, 326, p. 119947.

Bakar, N. N. A., J. M. Guerrero, N. Bazmohammadi, J. C. Vasquez (2022b) Optimal berth allocation in ports with the deployment of shore to ship power system, in: *2022 IEEE International Conference on Power and Energy (PECon)*, Langkawi, Kedah, Malaysia, p. 263–268.

Bakar, N. N. A., J. M. Guerrero, J. C. Vasquez, N. Bazmohammadi, Y. Yu, A. Abusorrah, Y. A. Al-Turki (2021) A review of the conceptualization and operational management of seaport microgrids on the shore and seaside, *Energies*, 14(23), p. 7941.

Bengio, Y., A. Lodi, A. Prouvost (2021) Machine learning for combinatorial optimization: A methodological tour d'horizon, *European Journal of Operational Research*, 290(2), p. 405–421.

Buhrkal, K., S. Zuglian, S. Ropke, J. Larsen, R. Lusby (2011) Models for the discrete berth allocation problem: A computational comparison, *Transportation Research Part E: Logistics and Transportation Review*, 47(4), pp. 461–473.

Chen, Z., D. Kuhn, W. Wiesemann (2024) Technical Note—Data-Driven Chance Constrained Programs over Wasserstein Balls, *Operations Research*, 72(1), pp. 410–424.

Chu, Z., R. Yan, S. Wang (2023) Evaluation and prediction of punctuality of vessel arrival at port: a case study of hong kong, *Maritime Policy & Management*, 51(6), p. 1096–1124.

Chu, Z., R. Yan, S. Wang (2025) Vessel arrival time to port prediction via a stacked ensemble approach: Fusing port call records and ais data, *Transportation Research Part C: Emerging Technologies*, 176, p. 105128.

Chu, Z., R. Yan, X. Yang, K.-W. Pang, S. Wang (2026) Integrating vessel arrival time forecasting into berth allocation decisions: A predictive-operational framework, *Advanced Engineering Informatics*, 69, p. 104010.

Clarksons Research (2025) World fleet register, URL https://www-clarksons-net.tudelft.idm.oclc.org/wfr/.

Conte, F., G. Natrella, D. Sasso, F. Silvestro, F. D'Agostino, F. D'Antoni, M. Merone (2025) Optimizing green port operations with reinforcement learning and model predictive control, *International Journal of Electrical Power & Energy Systems*, 173, p. 111437.

Crespo-Vazquez, J. L., C. Carrillo, E. Diaz-Dorado, J. A. Martinez-Lorenzo, M. Noor-E-Alam (2018) A machine learning based stochastic optimization framework for a wind and storage power plant participating in energy pool market, *Applied Energy*, 232, pp. 341–357.

ENTSO-E (2023) ENTSO-E transparency platform, URL https://transparency.entsoe.eu/.

European Commission (2019) The European Green Deal, Communication from the Commission to the European Parliament, the European Council, the Council, the European Economic and Social Committee and the Committee of the Regions COM(2019) 640 final, European Commission, Brussels.

European Commission (2023a) Alternative Fuels Infrastructure, URL https://transport.ec.europa.eu/transport-themes/clean-transport/alternative-fuels-sustainable-mobility-europe/alternative-fuels-infrastructure_en.

European Commission (2023b) Decarbonising maritime transport – fueleu maritime, URL https://transport.ec.europa.eu/transport-modes/maritime/decarbonising-maritime-transport-fueleu-maritime_en.

Fagerholt, K., N. T. Gausel, J. G. Rakke, H. N. Psaraftis (2015) Maritime routing and speed optimization with emission control areas, *Transportation Research Part C: Emerging Technologies*, 52, pp. 57–73.

Fagerholt, K., G. Laporte, I. Norstad (2010) Reducing fuel emissions by optimizing speed on shipping routes, *Journal of the Operational Research Society*, 61(3), pp. 523–529.

Gao, R., A. Kleywegt (2023) Distributionally robust stochastic optimization with wasserstein distance, *Mathematics of Operations Research*, 48(2), pp. 603–655.

Geerlings, H., R. Heij, R. van Duin (2018) Opportunities for peak shaving the energy demand of ship-to-shore quay cranes at container terminals, *Journal of Shipping and Trade*, 3, p. 3.

Gennitsaris, S. G., F. D. Kanellos (2019) Emission-aware and cost-effective distributed demand response system for extensively electrified large ports, *IEEE Transactions on Power Systems*, 34(6), pp. 4341–4351.

Grinsztajn, L., K. Flöge, O. Key, F. Birkel, P. Jund, B. Roof, B. Jäger, D. Safaric, S. Alessi, A. Hayler, M. Manium, R. Yu, F. Jablonski, S. B. Hoo, A. Garg, J. Robertson, M. Bühler, V. Moroshan, L. Purucker, C. Cornu, L. C. Wehrhahn, A. Bonetto, B. Schölkopf, S. Gambhir, N. Hollmann, F. Hutter (2025) Tabpfn-2.5: Advancing the state of the art in tabular foundation models, URL https://arxiv.org/abs/2511.08667.

Grundmeier, N., A. Hahn, N. Ihle, S. Runge, C. Meyer-Barlag (2014) A simulation based approach to forecast a demand load curve for a container terminal using battery powered vehicles, in: *2014 International Joint Conference on Neural Networks (IJCNN)*, Beijing, China, pp. 1711–1718, ISSN: 2161-4407.

Harnischmacher, C., L. Markefke, A. B. Brendel, L. Kolbe (2023) Two-sided sustainability: Simulating battery degradation in vehicle to grid applications within autonomous electric port transportation, *Journal of Cleaner Production*, 384, p. 135598.

He, J. (2016) Berth allocation and quay crane assignment in a container terminal for the trade-off between time-saving and energy-saving, *Advanced Engineering Informatics*, 30(3), pp. 390–405.

He, J., Y. Huang, W. Yan (2015a) Yard crane scheduling in a container terminal for the trade-off between efficiency and energy consumption, *Advanced Engineering Informatics*, 29(1), pp. 59–75.

He, J., Y. Huang, W. Yan, S. Wang (2015b) Integrated internal truck, yard crane and quay crane scheduling in a container terminal considering energy consumption, *Expert Systems with Applications*, 42(5), pp. 2464–2487.

He, P., J. G. Jin, W. Pan, J. Chen (2024) Route, speed, and bunkering optimization for LNG-fueled tramp ship with alternative bunkering ports, *Ocean Engineering*, 305, p. 117957.

He, P., L. Wu, J. G. Jin, S. Zhou, F. Schulte (2026) Distributionally robust optimization of sailing speed, bunkering, and fuel switching for dual-fuel liner services, *Transportation Research Part C: Emerging Technologies*, 184, p. 105528.

He, X., H. Ren, S. Wang, L. Zhen (2025) How to manage berths in ports with on-shore power supply technology, *IEEE Transactions on Engineering Management*, 72, p. 2583–2599.

HHLA (2022) Sustainability for container handling: AGV charging infrastructure completed, URL https://hhla.de/en/media/news/detail-view/cta-agv-charging-infrastructure-completed.

HHLA (2023a) Container Terminal Altenwerder (CTA), URL https://hhla.de/en/company/subsidiaries/container-terminal-altenwerder-cta.

HHLA (2023b) Innovation: FRESH, URL https://hhla.de/en/innovation/fresh.

HHLA (2025) Report vessel operations: Sailing list, URL https://coast.hhla.de/report?id=Standard-Report-Segelliste.

Hollmann, N., S. Müller, L. Purucker, A. Krishnakumar, M. Körfer, S. B. Hoo, R. T. Schirrmeister, F. Hutter (2025) Accurate predictions on small data with a tabular foundation model, *Nature*, 637(8045), p. 319–326.

Hong Kong Government (2025) Vessel traffic management system report, URL https://data.gov.hk/en-data/dataset/hk-md-mardep-vessel-traffic-management-system-report.

Imai, A., E. Nishimura, S. Papadimitriou (2001) The dynamic berth allocation problem for a container port, *Transportation Research Part B: Methodological*, 35(4), pp. 401–417.

Iris, Ç., J. S. L. Lam (2019a) Recoverable robustness in weekly berth and quay crane planning, *Transportation Research Part B: Methodological*, 122, pp. 365–389.

Iris, Ç., J. S. L. Lam (2019b) A review of energy efficiency in ports: Operational strategies, technologies and energy management systems, *Renewable and Sustainable Energy Reviews*, 112, pp. 170–182.

Iris, Ç., J. S. L. Lam (2021) Optimal energy management and operations planning in seaports with smart grid while harnessing renewable energy under uncertainty, *Omega*, 103, p. 102445.

Kaisermayer, V., D. Muschick, M. Horn, M. Gölles (2021) Progressive hedging for stochastic energy management systems, *Energy Systems*, 12(1), pp. 1–29.

Kanellos, F. D. (2017) Real-time control based on multi-agent systems for the operation of large ports as prosumer microgrids, *IEEE Access*, 5, pp. 9439–9452.

Kanellos, F. D. (2019) Multiagent-system-based operation scheduling of large ports' power systems with emissions limitation, *IEEE Systems Journal*, 13(2), pp. 1831–1840.

Kanellos, F. D., E.-S. M. Volanis, N. D. Hatziargyriou (2019) Power management method for large ports with multi-agent systems, *IEEE Transactions on Smart Grid*, 10(2), pp. 1259–1268.

Karakas, S., M. Kirmizi, B. Kocaoglu (2021) Yard block assignment, internal truck operations, and berth allocation in container terminals: introducing carbon-footprint minimisation objectives, *Maritime Economics & Logistics*, 23(4), p. 750–771.

Kermani, M., G. Parise, L. Martirano, L. Parise, B. Chavdarian (2018) Optimization of peak load shaving in STS group cranes based on PSO algorithm, in: *2018 IEEE International Conference on Environment and Electrical Engineering and 2018 IEEE Industrial and Commercial Power Systems Europe (EEEIC / I&CPS Europe)*, Palermo, Italy, pp. 1–5.

Knueven, B., C. Muir, J.-P. Watson, D. T. Mildebrath, J. D. Siirola, D. L. Woodruff (2020) A parallel hub-and-spoke system for large-scale scenario-based optimization under uncertainty – optimization online, URL https://optimization-online.org/2020/11/8088/.

Kolley, L., N. Rückert, M. Kastner, C. Jahn, K. Fischer (2023) Robust berth scheduling using machine learning for vessel arrival time prediction, *Flexible Services and Manufacturing Journal*, 35(1), pp. 29–69.

Li, Y., J. G. Jin, P. He, C. Lu (2025) Optimizing bunkering and speed for dry bulk carriers considering biofuel storage period limitation, *Ocean & Coastal Management*, 260, p. 107482.

Liu, C., X. Xiang, L. Zheng (2020) A two-stage robust optimization approach for the berth allocation problem under uncertainty, *Flexible Services and Manufacturing Journal*, 32(2), pp. 425–452.

Liu, M., X. Liu, F. Chu, M. Zhu, F. Zheng (2019) Liner ship bunkering and sailing speed planning with uncertain demand, *Computational and Applied Mathematics*, 39(1), p. 22.

Lundberg, S., S.-I. Lee (2017) A unified approach to interpreting model predictions, URL https://arxiv.org/abs/1705.07874.

Mao, A., T. Yu, Z. Ding, S. Fang, J. Guo, Q. Sheng (2022) Optimal scheduling for seaport integrated energy system considering flexible berth allocation, *Applied Energy*, 308, p. 118386.

Meng, Q., S. Wang, C.-Y. Lee (2015) A tailored branch-and-price approach for a joint tramp ship routing and bunkering problem, *Transportation Research Part B: Methodological*, 72, pp. 1–19.

Micallef, A., M. Apap, J. Licari, C. Spiteri Staines, Z. Xiao (2025) A comparative framework for evaluating machine learning models in forecasting electricity demand for port microgrids, *Energy and AI*, 20, p. 100494.

Mohajerin Esfahani, P., D. Kuhn (2018) Data-driven distributionally robust optimization using the wasserstein metric: Performance guarantees and tractable reformulations, *Mathematical Programming*, 171(1), pp. 115–166.

Norstad, I., K. Fagerholt, G. Laporte (2011) Tramp ship routing and scheduling with speed optimization, *Transportation Research Part C: Emerging Technologies*, 19(5), pp. 853–865.

Okumuş, F., A. Ekmekçioğlu, S. S. Kara (2021) Modelling ships main and auxiliary engine powers with regression-based machine learning algorithms, *Polish Maritime Research*, 28(1), pp. 83–96.

Omholt-Jensen, S., K. Fagerholt, F. Meisel (2025) Fleet repositioning in the tramp ship routing and scheduling problem with bunker optimization: A matheuristic solution approach, *European Journal of Operational Research*, 321(1), pp. 88–106.

Oyewola, O. M., A. A. Awonusi, O. S. Ismail (2024) Performance optimization of step-like divergence plenum air-cooled li-ion battery thermal management system using variable-step-height configuration, *Emerging Science Journal*, 8(3), p. 795–814.

Palensky, P., D. Dietrich (2011) Demand side management: Demand response, intelligent energy systems, and smart loads, *IEEE Transactions on Industrial Informatics*, 7(3), pp. 381–388.

Patnam, B. S. K., N. M. Pindoriya (2021) Demand response in consumer-centric electricity market: Mathematical models and optimization problems, *Electric Power Systems Research*, 193, p. 106923.

Pei, R., J. Xie, H. Zhang, K. Sun, Z. Wu, S. Zhou (2021) Robust multi-layer energy management and control methodologies for reefer container park in port terminal, *Energies*, 14(15), p. 4456.

Peng, Y., M. Dong, X. Li, H. Liu, W. Wang (2021) Cooperative optimization of shore power allocation and berth allocation: A balance between cost and environmental benefit, *Journal of Cleaner Production*, 279, p. 123816.

Peng, Y., X. Li, W. Wang, K. Liu, X. Bing, X. Song (2018) A method for determining the required power capacity of an on-shore power system considering uncertainties of arriving ships, *Sustainability*, 10(12), p. 4524.

Peng, Y., X. Li, W. Wang, Z. Wei, X. Bing, X. Song (2019) A method for determining the allocation strategy of on-shore power supply from a green container terminal perspective, *Ocean & coastal management*, 167, p. 158–175.

Peng, Y., H. Liu, X. Li, J. Huang, W. Wang (2020) Machine learning method for energy consumption prediction of ships in port considering green ports, *Journal of Cleaner Production*, 264, p. 121564.

Peng, Z., Y. Zhao, T. Notteboom, J. Zhou (2026) Optimizing hybrid power-fuel configurations for container ships under decarbonization uncertainty, *Energy Conversion and Management*, 365, p. 121784.

Psaraftis, H. N., C. A. Kontovas (2014) Ship speed optimization: Concepts, models and combined speed-routing scenarios, *Transportation Research Part C: Emerging Technologies*, 44, pp. 52–69.

Pu, Y., W. Chen, R. Zhang, H. Liu (2020) Optimal operation strategy of port integrated energy system considering demand response, in: *2020 IEEE 4th Conference on Energy Internet and Energy System Integration (EI2)*, Wuhan, China, pp. 518–523.

Qi, J., S. Wang, C. Peng (2020) Shore power management for maritime transportation: Status and perspectives, *Maritime Transport Research*, 1, p. 100004.

Qu, S., X. Li, C. Liu, X. Tang, Z. Peng, Y. Ji (2023) Two-stage robust programming modeling for continuous berth allocation with uncertain vessel arrival time, *Sustainability*, 15(13), p. 10560.

Raeesi, R., N. Sahebjamnia, S. A. Mansouri (2023) The synergistic effect of operational research and big data analytics in greening container terminal operations: A review and future directions, *European Journal of Operational Research*, 310(3), p. 943–973.

Roald, L. A., D. Pozo, A. Papavasiliou, D. K. Molzahn, J. Kazempour, A. Conejo (2023) Power systems optimization under uncertainty: A review of methods and applications, *Electric Power Systems Research*, 214, p. 108725.

Rockafellar, R. T., R. J.-B. Wets (1991) Scenarios and policy aggregation in optimization under uncertainty, *Mathematics of operations research*, 16(1), pp. 119–147.

Rumbe, G., M. Hamasha, S. Al Mashaqbeh (2024) A comparison of holts-winter and artificial neural network approach in forecasting: A case study for tent manufacturing industry, *Results in Engineering*, 21, p. 101899.

Sarantakos, I., S. Nikkhah, M. Peker, A. Bowkett, T. Sayfutdinov, A. Alahyari, C. Patsios, J. Mangan, A. Allahham, E. Bougioukou, A. Murphy, K. Pazouki (2024) A robust logistics-electric framework for optimal power management of electrified ports under uncertain vessel arrival time, *Cleaner Logistics and Supply Chain*, 10, p. 100144.

Schmidt, J., L.-P. Lauven, N. Ihle, L. Kolbe (2015) Demand side integration for electric transport vehicles, *International Journal of Energy Sector Management*, 9(4), pp. 471–495.

Sheng, D., P. Wu, Q. V. Guo, J. Jiang, B. Liu (2025) Integrated shore power deployment problem in an inland shipping network, *Transport Policy*, 169, p. 26–40.

Song, D.-P. (2024) A literature review of seaport decarbonisation: Solution measures and roadmap to net zero, *Sustainability*, 16(4), p. 1620.

Stoter, J., X. Tang, M. Cvetkovic, P. Palensky, H. Polinder, Ç. Iris, F. Schulte (2025) Energy management and stochastic operations planning for electrified container terminals with uncertain energy supply and demand, *Journal of Cleaner Production*, 527, p. 146383.

Tang, G., Z. Zhao, F. Schulte, Ç. Iris (2025a) Smart charging with demand response and energy peak shaving for reefer containers with internet-of-things, *International Journal of Production Research*, 63(20), pp. 7460–7485.

Tang, X., P. He, Ç. Iris, F. Schulte (2026a) Dual-fuel vessel operations under fuel supply uncertainty: Robust planning and scenario analysis, *Submitted to a journal*.

Tang, X., Ç. Iris, R. R. Negenborn, P. He, F. Schulte (2026b) Learning shore power demand and energy-aware berth allocation, *Submitted to a journal*.

Tang, X., Ç. Iris, F. Schulte (2025b) Fine-grained estimation of onshore power demand via operational phase segmentation of port call data, in: *Proceedings of the 16th International Conference on Computational Logistics*, Delft, The Netherlands.

Tjøstheim, D. (2025) Selected topics in time series forecasting: Statistical models vs. machine learning, *Entropy*, 27(3), p. 279.

UNCTAD (2025) Shipping data: UNCTAD releases new seaborne trade statistics, https://unctad.org/news/shipping-data-unctad-releases-new-seaborne-trade-statistics, Accessed: 02-03-2026.

UNFCCC (2015) The Paris Agreement (FCCC/CP/2015/10/Add.1), URL https://unfccc.int/process-and-meetings/the-paris-agreement.

Uyanık, T., Y. Yalman, O. Kalenderli, Y. Arslanoğlu, Y. Terriche, C.-L. Su, J. M. Guerrero (2022) Data-driven approach for estimating power and fuel consumption of ship: A case of container vessel, *Mathematics*, 10(22), p. 4167.

Uzun, D., D. Okumus, O. Canbulat, S. Anil Gunbeyaz, S. Karamperidis, D. Hudson, O. Turan, R. Allan (2024) Port energy demand model for implementing onshore power supply and alternative fuels, *Transportation Research Part D: Transport and Environment*, 136, p. 104432.

van Duin, J. H. R. R., H. H. Geerlings, A. A. Verbraeck, T. T. Nafde (2018) Cooling down: A simulation approach to reduce energy peaks of reefers at terminals, *Journal of Cleaner Production*, 193, pp. 72–86.

Vanderschueren, T., T. Verdonck, B. Baesens, W. Verbeke (2022) Predict-then-optimize or predict-and-optimize? an empirical evaluation of cost-sensitive learning strategies, *Information Sciences*, 594, p. 400–415.

Ventikos, N. P., P. Sotiralis, M. Annetis, M.-A. Koimtzoglou, L. Keratsa (2025) Defining the power and energy demands from ships at anchorage for offshore power supply solutions, *Energies*, 18(7), p. 1766.

Wang, B., Q. Liu, L. Wang, Y. Chen, J. Wang (2023) A review of the port carbon emission sources and related emission reduction technical measures, *Environmental pollution*, 320, p. 121000.

Wang, J., H. Li, Z. Yang, Y.-E. Ge (2024a) Shore power for reduction of shipping emission in port: A bibliometric analysis, *Transportation Research Part E: Logistics and Transportation Review*, 188, p. 103639.

Wang, S., Q. Meng (2015) Robust bunker management for liner shipping networks, *European Journal of Operational Research*, 243(3), pp. 789–797.

Wang, X., Z. Dong, Y. Wang, H. Xiao (2024b) Joint optimization of berth-quay crane-shore power allocation under time-of-use pricing, *Jiaotong Yunshu Xitong Gongcheng Yu Xinxi/Journal of Transportation Systems Engineering and Information Technology*, 25(2), p. 314–327.

Wang, Y., Ç. Iris (2025) Transition to near-zero emission shipping fleet powered by alternative fuels under uncertainty, *Transportation Research Part D: Transport and Environment*, 142, p. 104689.

Wang, Y., Q. Meng, H. Kuang (2018) Jointly optimizing ship sailing speed and bunker purchase in liner shipping with distribution-free stochastic bunker prices, *Transportation Research Part C: Emerging Technologies*, 89, pp. 35–52.

Wu, Y., H. Guo, J. Qi, S. Wang, L. Zhen (2024) Ship refueling optimization for dual-fuel ships considering carbon intensity indicator rating limit and uncertain fuel prices, *Multimodal Transportation*, 3(3), p. 100138.

Wu, Y., H. Zhang, F. Li, S. Wang, L. Zhen (2023) Optimal selection of multi-fuel engines for ships considering fuel price uncertainty, *Mathematics*, 11(17).

Xiao, M., Q. Zhou, Z. Zhang, J. Yin (2024) Real-time intrusion detection in power grids using deep learning: Ensuring dpu data security, *HighTech and Innovation Journal*, 5(3), p. 814–827.

Xiong, C., Y. Su, H. Wang, D. Zhang, B. Xiong (2024) Optimal distributed energy scheduling for port microgrid system considering the coupling of renewable energy and demand, *Sustainable Energy, Grids and Networks*, 39, p. 101506.

Yan, R., Z. Chu, L. Wu, S. Wang (2024) Predicting vessel service time: A data-driven approach, *Advanced Engineering Informatics*, 62, p. 102718.

Yu, D., D. Li, M. Sha, D. Zhang (2019) Carbon-efficient deployment of electric rubber-tyred gantry cranes in container terminals with workload uncertainty, *European Journal of Operational Research*, 275(2), p. 552–569.

Yu, F., Q. Shan, Y. Xiao, F. Teng (2022a) Robust low-carbon discrete berth allocation under uncertainty, *International Transactions on Electrical Energy Systems*, 2022(1), p. 5310004.

Yu, H., N. Xu, K. Li (2025) Distributed robust optimization of integrated seaport energy systems under multiple uncertainties, in: *20th IEEE Conference on Industrial Electronics and Applications, ICIEA 2025*, Institute of Electrical and Electronics Engineers Inc., Yantai, China, pp. 1–6.

Yu, J., P. Cammin, S. Voß (2023a) Allocation of shore side electricity: The case of the port of hamburg, in: Daduna, J. R., G. Liedtke, X. Shi, S. Voß, eds., *Lecture Notes in Computer Science*, Springer Nature Switzerland, Cham, pp. 139–153.

Yu, J., G. Tang, S. Voß, X. Song (2023b) Berth allocation and quay crane assignment considering the adoption of different green technologies, *Transportation Research Part E: Logistics and Transportation Review*, 176, p. 103185.

Yu, J., S. Voß, X. Song (2022b) Multi-objective optimization of daily use of shore side electricity integrated with quayside operation, *Journal of Cleaner Production*, 351, p. 131406.

Zhai, J., X. Wu, S. Zhu, B. Yang, H. Liu (2020) Optimization of integrated energy system considering photovoltaic uncertainty and multi-energy network, *IEEE Access*, 8, pp. 141558–141568.

Zhang, X., Y. Gu, Y. Yang, B. Liu (2023) Comparing the efficiency of two types of yard layout in container terminals, *Sustainability*, 15(9), p. 7195.

Zhang, Y., C. Liang, J. Shi, G. Lim, Y. Wu (2022) Optimal port microgrid scheduling incorporating onshore power supply and berth allocation under uncertainty, *Applied energy*, 313, p. 118856.

Zhang, Z., Y. Zhu, J. Zhu, D. Huang, C. Yin, J. Li (2025) Collaborative optimization of shore power and berth allocation based on economic, environmental, and operational efficiency, *Journal of Marine Science and Engineering*, 13(4), p. 776.

Zhao, W., K. Ma, J. Yang, S. Guo (2024) A risk-averse logistics-energy coordination optimization strategy for port energy system considering demand response program, *Electric Power Systems Research*, 231, p. 110297.

Zhao, Y., Z. Peng, J. Zhou, T. Notteboom, Y. Ma (2025) Toward green container liner shipping: joint optimization of heterogeneous fleet deployment, speed optimization, and fuel bunkering, *International Transactions in Operational Research*, 32(6), pp. 3347–3384.

Zhen, L., S. Wang, D. Zhuge (2017) Dynamic programming for optimal ship refueling decision, *Transportation Research Part E: Logistics and Transportation Review*, 100, pp. 63–74.

Zhou, L., J. G. Jin, Y. Gao, Ç. Iris, T. Bektaş, J. H. Chen (2026) Techno-economic optimization for containership green transition under net-zero emission target: a predict-then-optimize framework, *Transportation Research Part E: Logistics and Transportation Review*, 209, p. 104731.

Glossary

List of symbols and notations

Below follows a list of the most frequently used symbols and notations in this thesis.

a_i	earliest feasible arrival period of vessel i
$a_{r,n}$	arrival time at port call n on route r
B	set of berths
b	index of berths
$b_f^{r,n}$	amount of fuel f bunkered at port call n on route r
C_i	set of feasible shore-power connection start periods for vessel i
C_{zt}	shore-power capacity of electrical zone z in time period t
c_t	electricity price in time period t
$d_{r,n}$	departure time from port call n on route r
F	set of fuel types
f	index of fuel types
H	length of the planning horizon
I	set of vessels
K_i	length of the shore-power demand profile of vessel i
$L_{i,w}$	operational lateness of vessel i in scenario w
L_r	set of sailing legs on route r
M	sufficiently large positive constant
N_r	ordered set of port calls on route r

n	index of port calls
P	set of physical ports
$P_{i,k}$	shore-power demand of vessel i at relative time index k
P_t^{da}	power purchased in the day-ahead electricity market at time t
$P_{t,w}^{\text{shor}}$	power shortage at time t in scenario w
$P_{t,w}^{\text{sur}}$	power surplus at time t in scenario w
$q_f^{r,n}$	remaining amount of fuel f upon arrival at port call n
R	set of shipping routes
r	index of shipping routes
S	set of scenarios
S_i	set of feasible service start periods for vessel i
$S_{i,w}$	berthing start time of vessel i in scenario w
$\widetilde{S}_{if}$	uncertain supply of fuel f at physical port i
$\widehat{S}_{if,k}$	historical observation k of fuel supply at port i
T	set of discrete time periods
t	index of time periods
V	set of alternative sailing speeds
v	index of alternative sailing speeds
w	index of uncertainty scenarios
x_{is}	binary variable indicating whether vessel i starts service at time s
$x_{vf}^{r,n}$	binary variable indicating the selected speed–fuel combination
y_{ibs}	binary variable indicating a shore-power connection start
Z	set of electrical zones
z	index of electrical zones
z_{it}	binary shore-power connection state of vessel i at time t

Δ	duration of one discrete time period
ε_{if}	allowable chance-constraint violation probability
η	carbon emission cost per unit of carbon dioxide emissions
π_w	probability of scenario w
ρ_{if}	radius of the Wasserstein ambiguity set
ξ_{zt}	nonnegative slack for the capacity of zone z at time t
$\psi_{r,n}$	arrival delay at port call n on route r
$\zeta_f^{r,n}$	binary variable indicating whether fuel f is bunkered at port call n on route r

List of abbreviations

The following abbreviations are used in this thesis:

AFIR	Alternative Fuels Infrastructure Regulation
AGV	Automated Guided Vehicle
AIS	Automatic Identification System
ANN	Artificial Neural Network
ATA	Actual Arrival Time
ATD	Actual Departure Time
BAP	Berth Allocation Problem
BAQAP	Berth Allocation and Quay Crane Assignment Problem
BBX	Baltic Bridge Express
BP	Backpropagation
CCP	Chance-Constrained Programming
CO_2	Carbon Dioxide
CPP	Critical Peak Pricing
CT	Container Terminal
CTA	Container Terminal Altenwerder
DBAP	Discrete Berth Allocation Problem
DR	Demand Response
DRCC	Distributionally Robust Chance Constraint
DRO	Distributionally Robust Optimization
DWT	Deadweight Tonnage
EC	Energy-Related Cost
ECA	Emission Control Area
EEV	Expectation of the Expected Value Problem
EFT	Expected Finishing Time
EG	Electricity Grid
EMS	Energy Management System

ENTSO-E	European Network of Transmission System Operators for Electricity
ES	Exponential Smoothing
ESS	Energy Storage System
ETA	Estimated Time of Arrival
EU	European Union
EVPI	Expected Value of Perfect Information
FC	Flexibility Coefficient
FI1	Finland Express 1
GB	Gradient Boosting
GHG	Greenhouse Gas
GT	Gross Tonnage
HHLA	Hamburger Hafen und Logistik AG
IBC	Iberia Europe Service
IMO	International Maritime Organization
KC	Kwai Chung Container Terminal
KNN	K-Nearest Neighbor
LightGBM	Light Gradient Boosting Machine
LNG	Liquefied Natural Gas
LOA	Length Overall
LR	Linear Regression
MAE	Mean Absolute Error
MGO	Marine Gas Oil
MHE	Material Handling Equipment
MILP	Mixed-Integer Linear Programming
MIP	Mixed-Integer Programming
ML	Machine Learning
MLP	Multi-Layer Perceptron
MO	Multi-Objective Optimization
MOIP	Multi-Objective Integer Programming
MPSO	Multi-Objective Particle Swarm Optimization
MRV	Monitoring, Reporting, and Verification
NP	No Pricing
NSGA-III	Non-Dominated Sorting Genetic Algorithm III
ONE	Ocean Network Express
OPS	Onshore Power Supply
OR	Operational Research
PAR	Peak-to-Average Ratio
PE	Port Electricity
PH	Progressive Hedging
PLS	Poland Shuttle
PV	Photovoltaic Panel
QC	Quay Crane
R^2	Coefficient of Determination
RE	Reactive Problem
RF	Random Forest
RMSE	Root Mean Squared Error

RR	Ridge Regression
RTP	Real-Time Pricing
SAA	Sample Average Approximation
SC	Schedule-Related Cost
SHAP	SHapley Additive exPlanations
SP	Shore Power
SP-BAP	Shore-Power-Aware Berth Allocation Problem
SPAP	Shore Power Allocation Problem
TC	Total Cost
TEN-T	Trans-European Transport Network
TEU	Twenty-Foot Equivalent Unit
TOS	Terminal Operating System
TOU	Time-of-Use Pricing
UNCTAD	United Nations Conference on Trade and Development
V2G	Vehicle-to-Grid
VSS	Value of the Stochastic Solution
WFR	World Fleet Register
WS	Wait-and-See Solution
WT	Wind Turbine
XGB	Extreme Gradient Boosting
YC	Yard Crane

Summary

Maritime decarbonization has become a major research and industrial focus in recent years under increasing environmental concerns and international climate policies. The maritime sector is under growing pressure to reduce greenhouse gas emissions through various green strategies such as the adoption of shore power systems, port electrification, renewable energy integration, and alternative marine fuels. However, the transition toward decarbonized maritime transport also introduces substantial operational and energy-related challenges. The increasing electrification of port operations creates strong interactions between terminal operations and energy systems, while the deployment of alternative fuels further complicates operational planning in shipping networks. In addition, uncertainties related to vessel arrivals, operational demand, electricity prices, and fuel availability make decision-making increasingly complex. Despite the growing attention to maritime decarbonization, existing studies often treat operational planning, energy management, demand prediction, and uncertainty handling separately, limiting their applicability in highly integrated and uncertain maritime environments.

Motivated by these challenges, this thesis investigates energy-aware operations for ports and shipping systems under uncertainty. The thesis aims to support the transition toward low-carbon maritime transport systems by jointly considering operational planning, energy management, and uncertainty handling. In particular, the research explores the interactions between port operations and energy systems, the integration of shore power demand prediction into operational decision-making, and robust optimization for shipping network systems.

At the terminal energy system level, this thesis investigates the integration of port operations and energy management in electrified container terminals (Chapter 2). An integrated stochastic programming framework is developed to jointly model terminal operations and energy flows under uncertain conditions. Multiple operational components, including vessels, quay cranes, yard cranes, reefers, and automated guided vehicles, are modeled as energy consumers within the terminal energy system. The results demonstrate that jointly considering operational planning and energy management can improve both operational efficiency and energy utilization under uncertainty.

Building upon the terminal-level energy perspective, this thesis further explores shore power demand modeling, prediction, and its interaction with berth allocation decisions at the berth-area level (Chapter 3). A data-driven framework is proposed to reconstruct operationally segmented shore power demand profiles from historical port event data and to predict time-granular shore power demand using machine learning approaches. The predicted demand profiles are then integrated into an energy-aware berth allocation framework. The results show that incorporating predicted shore power demand into berth allocation decisions can effectively reduce energy-related operational costs and mitigate peak electricity demand. In addition, the findings reveal

that the prediction model with the best forecasting accuracy does not necessarily lead to the best optimization performance, highlighting the importance of jointly considering prediction and optimization in energy-aware port operations.

Extending the research scope from terminal operations to maritime shipping networks, this thesis investigates uncertainty-aware operational planning for dual-fuel liner shipping systems under uncertain fuel supply conditions (Chapter 4). An integrated distributionally robust optimization framework is developed to jointly determine sailing speeds, bunkering locations and quantities, and fuel choices across sailing legs. The experiments show that explicitly accounting for fuel supply uncertainty can substantially improve operational reliability. The methanol uptake experiments further reveal that bunkering fuel supply availability and fuel price competitiveness play complementary roles. Supply expansion determines the operational upper bound on methanol use, whereas price reductions influence how closely operators approach that bound.

Overall, the framework proposed in this thesis provides practical insights for supporting the transition toward more efficient, resilient, and sustainable maritime transport systems, while demonstrating the potential of combining operations research and data-driven approaches in advancing net-zero maritime shipping.

Samenvatting

De decarbonisatie van de scheepvaart is de afgelopen jaren, tegen de achtergrond van toenemende milieuzorgen en internationaal klimaatbeleid, een belangrijk aandachtspunt geworden voor zowel onderzoek als de industrie. De maritieme sector staat onder toenemende druk om de uitstoot van broeikasgassen te verminderen door middel van diverse groene strategieën, zoals de invoering van walstroomsystemen, de elektrificatie van havens, de integratie van hernieuwbare energie en het gebruik van alternatieve scheepsbrandstoffen. De overgang naar een koolstofarm zeevervoer brengt echter ook aanzienlijke operationele en energiegerelateerde uitdagingen met zich mee. De toenemende elektrificatie van havenactiviteiten zorgt voor sterke interacties tussen terminalactiviteiten en energiesystemen, terwijl de inzet van alternatieve brandstoffen de operationele planning in scheepvaartnetwerken verder compliceert. Bovendien maken onzekerheden met betrekking tot de aankomst van schepen, de operationele vraag, elektriciteitsprijzen en de beschikbaarheid van brandstof de besluitvorming steeds complexer. Ondanks de groeiende aandacht voor de decarbonisatie van de maritieme sector, behandelen bestaande studies operationele planning, energiebeheer, vraagvoorspelling en het omgaan met onzekerheid vaak afzonderlijk, waardoor hun toepasbaarheid in sterk geïntegreerde en onzekere maritieme omgevingen beperkt blijft.

Gemotiveerd door deze uitdagingen onderzoekt dit proefschrift energiebewuste activiteiten voor havens en scheepvaartsystemen onder onzekerheid. Het proefschrift heeft tot doel de overgang naar koolstofarme maritieme transportsystemen te ondersteunen door operationele planning, energiebeheer en het omgaan met onzekerheid gezamenlijk in overweging te nemen. Het onderzoek verkent met name de interacties tussen havenactiviteiten en energiesystemen, de integratie van vraagvoorspelling voor walstroom in operationele besluitvorming, en robuuste optimalisatie voor scheepvaartnetwerksystemen.

Op het niveau van het energiesysteem van de terminal onderzoekt dit proefschrift de integratie van havenactiviteiten en energiebeheer in geëlektrificeerde containerterminals (Chapter 2). Er wordt een geïntegreerd stochastisch programmeerkader ontwikkeld om terminalactiviteiten en energiestromen onder onzekere omstandigheden gezamenlijk te modelleren. Meerdere operationele componenten, waaronder schepen, kade- en stapelkranen, koelcontainers en automatisch geleide voertuigen, worden gemodelleerd als energieverbruikers binnen het energiesysteem van de terminal. De resultaten tonen aan dat het gezamenlijk in aanmerking nemen van operationele planning en energiebeheer zowel de operationele efficiëntie als het energiebenutting onder onzekerheid kan verbeteren.

Voortbouwend op het energieperspectief op terminalniveau onderzoekt dit proefschrift verder de modellering en voorspelling van de vraag naar walstroom en de interactie daarvan met beslissingen over de toewijzing van ligplaatsen op het niveau van het ligplaatsgebied (Chapter 3). Er wordt een datagestuurd raamwerk voorgesteld om operationeel gesegmenteerde vraagprofielen

voor walstroom te reconstrueren op basis van historische havengebeurtenisgegevens en om de tijdsgranulaire walstroomvraag te voorspellen met behulp van machine learning-benaderingen. De voorspelde vraagprofielen worden vervolgens geïntegreerd in een energiebewust kader voor ligplaatsallocatie. De resultaten tonen aan dat het meenemen van de voorspelde vraag naar walstroom in beslissingen over ligplaatsallocatie de energiegerelateerde operationele kosten effectief kan verlagen en de piekvraag naar elektriciteit kan verminderen. Bovendien laten de bevindingen zien dat het voorspellingsmodel met de beste voorspellingsnauwkeurigheid niet noodzakelijkerwijs leidt tot de beste optimalisatieprestaties, wat het belang onderstreept van het gezamenlijk overwegen van voorspelling en optimalisatie in energiebewuste havenoperaties.

Door het onderzoeksgebied uit te breiden van terminalactiviteiten naar maritieme scheepvaartnetwerken, onderzoekt dit proefschrift onzekerheidsbewuste operationele planning voor dual-fuel lijnvaartsystemen onder onzekere brandstofvoorzieningsomstandigheden (hoofdstuk 4). Er wordt een geïntegreerd, distributioneel robuust optimalisatiekader ontwikkeld om vaarsnelheden, bunkeringlocaties en -hoeveelheden, en brandstofkeuzes over de verschillende vaartrajecten heen gezamenlijk te bepalen. De experimenten tonen aan dat het expliciet rekening houden met onzekerheid in de brandstofvoorziening de operationele betrouwbaarheid aanzienlijk kan verbeteren. De experimenten met methanolgebruik laten verder zien dat de beschikbaarheid van bunkerbrandstof en de prijsconcurrentie van brandstoffen complementaire rollen spelen. Uitbreiding van het aanbod bepaalt de operationele bovengrens voor het gebruik van methanol, terwijl prijsdalingen van invloed zijn op de mate waarin exploitanten die grens benaderen.

Over het geheel genomen biedt het in dit proefschrift voorgestelde raamwerk praktische inzichten ter ondersteuning van de transitie naar efficiëntere, veerkrachtigere en duurzamere maritieme transportsystemen, terwijl het potentieel wordt aangetoond van het combineren van operations research en datagestuurde benaderingen bij het bevorderen van een netto-nul zeevaart.

About the author

Xinyu Tang was born in Zhoushan, China. She obtained her B.Sc. degree in Transport Management from Dalian Maritime University in 2019. She subsequently pursued her M.Sc. degree in Transportation Engineering under supervision of Prof. Jiangang Jin at Shanghai Jiao Tong University, where she graduated in 2022.

In October 2022, Xinyu joined the Department of Maritime and Transport Technology, at Delft University of Technology as a PhD candidate. Her doctoral research was supervised by Prof. Rudy Negenborn and Dr. Frederik Schulte. Her PhD research focuses on energy-aware port and maritime operations under uncertainty with integrated optimization and learning-based approaches.

Publications

1. J. Stoter, **X. Tang**, M. Cvetkovic, P. Palensky, H. Polinder, Ç. Iris, F. Schulte (2025) Energy management and stochastic operations planning for electrified container terminals with uncertain energy supply and demand, Journal of Cleaner Production, 527, p. 146383

2. **X. Tang**, Ç. Iris, R. R. Negenborn, P. He, F. Schulte (2026) Learning shore power demand and energy-aware berth allocation, Submitted to a journal.

3. **X. Tang**, P. He, F. Schulte (2026) Dual-Fuel Vessel Operations under Fuel Supply Uncertainty: Robust Planning and Scenario Analysis, Submitted to a journal.

4. **X. Tang**, F. Schulte (2023) Stockyard storage space allocation in dry bulk terminals considering mist cannons and energy expenditure, in Proceedings of the 14th International Conference on Computational Logistics (ICCL 2023), Berlin, Germany

5. **X. Tang**, Ç. Iris, F. Schulte (2025) Fine-grained estimation of onshore power demand via operational phase segmentation of port call data, in Proceedings of the 16th International Conference on Computational Logistics (ICCL 2025), Delft, The Netherlands.

TRAIL Thesis Series

The following list contains the most recent dissertations in the TRAIL Thesis Series. For a complete overview of more than 400 titles, see the TRAIL website: www.rsTRAIL.nl.

The TRAIL Thesis Series is a series of the Netherlands TRAIL Research School on transport, infrastructure and logistics.

Tang, X., *Energy-Aware Operations for Decarbonizing Ports and Shipping under Uncertainty: Learning- and optimization-based approaches*, T2026/22, September 2026, TRAIL Thesis Series, The Netherlands

Yoo, S., *Perceived Accessibility by Air Transportation: Determinants, Heterogeneity, and Climate Policy Implications*, T2026/21, September 2026, TRAIL Thesis Series, The Netherlands

Cunillera Pérez, A., *Robust Train Trajectory Optimization and Train Motion Model Calibration*, T2026/20, September 2026, TRAIL Thesis Series, The Netherlands

Öztürker, M., *On the Bright Side of Vehicle Automation: The effects of service quality improvements and ride experience on users' preferences for automated public transport*, T2026/19, July 2026, TRAIL Thesis Series, The Netherlands

Faber, R.M., *Travel in Transition: A longitudinal exploration of travel behaviour*, T2026/18, June 2026, TRAIL Thesis Series, The Netherlands

Xiong, X., *Hydrodynamics-Aware Model Predictive Formation Control for Energy-Efficient Multi-Vessel Systems*, T2026/17, July 2026, TRAIL Thesis Series, The Netherlands

Louro, T.V., *Electric Bicycles: impacts on job accessibility and spatial equity in Brazilian megacities*, T2026/16, July 2026, TRAIL Thesis Series, The Netherlands

Knaap, R.J.H. van der, *Multi-period Line Planning and Timetabling for Varying Railway Passenger Demand*, T2026/15, June 2026, TRAIL Thesis Series, The Netherlands

Liang, K., *Adaptive Takeover Time Budgets in Conditionally Automated Driving*, T2026/14, June 2026, TRAIL Thesis Series, The Netherlands

Suryana, L.E., *Operationalising Meaningful Human Control for Reason-Responsive Decision-*

Making in Automated Vehicles, T2026/13, June 2026, TRAIL Thesis Series, The Netherlands

Yan, H., *Cycling Speed: Variation and Stability within Rides*, T2026/12, May 2026, TRAIL Thesis Series, The Netherlands

Abhishek, D., *Safe Navigation of Autonomous Vessels in Inland Waterways under Uncertain and Abnormal Operational Condition*, T2026/11, June 2026, TRAIL Thesis Series, The Netherlands

Garrido-Valenzuela, F., *Pixels, People, Places: Computer Vision and Image Embeddings for Perception-Aware Urban Analytics*, T2026/10, April 2026, TRAIL Thesis Series, The Netherlands

Spierenburg, L., *Advances in the Analysis of Residential Segregation and Urban Riots*, T2026/9, April 2026, TRAIL Thesis Series, The Netherlands

Boot, M., *Evaluating Experiences with Smart Cycling Technologies: Sensor-based evaluations of outdoor cycling experiences with Smart Cycling Technologies*, T2026/8, March 2026, TRAIL Thesis Series, The Netherlands

Wen, X., *Data-Driven Spatial-Temporal Modeling for Bicycle Traffic Prediction*, T2026/7, March 2026, TRAIL Thesis Series, The Netherlands

Wang, Z., *Optimising Performance of Automatic Train Operation on Railway Networks*, T2026/6, March 2026, TRAIL Thesis Series, The Netherlands

Hadi, A.H., *DEM Modelling of Multi-Component Segregation in the Blast Furnace Charging System*, T2026/5, February 2026, TRAIL Thesis Series, The Netherlands

Farhani, M., *Demand Management Strategies for Operations of Shared Mobility Services*, T2026/4, February 2026, TRAIL Thesis Series, The Netherlands

Yao, X., *Driving Heterogeneity in Traffic Flow Theory: An action-based framework for identification, modelling, and simulation*, T2026/3, January 2026, TRAIL Thesis Series, The Netherlands

Versluis, N.D., *Optimising Railway Traffic Management under Radio-Based Distance-to-Go Signalling*, T2026/2, January 2026, TRAIL Thesis Series, The Netherlands

Jiao, Y., *Proactive Collision Risk Quantification in Multi-directional Traffic Interactions*, T2026/1, January 2026, TRAIL Thesis Series, The Netherlands

Asadi, M., *Accessibility and Road Safety: Integration of road safety in accessibility evaluation*, T2025/20, November 2025, TRAIL Thesis Series, The Netherlands

Akse, R., *Understanding and untangling the uncertainty knot: How to catalyse decision-making in mobility innovations*, T2025/19, November 2025, TRAIL Thesis Series, The Netherlands

Führer, K., *Participatory Decision-making under Deep Uncertainty: Modelling mobility transi-*

tions, T2025/18, November 2025, TRAIL Thesis Series, The Netherlands

Picco, A., *Monitoring and Feedback in Driving*, T2025/17, October 2025, TRAIL Thesis Series, The Netherlands

Cebeci, M.S., *Behaviour of Prosumers in Last-mile Logistics: The case of crowdshipping*, T2025/16, September 2025, TRAIL Thesis Series, The Netherlands

Summary

Decarbonizing ports and shipping introduce operational and energy-related challenges under uncertainty. This thesis develops learning- and optimization-based approaches for energy-aware maritime operations. It combines stochastic terminal energy management, data-driven shore power demand prediction and berth allocation, and distributionally robust planning for dual-fuel liner services. Together, these approaches provide integrated decision support for the decarbonization of port and maritime transport systems.

About the Author

Xinyu Tang received an MSc in Transportation Engineering from Shanghai Jiao Tong University. In 2022, she began her PhD research in the Department of Maritime and Transport Technology at Delft University of Technology.

TRAIL Research School ISBN 978-90-5584-397-8

Erasmus University Rotterdam · Radboud University · rijksuniversiteit groningen

TU Delft Delft University of Technology · UNIVERSITY OF TWENTE. · TU/e Technische Universiteit Eindhoven University of Technology